Mechanical and conformational aspects of protein layers on water

Promotor	Prof. dr. ir. M.A. Cohen Stuart hoogleraar in de Fysische Chemie met bijzondere aandacht voor de Kolloïdchemie
Co-promotoren	Dr. ir. M.A. Bos wetenschappelijk hoofmedewerker TNO Voeding
	Dr. ir. T. van Vliet projectleider WCFS / universitair hoofddocent
Promotiecommissie	Prof. dr. E. Dickinson (University of Leeds, UK) Prof. dr. G. Frens (TU Delft) Prof. dr. E.J.R. Sudhölter (Wageningen Universiteit) Dr. ir. W. Norde (Wageningen Universiteit)

Mechanical and conformational aspects of protein layers on water

A.H. Martin

Proefschrift
ter verkrijging van de graad van doctor
op gezag van de rector magnificus
van Wageningen Universiteit,
prof. dr. ir. L. Speelman,
in het openbaar te verdedigen
op vrijdag 9 mei 2003
des namiddags te vier uur in de Aula.

ISBN: 90-5808-810-3

A.H. Martin (2003)
Mechanical and conformational aspects of protein layers on water
Ph.D. Thesis, Wageningen University, The Netherlands, 125 p.

Keywords: protein film, protein conformation, air/water interface, network formation, foam formation, foam stability, interfacial rheology, fracture behaviour

ABSTRACT

The aim of this thesis was to obtain systematic information on the importance of mechanical and conformational aspects for the formation of a visco-elastic protein network at the air/water interface. Such a protein network is formed upon adsorption at the interface and is assumed to play a role in the formation and stabilisation of emulsions and foams. To understand the formation of a visco-elastic layer with specific mechanical properties, one has to study the molecular processes occurring at the interface, namely protein adsorption, conformational changes that occur upon adsorption and the interactions between the adsorbed proteins. A series of proteins was studied with a tertiary structure varying from random coil (flexible) to rigid (globular): β-casein, β-lactoglobulin, ovalbumin and (soy) glycinin. Glycinin has only been studied preliminary in the past but, being an interesting substitute for animal proteins, it was investigated quite extensively in this thesis. The conformation of glycinin was found to be pH-dependent and this change in conformation strongly affected the adsorption behaviour and rheological properties of interfacial glycinin layers. The monomeric glycinin form present at pH 3 behaved as a good foaming agent whereas at pH 6.7 (hexamer form) no foam could be formed. Infrared Reflection Absorption Spectroscopy (IRRAS) showed that only minor changes occurred in the secondary structure of a protein upon adsorption at the interface. Ovalbumin and β-lactoglobulin showed a 10% loss of β-sheet structures whereas glycinin (pH 3) formed intermolecular anti-parallel β-sheets. The latter is an indication for interfacial aggregation. Mechanical properties were determined by deformation in shear and dilation. Upon large deformations most protein films were found to exhibit fracture behaviour. The differences observed for ovalbumin, β-lactoglobulin and glycinin indicated a transition from a more yielding behaviour to a more brittle fracture behaviour. A correlation was found between several mechanical properties of adsorbed protein films and the stability against disproportionation of foams made with the corresponding proteins. Furthermore, correlations between macroscopic film properties and molecular properties of the proteins in terms of molecular dimensions and secondary structure were studied. It was discovered that the molecular area at the onset of surface pressure per unit protein molecular weight was strongly correlated to the steady-state shear stress of a saturated protein film. This means that protein 'hardness' largely determines the film properties but a quantitative model is yet to be developed. Practical relevance of the mechanical properties of adsorbed protein layers for the stability of emulsions and foams is discussed.

Table of Contents

1 Introduction

1.1 General introduction

The physical stability of foams and emulsions is a very important topic for the food industry both in terms of assuring a good quality during storage and in obtaining a controlled instability during processing, handling and consumption. Moreover, ongoing product and process development requires knowledge and tools that allow better control of the formation and stability of food emulsions and foams. Therefore research is needed on mechanisms determining formation and stability of emulsions and foams from molecular to macroscopic scale: from monolayers of single components via well-defined simple model systems to complex ones.

In food emulsions and foams proteins are often the main interfacial components. The physical-chemical role of proteins in the formation and stabilisation of emulsions and foams has been studied extensively and was reviewed by Walstra [1], Dickinson [2] and Wilde [3] among others. Upon adsorption at interfaces proteins may form a coherent film or interfacial protein network. Little attention has been paid to this process of network formation by proteins at the interface. The extent to which the properties of such interfacial protein layers are important for the stability of emulsions and foams is also not exactly known yet. It is thought that a rigid protein network around air bubbles or oil droplets retards destabilisation processes of foams and emulsions such as coalescence [3,4], drainage [5,6] and disproportionation [7,8].

To understand the role of visco-elastic protein layers in the formation and stability of emulsions and foams one has to take a closer look at the molecular processes occurring at the interface. In this thesis a rather simple, schematic distinction is made between these molecular processes, namely: (i) protein adsorption, (ii) conformational changes that occur upon adsorption and (iii) the formation of a visco-elastic layer with specific mechanical properties. These three processes depend on the type of protein and on solution conditions like pH and ionic strength. By studying a series of proteins in which the structure varies, the importance of mechanical and conformational aspects for the formation of a visco-elastic protein network can be assessed. This may lead to the formulation of general mechanisms and, hence, to a better understanding of foam and emulsion stability.

1.2 Protein structure

Proteins are large molecules with complex structures. In chemical terms, they are defined as linear polymers of amino acids linked by peptide bonds. Four levels of structure are usually distinguished: the primary, secondary, tertiary and for some proteins also a quaternary structure. The primary structure is the sequence of the amino acids in the polypeptide chain; the secondary structure refers to the ordered regions in the polypeptide chain, such as α-helices and β-sheets (see Figure 1.1).

The way in which twists or bends of the whole polypeptide are folded together is called the tertiary structure (see Figure 1.1). Generally, hydrophilic amino acid side groups reside predominantly at the surface, and hydrophobic ones in the core of the structure. The association of proteins by non-covalent bonds in order to form larger units is termed quaternary structure. Many globular proteins (‘monomers’) form dimers, trimers or larger aggregates. Secondary, tertiary and quaternary structures together determine the conformation of the protein.

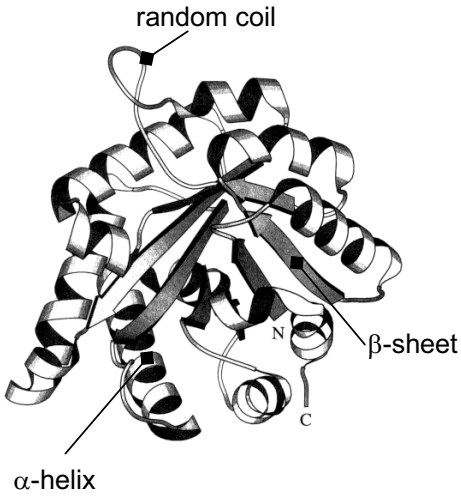

Figure 1.1 Protein folding: secondary and tertiary structure

On the basis of their shape proteins can be classified into three groups: globular, fibrous and disordered. A globular protein is tightly folded into a roughly spherical shape; fibrous proteins have a very elongated structure and disordered proteins have a range of conformations closer to random coil than the other two types. Another useful distinction is that between ‘hard’ and ‘soft’ proteins. The term ‘hard’ is used for proteins that have a relatively stable globular conformation characterised by a high Gibbs activation energy for denaturation (unfolding).

Several interactions and linkages are known to contribute to the formation of the secondary, tertiary and quaternary structures: van der Waals interactions, electrostatic interactions, hydrogen bonding, hydrophobic interactions and covalent disulphide cross-links. All these interactions may be intra- or intermolecular. Also, they may depend on, for example, the solvent quality, the pH and ionic strength of the solution [9,10].

1.3 Protein adsorption at liquid interfaces

Most water-soluble proteins accumulate spontaneously at liquid interfaces. This implies that the adsorption process is accompanied by a lowering of the Gibbs energy of the interfacial system. The Gibbs energy of adsorption ΔG_{ads} consists of an enthalpy term ΔH_{ads} and an entropy term ΔS_{ads}

$$\Delta G_{ads} = \Delta H_{ads} - T \cdot \Delta S_{ads} \tag{1.1}$$

in which T is the temperature. The large positive entropy change ΔS_{ads} provides the major contribution to ΔG_{ads} while ΔH_{ads} is relatively less important. The main contributors to ΔS_{ads} are the hydration of polar side groups and peptide bonds of the protein and the changes in protein secondary and tertiary structure (=unfolding) upon adsorption.

The surface activity of a protein depends on the protein concentration, the molecular weight of the protein, protein structure and solution conditions like pH and ionic strength. In literature also protein hydrophobicity is considered to play a role. Furthermore, the type of interface (liquid/gas, liquid/liquid or solid/liquid) is of importance. These factors lead to differences in adsorption kinetics (the rate at which protein adsorbs to the interface), in the extent to which proteins change conformation upon adsorption and in the mechanical properties of the adsorbed protein layer.

Adsorption processes play an important role in the formation of foams and emulsions. If a protein or another surface-active agent cannot adsorb in a sufficient amount within the characteristic time-scale of the production process, no foam or emulsion is formed. Foam formation or emulsification will therefore in the first place depend on the adsorption rate of the protein. Obviously, this requires transport of protein to the surface by convection and diffusion and, subsequently, attachment of the protein at the surface. A rough qualitative measure for protein adsorption at liquid interfaces is the decrease in surface tension γ (mN/m) with time. If the extent to which proteins adsorb is to be assessed quantitatively one should measure the adsorbed amount Γ (mg/m^2). Techniques commonly used to measure the surface tension are the Wilhelmy-plate method and drop shape analysis; optical reflection ellipsometry or infra-red reflection absorption spectroscopy (IRRAS) can be used to determine the adsorbed amount. Surface tension and adsorbed amount data are often used to check quantitative theoretical models of protein adsorption at interfaces.

1.4 Conformational changes

It is generally believed that proteins undergo structural or conformational changes upon adsorption at an interface. The extent to which this happens depends on the interface, the local environment, the protein and its concentration. The type of interface (either liquid/gas, liquid/liquid or liquid/solid) appears to have considerable

effects on the unfolding of adsorbed proteins [11]. Both oil and air provide hydrophobic surfaces, where the main driving force for adsorption is hydrophobic interaction. Since most a-polar residues are buried in the core of a globular protein, adsorption generally involves changes in conformation. It is expected that at low protein concentration the increase in adsorbed amount is slow, allowing adsorbed molecules to expand laterally, which implies relatively extensive conformational change. If the increase in adsorbed amount is fast (at high protein concentration), a densely packed adsorbed layer is rapidly formed, which could prevent lateral expansion of individual molecules.

There are only few techniques that allow determination of conformational changes of proteins upon adsorption at the interface. Information on conformational changes is mostly deduced from adsorption experiments relating surface excess, surface pressure and protein layer thickness to protein molecular dimensions [12-14]. These studies suggest that adsorption of globular proteins at the air/water interface results in partial unfolding of the protein structures in terms of tertiary structure. The techniques most commonly used to directly study conformational changes of proteins upon adsorption are Fourier Transform Infra-Red (FTIR) or Infra-Red Reflection Absorption Spectroscopy (IRRAS).

IRRAS is a relatively new and promising technique. It offers the possibility to detect changes in protein secondary structure as well as in the orientation of the protein at the interface. In this thesis we will use IRRAS to study the adsorption of protein at the air/water interface simultaneously with the conformational changes that may take place upon adsorption.

1.5 Mechanical properties of protein layers

Upon adsorption proteins may form a visco-elastic network, the mechanical properties of which are of interest for the formation and stabilisation of emulsions and foams. Mechanical properties of protein layers give information on the rigidity, visco-elasticity or strength of such a layer. Determination of the mechanical properties can be done by surface rheological measurements in which the interfacial protein layer is exposed to deformation of the surface. The most important types of surface deformation in relation to the formation and stability of foams and emulsions are: shape changes (shear) and area changes (dilation) (see Figure 1.2). Deformation in shear may be associated with cohesive interactions between protein molecules. By changing only the shape of the surface (and not the area) no protein will adsorb or desorb during the measurement and therefore protein interactions in the plane of the interface can be probed. Other factors of importance in shear rheology are the internal cohesion and the surface density of the proteins present at the surface. The structure of the protein network formed at the interface may have an open or a

compact character, and this has an influence on the deformation and relaxation of the surface. Unlike with shear rheology, deformation in dilation leads to changes in area of the surface plane. Therefore, dilation may be associated with some adsorption/desorption of the surface-active agent. During enlargement of the surface 'new' protein can adsorb to the bare interface that has been created, whereas during compression (segments of) proteins may desorb from the interface. Oscillatory area changes are related to adsorption and desorption processes as well and to some extent they can also probe cohesive and repulsive interactions between protein molecules. Interactions between protein molecules however, are better probed by deformation in shear as mentioned above [15].

Various methods have been developed in order to determine the surface rheological properties of protein layers. The equipment used in this thesis involves the ring trough, the overflowing cylinder, a surface shear rheometer, an automated drop tensiometer (ADT) and a Langmuir trough with an endless caterpillar belt.

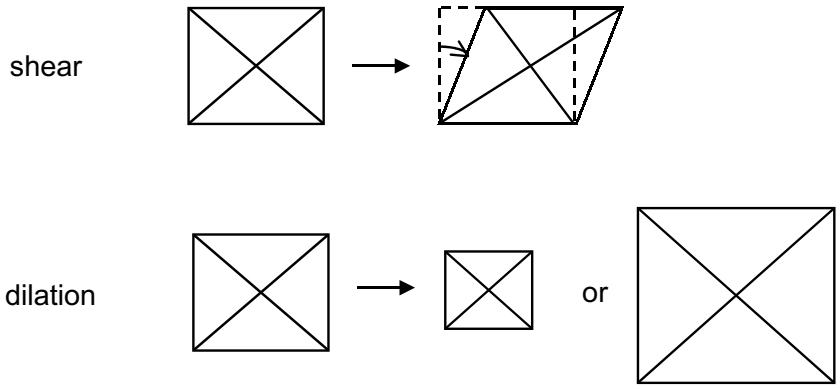

Figure 1.2 Deformation of surfaces in shear (shape) and dilation (area)

1.6 Stability of emulsions and foams

Foams and emulsions are meta-stable systems in which one (fluid) phase (air for foams and oil for oil-in-water emulsions) is dispersed in another (liquid) phase. Emulsions and foams are only formed if protein or another surface-active agent adsorbs in a sufficient amount within the time-scale of the production process. Surfactants do not only play a role in the formation of foam and emulsions but also in preventing the bubbles and droplets from becoming unstable.

Foams and emulsions are subject to changes in state through various processes. Some of these processes just change the distribution of dispersed and continuous phase (creaming, drainage) but others affect the stability (disproportionation, aggregation and coalescence) (see Figure 1.3) [8]. For foams

creaming and aggregation are normally not important. Drainage is the process of liquid flow due to gravitational forces resulting in a lower continuous phase content of the foam. Coalescence is the merging of two bubbles into one bigger bubble. Disproportionation (or Ostwald ripening) involves gas transport from smaller bubbles to larger ones due to the difference in Laplace-pressure. Large bubbles will therefore grow at the expense of smaller bubbles, which decrease in size and eventually disappear. This process leads to coarsening of the foam.

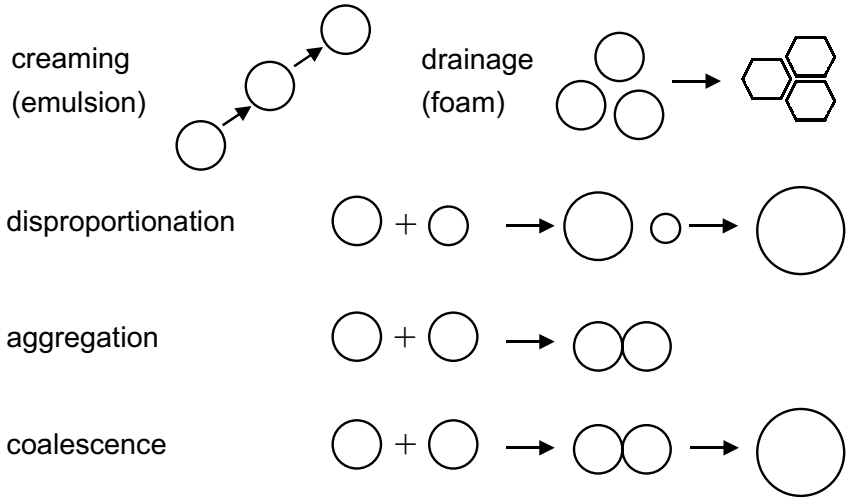

Figure 1.3 Instability mechanisms of foams and emulsions

Various interfacial properties of proteins are claimed to have some sort of influence on the stabilisation of foams and emulsions. A gel-like adsorbed film with a finite yield stress would slow down disproportionation [6,7,16]. The mechanical resistance of the protein film could oppose the area change that occurs during disproportionation. It has also been suggested that a kind of skin slows down gas transport because of lack of solubility in this skin. During film drainage surface shear rheological properties seem to be important. The moving liquid exerts a shear stress on the film surfaces, which is counteracted by a surface tension gradient $\Delta\gamma$ (caused by the same liquid flow) acting from bottom to top of the film. If the stress in the interface due to $\Delta\gamma$ is large enough, lateral movement of the surface can be arrested. Hence, the higher the surface shear stress, the slower drainage, and the more stable the foam [5,6]. A surface tension gradient is also a prerequisite for stability against re-coalescence during foaming/emulsification. When two bubbles come close to each other, the outflow of liquid from the thin film causes a $\Delta\gamma$. As a result, $\Delta\gamma$ leads to flow of adjacent liquid(s) in the direction of increasing γ. The inflow of continuous phase

drives the bubbles/droplets apart. This stabilising mechanism is called the Gibbs-Marangoni effect. Coalescence requires a near approach of two bubbles/droplets and also hole formation implying film rupture. Coalescence can be induced by shear flow, enhancing the encounter of bubbles/droplets. The rate of film rupture depends on the film thickness and on its mechanical properties, in particular on the Gibbs elasticity of the film and the stress at which the film breaks [3,4].

1.7 Outline of thesis

The central theme of this thesis is the formation of visco-elastic protein layers upon adsorption at the air/water interface. Three molecular processes are distinguished: (i) protein adsorption, (ii) conformational changes that occur upon adsorption and (iii) the formation of a visco-elastic layer with specific mechanical properties. Our aim was to obtain systematic information on the importance of mechanical and conformational aspects for the formation of a visco-elastic protein network. A series of proteins was selected varying in structure from flexible to rigid/globular. These proteins were β-casein (from milk), β-lactoglobulin (from milk), (egg) ovalbumin and (soy) glycinin.

Chapters 2 and 3 discuss the conformational aspects of proteins upon adsorption at the air/water interface. In *Chapter 2* the conformation of glycinin is studied as a function of pH; the association/dissociation behaviour as a result of the change in pH is related to differences in interfacial rheological properties. Interfacial parameters such as adsorbed amount, dilational modulus, surface shear viscosity and foaming properties are linked to the conformation of glycinin. *Chapter 3* discusses the conformational changes that various proteins may undergo upon adsorption at the air/water interface. For this study a relatively new technique was used, namely Infra-Red Reflection Absorption Spectroscopy (IRRAS). This technique enables us to determine surface pressure, adsorbed amount and changes in conformation on a secondary folding level simultaneously as a function of time.

Chapter 4 and 5 deal with the mechanical aspects of the visco-elastic protein layer formed at the interface. Whereas *Chapter 4* only deals with the mechanical properties determined by deformation in shear, *Chapter 5* discusses both shear and dilation. From the stress-strain curves information on fracture stress and fracture strain is derived for different proteins. Transients in surface shear experiments and the meaning of stresses and strains involved are discussed (see *Chapter 4*). *Chapter 5* continues and expands the shear measurements. Also, experiments in dilation are discussed. All four proteins mentioned above are studied and the protein layers are mechanically characterised. The mechanical properties are correlated with foamability and foam stability of the proteins studied.

Chapter 6 provides a general discussion on the relation between the mechanical properties of interfacial protein layers (chapter 4 and 5) and the molecular properties of each of the proteins (chapter 2 and 3). Molecular properties such as the molecular dimensions and secondary structure are related to the mechanical properties determined by deformation in shear and dilatation and to the relaxation behaviour after deformation.

Finally, *Chapter 7* describes the relevance of the research performed in this thesis for selected practical applications, as may occur in industrial processes.

References

1. Walstra, P. In: *Encyclopedia of emulsion technology*; Ed. P. Becher, Marcel Dekker; 1996, 2-62.
2. Dickinson, E. *J. Chem.Soc.Far.Trans.* **1998**, *94*, 1657-1669.
3. Wilde, P.J. *Curr. Op. Coll.Interface Sci.* **2000**, *5*, 176-181.
4. Dickinson, E. *Colloids Surf. B* **1999**, *15*, 161-176.
5. Prins, A. *Colloids Surf. A* **1999**, *149*, 467-473.
6. Prins, A.; van Kalsbeek, H.K. *Curr. Op. Coll.Interface Sci.* **1998**, *3*, 639-642.
7. Gandolfo, F.G.; Rosano, H.L. *J. Coll. Interface Sci.* **1997**, *194*, 31-36.
8. Prins, A. In: *Adv. Food Emulsions and Foams*; Ed. E. Dickinson and G. Stainsby, Elsevier; 1988, 91-122.
9. Damodaran, S. In: *Food Chemistry*; Ed. O.R. Fennema, Marcel Dekker; 1996, chapter 6.
10. Creighton, T.E. Proteins: Structures and molecular properties; Freeman; New York ; 1993.
11. Green, R.J.; Hopkinson, I.; Jones, R.A.L. *Langmuir* **1999**, *15*, 5102-52110.
12. Graham, D.E.; Phillips, M.C. *J. Coll. Interface Sci.* **1979**, *70*, 427-439.
13. Lu, J.R.; Su, T.J.; Thomas, R.K.; Penfold, J.; Webster, J. *J. Chem.Soc.Far.Trans.* **1998**, *94*, 3279-3287.
14. Clark, D.C.; Smith, L.J.; Wilson, D.R. *J. Coll. Interface Sci.* **1988**, *121*, 136-147.
15. Bos, M.A.; van Vliet, T. *Adv. Coll. Interface Sci.* **2001**, *91*, 437-471.
16. Kloek, W.; van Vliet, T.; Meinders, M.B.J. *J. Coll. Interface Sci.* **2001**, *237*, 158-166.

2 Interfacial rheological properties and conformational aspects of soy glycinin at the air/water interface

AH Martin, MA Bos & T van Vliet
Food Hydrocolloids (2002) 16: 63-71

ABSTRACT

Interfacial (rheological) properties of soy glycinin were studied at different pH. At acidic and high alkaline pH glycinin (11S form, M~350 kDa) dissociates into smaller subunits, the so called 3S form (M~44 kDa) and 7S form (M~175 kDa). This dissociation behaviour is expected to affect the interfacial rheological properties of glycinin. Adsorption kinetics at the air/water interface were followed with an Automated Drop Tensiometer (ADT) and ellipsometer. The changes in surface concentration, surface pressure, dilational modulus and layer thickness were determined. At acidic pH where glycinin is in the 3S/7S form, it adsorbs much faster at the air/water interface giving a higher surface concentration and a higher dilational modulus than at pH 6.7 (where glycinin is in the 11S form). Surface shear viscosity measurements showed that after short ageing times glycinin gives a protein network that is much more resistant to deformation in shear at pH 3 than at pH 6.7. After ageing for 24 hours the surface shear viscosity is about the same at both pH. Foaming experiments failed to give a glycinin stabilised foam at pH 6.7 while at pH 3 glycinin behaves as a good foaming agent. All results indicate that changing the pH influences the conformation of glycinin and that this has a great impact on the interfacial rheological properties and foaming properties. Based on the results a model is postulated for the modes of glycinin adsorption at pH 3 and pH 6.7, respectively.

2.1 Introduction

The interfacial rheological properties of various well-known animal proteins have been studied extensively. Vegetable proteins, like those from soy, have only been studied preliminarily although they may be interesting substitutes for proteins of animal origin for use in foams and emulsions. Soy proteins are presently used more and more in fabricated food products as emulsifier, foaming agent, thickener, and water absorption and retention agent. However, optimum use of soy protein in, for example, emulsion and foam-type food products requires much more knowledge of their surface properties under various conditions than is presently available [1].

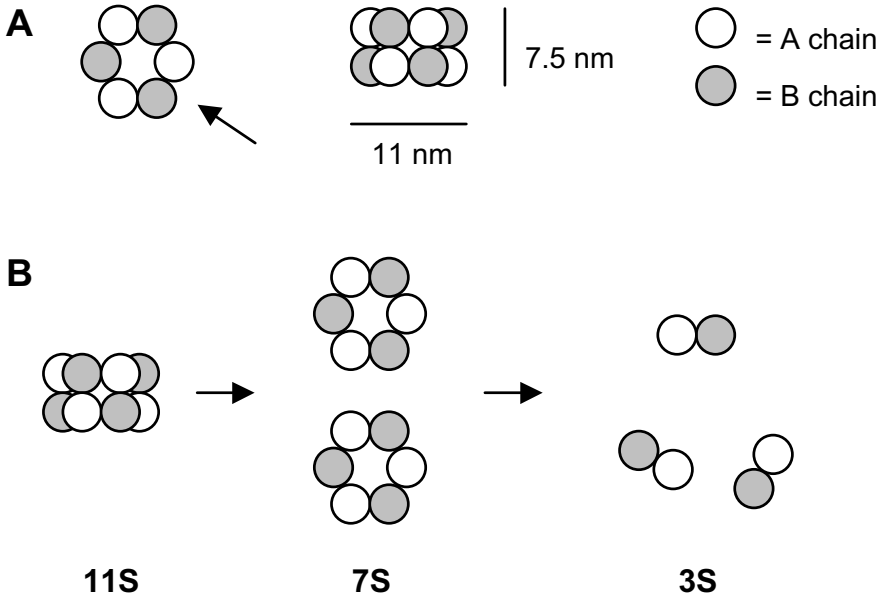

Figure 2.1 Schematic drawing of the structure of glycinin according to Badley [2]; A. Structure of (soy) glycinin; B. Dissociation of glycinin

Glycinin (11S) is the most important storage protein of soybeans and is a globular protein. The currently most accepted model of glycinin is that of a hexamer. The six monomeric subunits have the generalised structure AB, where A represents an acidic polypeptide (M = 34-44 kDa) and B a basic polypeptide (M = 20 kDa). The A and B chains are linked by a single SS bond [3]. Native glycinin (11S) consists of 6 acidic (A) and basic (B) subunits (= 6 AB subunits $(AB)_6$). According to Badley *et al.* [2] the AB subunits associate into two hexagonal rings forming a hollow cylinder of $11 \times 11 \times 7.5$ nm (see Figure 2.1) held together by hydrophilic interactions (electrostatic interactions/H-bridges) [1,2,4,5]. Depending on solubility, pH and ionic

strength, glycinin (11S) dissociates into the 7S form ($(AB)_3$) and/or the 3S form (AB). The dissociation is mainly driven by electrostatic repulsion. Also association into the 15S form (dimer of 11S) may occur. Molecular weights of the 3S, 7S, 11S and 15S forms are approximately 44 kDa, 175 kDa, 350 kDa and 780 kDa, respectively [4].

The model of Badley *et al.* however, is not in complete agreement with the observations of Plietz *et al.* [6] and Lakemond and co-workers [7] who found that the hydrophobic 'basic' type subunits are located predominantly in the interior of the molecule whereas the more hydrophilic 'acid' subunits remain at the outside of the molecule. Obviously, the structure of glycinin is not known exactly and therefore only schematic drawings can be made. The results found in this paper will be primarily explained through the structure model according to Badley *et al.* but for a more detailed analysis of the observations the findings of Plietz *et al.* and Lakemond *et al.* will be taken into account.

The foaming properties of native glycinin (11S form) have been extensively studied [8] and were shown to be limited by the protein's close packed globular conformation [9]. Glycinin does not adsorb rapidly at the air/water interface due to its low surface hydrophobicity, low molecular flexibility and large molecular size [8,10,11]. Surface behaviour and functionality of the 11S-type proteins can be enhanced by appropriate and controlled modification of its structure by reduction, succinylation, or acetylation. Wagner *et al.* [11] showed that dissociation, deamidation and reduction resulted in a decreased molecular size, increased surface hydrophobicity and increased protein charge. These modifications improve the ability of glycinin to adsorb at the interface and to act as a foaming or emulsifying agent [12,13]. Reduction of soy glycinin with DTT (dithiothreitol) also resulted in enhanced molecular hydrophobicity and increased surface viscosity causing an increase in the surface yield stress, the stability of foams and the elasticity of surface films [10].

Besides by chemical modifications, the structure of glycinin can also be modified by varying environmental factors such as ionic strength, pH or temperature [4]. The acidic subunits isolated from soy glycinin (AS11S) were significantly more surface-active than glycinin 11S. AS11S adsorbed faster at the air/water interface and the saturated surface concentration was higher than that of 11S. Similarly, the rate of increase as well as the final surface pressure value was higher for AS11S [14].

In this paper the interfacial rheological properties of glycinin will be presented as a function of pH (and therefore the quaternary structure). Interfacial parameters, such as adsorbed amount, dilational modulus, surface shear viscosity and foaming properties, will be linked to the dissociation behaviour of glycinin. Furthermore, a schematic model for the adsorption of glycinin at pH 3 and pH 6.7 will be presented.

2.2 Materials & Methods

2.2.1 Materials

Soy glycinin was isolated from soybeans according to the fractionation scheme given by Tanh and Shibasaki [15]. The glycinin isolate (135 g/l) was dissolved in 10 mM phosphate buffer pH 7.8 at 4°C in the presence of 10 mM 2-mercaptoethanol and 20% glycerol. It was stored in small aliquots at –40°C. Glycerol was used because of its protecting function against aggregation of glycinin upon freezing; the native state of glycinin is therefore better maintained (unpublished results).

Prior to performing measurements, glycinin was defrosted at 20°C for one hour and dialysed against phosphate buffer with the desired pH and ionic strength. For pH 6.7 a phosphate buffer was used and for pH 3 a citric acid/phosphate buffer. The buffer itself established the ionic strength (=30 mM). Glycinin was diluted with buffer to the desired concentration of 0.01 g/l and 0.1 g/l.

Tween 20 and the chemicals used for the buffer, Na_2HPO_4, NaH_2PO_4 and $C_6H_8O_7 \cdot H_2O$, were purchased from Merck (Darmstadt, Germany, analytical grade). All solutions were made with distilled water.

2.2.2 Methods

All experiments were performed at least twice. For most of the techniques used the experimental error was lower than 5%, except for the surface shear rheometer where the inaccuracy was around 10%.

Automated Drop Tensiometer

The Automated Drop Tensiometer (ADT) [16,17] was used to measure the interfacial tension either between two fluids (liquid/liquid) or between liquid and gas. The interfacial tension was determined by means of drop shape analysis of a bubble of gas formed within a cuvette containing the protein solution. The bubble was illuminated by a uniform light source and its profile was imaged and digitised by a CCD-camera and a computer. The profile was used to calculate the interfacial tension using Laplace's equation. The ADT can be run in different configurations; the one used here is the rising drop configuration.

During the measurements the decrease in surface tension was followed; the dilational modulus was obtained by dynamic oscillation of the bubble area at the beginning and at the end of each measurement. The bubble volume used was 4 μl and the area change during oscillation was approximately 8%. This change in area was within the linear region. Temperature was kept constant at 22°C.

Ellipsometry

Ellipsometry measurements were performed at the Colloid and Interface Science Group at the Max Planck Institute (Golm, Germany). A null-ellipsometer (Optrel) was used. Calculations were done with the program 'Ellipsometry' designed by Plamen Petrov (version 1.31, 1997) (personal communication).

The angle of incidence used was 50° and the wavelength was set at 532 nm. From the change in ellipsometric angles Δ and Ψ the layer thickness and the refractive index were calculated estimating that the protein density profile could be described by a stratified layer model. For the refractive-index increment, dn/dc, of protein solutions 0.18 cm^3/g was taken [18].

Before measurements were started the surface was cleaned by suction of the air/water interface. As reference solution pure buffer was used. Ellipsometry measurements were done at pH 6.7 and pH 3 (both 30 mM) and at the protein concentrations of 0.01 and 0.1 g/l. Temperature was 22 °C.

The overflowing cylinder

The overflowing cylinder technique used in this study has been described by Bergink-Martens [19] and Boerboom [20]. The overflowing cylinder consists of an inner cylinder through which the liquid is pumped at a constant flow rate. Liquid flows over the upper rim of the inner cylinder along the inner cylinder wall into the circular container formed by the inner and outer cylinder. From this vessel the liquid is pumped back to the inner cylinder. The difference between the level of the liquid in the outer cylinder and the rim is called the falling film length L [20]. At the top of the inner cylinder the surface expands radially at a constant relative expansion rate dlnA/dt. For water dlnA/dt is independent of the falling film length while for surfactants it is not. By increasing the length L of the falling film, dlnA/dt of an aqueous surfactant solution can be increased beyond the value for pure water, whereas below a certain value of L the expansion rate can be made lower than that of pure water. By decreasing L even further the surface can stop expanding completely so that it stands still. The falling film length at which this occurs is called L_{still} (dlnA/dt~0). This behaviour depends strongly on the nature of the surfactant used [21]. L_{still} can be translated to the ability of a surfactant to build up an elastic network preventing the surface from flowing. The critical falling film height, L_{still}, was determined at a flux of 31.4 cm^3/s and a temperature of 26°C; dlnA/dt values were determined going from high to low falling film length.

Surface shear rheometer

The apparent surface shear viscosity (η^s_{app}) was measured using a two-dimensional Couette-type interfacial viscometer as described by Dickinson and co-

workers [22-24]. A stainless steel biconical disc (diameter 30 mm) was suspended by a torsion wire such that the disc edge was in the plane of the air/water interface. The protein solution was contained in a thermostated circular glass dish (diameter 145 mm). The thickness of the torsion wire was 0.20 mm and its length was 740 mm. The apparent surface shear viscosity was determined over an ageing period of 24 hours.

To determine η^s_{app}, the protein film was subjected to intermittent shear at an angular velocity of the dish of 1.27×10^{-3} rad/s until a steady-state interfacial stress was obtained, usually after 10-15 minutes. The interfacial stress was monitored by measuring the rotation of the bob via a light beam reflected onto a circular scale with a radius of 600 mm. The apparent surface shear viscosity η^s_{app} (N·s/m) could be calculated as follows:

$$\eta_s = \frac{\tau}{4 \cdot \pi \cdot \Omega} \cdot \left(\frac{1}{R_1^2} - \frac{1}{R_2^2} \right) \tag{2.1}$$

where τ is the torque on the disc, Ω the angular velocity and R_1 and R_2 the radius of the (inner) disc and the (outer) dish, respectively. The torque on the disc can be calculated from the reading of the reflected laser beam and the torsion constant of the wire

$$\tau = K \cdot \frac{P_1 - P_2}{2 \cdot r} \tag{2.2}$$

where K is the torsion wire constant, P_1 and P_2 the final and initial position of the laser beam on the scale, respectively and r the radius of the scale [24-26].

Continuous expansion/compression measurements

The dynamic surface tension in steady state expansion and compression was determined using a Langmuir trough with an endless caterpillar belt with moving barriers [27]. The dimensions of the trough were length x width x depth = 400 × 190 × 30 mm. Six Teflon barriers were mounted on the endless belt. Measurements were performed first in expansion going from highest to lowest speed and then in compression from lowest to highest compression speed (dlnA/dt varies from around 10^{-3} to 10^{-1} s^{-1}).

The surface tension was measured by use of the Wilhelmy plate method. Measurements were performed at 23°C.

Foam experiments

Foams were made using a 'fanflutter' (high speed, single fan at the bottom of the cylinder, diameter of fan = 4.6 cm) and the Ledoux whipping apparatus (Ledoux b.v., Dodewaard, the Netherlands; medium speed, double beaters, diameter of each beater = 4 cm). With the 'fanflutter' 100 ml of protein solution was mixed at 3000 rpm for 2 minutes. The sample container was a volumetric cylinder 11 cm high and 6.2 cm of diameter. With the Ledoux, the protein solution (200 ml) was mixed for 2 minutes at 450 rpm; the cylindrical sample container was 14 cm high and had a diameter of 9.2 cm.

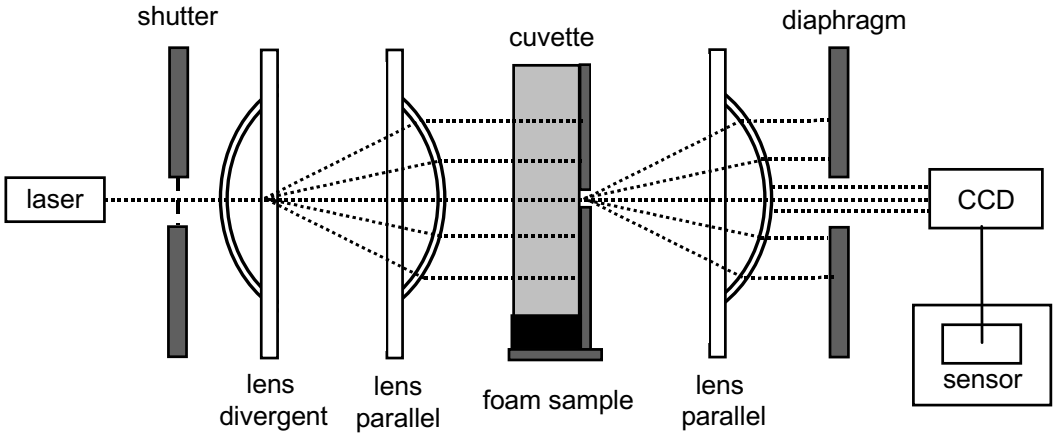

Figure 2.2 Experimental set-up of the laser transmission used for the foam experiments

Foam drainage and drainage height were monitored for a period of 20 minutes in the sample container in which the foam was made. From the foam a sample was taken (with a pipette with an opening of 3 mm in diameter) to determine the mean bubble size, d_{21} by using laser light transmission (see Figure 2.2). The laser beam (Ne-He, λ=633 nm) was interrupted by a timed shutter which opened at set intervals. The cuvette was made of glass, path length 0.5 cm. The transmitted light was measured with a Silicon power meter and recorded by a multimeter and a recorder. The light transmission through the cuvette filled with foam was measured at a set height at intervals of 30 seconds during a period of 15 minutes. The laser beam passes through the foam during 3 seconds per interval to avoid heating up of the foam.

The light transmission set up was calibrated with a Tween foam. Such a foam was analysed by light microscopy and light transmission and the amount of light transmission was correlated to the mean bubble size d_{21} determined by light

microscopy. This size parameter was chosen because the relation between d_{21} and light transmission is linear as shown by Durian *et al.* [28]. Light transmission for glycinin foam was recalculated to an equivalent (mean) d_{21} by using the calibration curve of Tween 20 foam.

2.3 Results

2.3.1 Adsorption behaviour

The adsorption of glycinin at the air/water interface was followed by measuring the decrease in surface tension γ with time as shown in Figure 2.3. The glycinin subunits at pH 3 adsorb much faster than the hexameric structure of glycinin at pH 6.7 at both concentrations. This is due to the lower surface hydrophobicity and higher molecular size (lower diffusion coefficient) of the 11S form compared to the 3S form. These results are in line with the findings of Wagner *et al.* [11]. They showed that the adsorption rate at the beginning of the process was strongly dependent on the conformational state of the 11S-type glycinin. Interfacial tension decreased faster as the dissociation-deamidation degree and/or the reduction of disulphide bridges increased although they found no significant difference in the equilibrium surface tension. Deamidation and/or reduction of the glycinin molecule caused partly unfolding and enhanced flexibility, which resulted in a faster decrease of γ. Reduction of the disulphide bridge in the AB subunit results in even faster decrease of γ and likely in a faster adsorption [11].

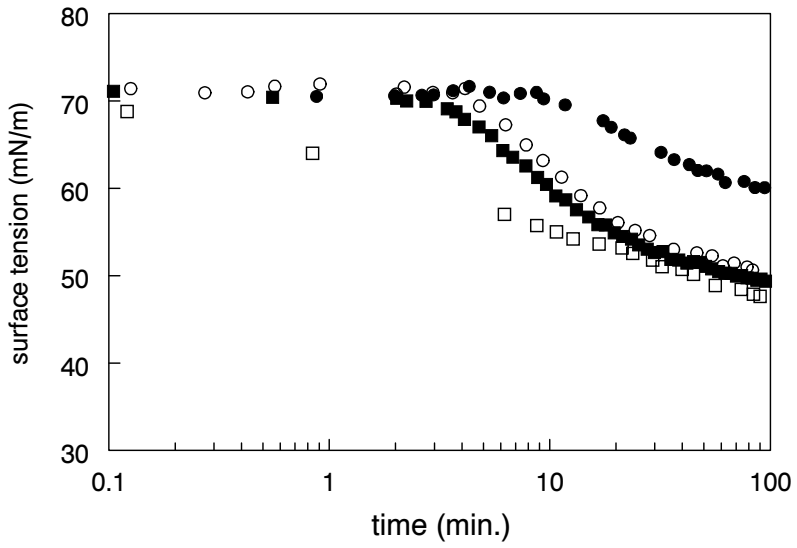

Figure 2.3 Surface tension of a glycinin solution as a function of ageing time at different pH and concentration (g/l), measured with ADT; (•) pH6.7, 0.01 g/l; (o) pH3, 0.01 g/l; (■) pH6.7, 0.1 g/l; (□) pH3, 0.1 g/l)

When measuring the surface tension, a lag time was often observed for lower protein concentrations before γ started to decrease. A minimum adsorbed amount of protein is needed to get a decrease in γ. In Figure 2.4 the adsorbed amount (Γ) as determined by ellipsometry is plotted versus time. Directly from the start of the measurement glycinin adsorbed very rapidly, especially the 3S form at pH 3. After a couple of hours a pseudo equilibrium (Γ_{eq}) was reached. According to Figure 2.4, at low protein concentration pH 3 gives a higher Γ_{eq} compared to pH 6.7. At higher concentration Γ_{eq} is more or less the same for pH 3 and pH 6.7 (though Γ is still increasing very slowly). Apparently the 11S and 3S/7S form adsorb differently and this will be discussed further below. This difference in adsorption is also reflected in the ellipsometric layer thickness. The 11S form gave a layer thickness of about 8.9 and 12 nm (±0.5 nm) at a concentration of 0.01 g/l and 0.1 g/l respectively; the 3S/7S form gave a layer thickness of 8.6 and 7.7 nm (±0.5 nm), respectively. In view of the size of the 11S glycinin molecule (7.5 by 11 nm, see Figure 2.1) these values are reasonable. Just as for the adsorbed amount the influence of the concentration on layer thickness is larger at pH 6.7 than at pH 3.

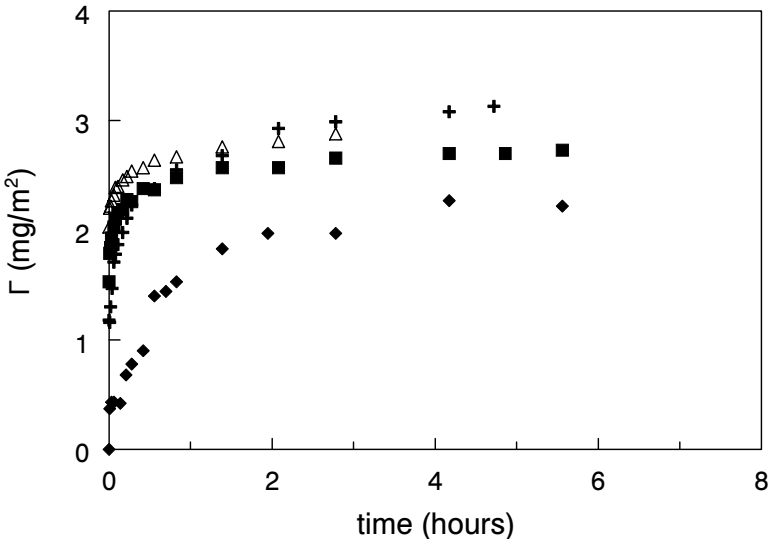

Figure 2.4 Adsorbed amount Γ (mg/m^2) of glycinin as a function of ageing time at different pH and concentration, determined by ellipsometry; (♦) pH 6.7, 0.01 g/l; (+) pH6.7, 0.1 g/l; (■) pH 3, 0.01 g/l; (Δ) pH 3, 0.1 g/l)

For a continuously expanding interface (measured with the Langmuir trough with caterpillar belt) the decrease in γ upon protein adsorption, depends on the expansion rate. Figure 2.5 shows the difference in ability to lower the surface tension at an expanding interface between the 3S/7S form (pH 3) and the 11S form (pH 6.7)

of glycinin. At higher expansion rates both types of glycinin were unable to adsorb in quantities sufficient to lower γ while at low expansion rates γ was reduced. The 3S/7S form was more able to lower γ at higher expansion rates (dlnA/dt~0.06 s^{-1}) than the 11S form. The 11S form lowered γ only at very low expansion rates (dlnA/dt < 0.002 s^{-1}) and γ was only lowered by 5 mN/m. In contrast, the 3S/7S form was able to lower γ by 11 mN/m at this low dlnA/dt (<0.002 s^{-1}) because its adsorption rate is higher (see Figures 2.3 and 2.4). Conclusively, smaller proteins can lower γ at relatively higher expansion rates than larger proteins because their adsorption rate related to the diffusion rate is higher under these circumstances.

At the expanding interface in the overflowing cylinder even higher expansion rates were obtained. As a result the 11S form was not able to lower γ measurably while the 3S/7S form lowered γ only by 2-3 mN/m. These results on expanding interfaces are important for the foaming properties of glycinin as will be discussed below.

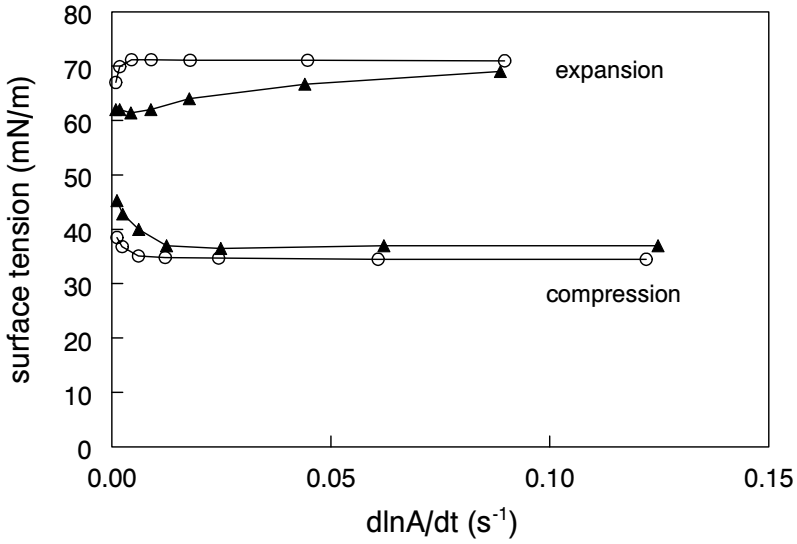

Figure 2.5. Surface tension of a glycinin solution (conc. 0.1 g/l) as a function of the expanding/compressing strain rate dlnA/dt, measured with the caterpillar; (o) pH 6.7; (▲) pH 3

2.3.2 Properties of the adsorbed protein layer

Going from high to low falling film length in the overflowing cylinder, glycinin is able to slow down the motion of the surface. This behaviour was found for other proteins as well. Due to the formation of a protein network the radial surface expansion is counteracted; at L_{still} the surface did not expand anymore (dlnA/dt~0). In Figure 2.6 dlnA/dt is given as a function of the falling film length L for the 3S/7S form

and the 11S form. The 3S/7S form has a higher L_{still} (=2.3 cm) than the 11S form (1.9 cm) which means that the 3S form is able to form a stronger network. Probably, this is due to the fact that the 3S/7S form has a higher ability to unfold and interact with other molecules (the denaturation temperature T_d is lower for the 3S/7S form than for the 11S form [7]). Increasing L (from L_{still} on) leads to protein film rupture; L_{still} can therefore be seen as a measure of the yield/fracture stress of the adsorbed layer [29].

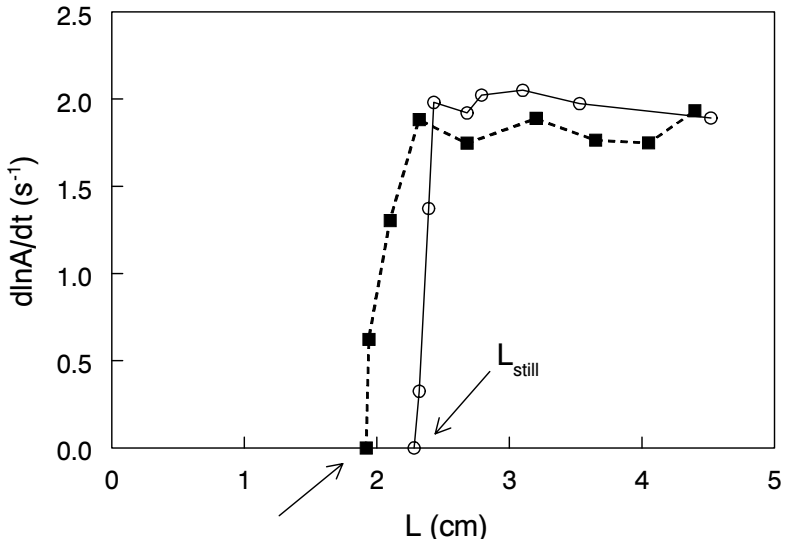

Figure 2.6 Relative expansion rate (dlnA/dt) of the surface of an overflowing cylinder as a function of the falling film length L (L_{still} is L for dlnA/dt goes to 0 and is indicated by an arrow); (■) pH 6.7; (o) pH 3

In general, it can be said that most adsorbed protein molecules are able to form a network at the interface, the properties of which depend on the kind of protein used. Parameters to express the rheological properties of an adsorbed protein layer are among others the dilational modulus and the apparent surface shear viscosity.

The dilational modulus, E, was measured with the ADT at 100 seconds after bubble formation and at the end of the surface tension measurements as shown in Figure 2.3. Table 2.1 shows the results for both pH values. Due to the rapid adsorption of the 3S/7S form, E is already 47 mN/m at t=100 s while the modulus of the 11S form is then only 3 mN/m (for a concentration of 0.1 g/l). From Figures 2.3 and 2.4 it can be deduced that after an adsorption time of ~100 s the 3S/7S form already lowers γ clearly while the 11S form still gives a surface tension of around 70 mN/m. After 1.7 hours the dilational modulus of both the 3S/7S and the 11S form has increased to 60 and 41 mN/m, respectively. Though both the 3S and 11S form are able to form a network, the network of the 11S form is less stiff. The difference in

rigidity lies in the more compact structure of the 11S form and the occurrence of other types of interactions between the molecules. The 3S form is more flexible due to a higher electrostatic repulsion inside the molecule. Therefore it will more easily unfold upon adsorption; the chances to form physical and covalent intermolecular bonds are therefore probably larger at pH 3. This is in agreement with the denaturation temperature T_d which was found to be in the order 11S > 7S > 3S [7].

Table 2.1 Dilational modulus (mN/m) of glycinin at pH 3 and pH 6.7, determined with the ADT

	E (mN/m) at t=100 s	*E* (mN/m) at t=1.7 h
pH 3, 0.01 g/l	4	54
pH 3, 0.1 g/l	47	60
pH 6.7, 0.01 g/l	-	33
pH 6.7, 0.1 g/l	3	41

Interfacial shear rheology of adsorbed protein films is considered to be very sensitive to the molecular structure and to the nature of intermolecular interactions in the adsorbed layer [30]. For most proteins a lag time is observed in time-dependent measurements of the apparent surface shear viscosity [24] but for glycinin (for both concentrations and both pH's), η^s_{app} starts to increase directly from the beginning. In Figure 2.7 the increase of η^s_{app} over an ageing period of 24 hours is shown. Since glycinin at pH 3 (0.1 g/l) adsorbs readily and is able to form intermolecular bonds, η^s_{app} is very high directly from the start and increases further over an ageing period of 24 hours. Glycinin at pH 6.7 (0.1 g/l) starts with a much lower apparent surface shear viscosity but after 8 hours it has reached the same level as at pH 3. Probably it is only a matter of time for glycinin pH 6.7 to adsorb, unfold and rearrange at the interface in such a way that intermolecular bonds can be formed or that the interface becomes so closely packed that it gives a apparent surface shear viscosity as high as pH 3. According to Figures 2.3 and 2.4, the surface tension and surface concentration did not increase much further after 3 hours. From that point on, it is likely that the increase in apparent surface shear viscosity is mainly caused by restructuring of the proteins at the interface and hardly by additional adsorption from the bulk solution.

Compared to other proteins [24] the apparent surface shear viscosity of glycinin takes intermediate values; at pH 3 it is larger than that of lysozyme and smaller than that of myosin, while at pH 6.7 it is smaller than that of lysozyme but larger than that of β-lactoglobulin and ovalbumin at the same pH.

Concerning these results and experiments with the surface shear rheometer, a remark has to be made. In fact, it is very difficult to say what is actually measured and therefore it seems that a clear definition of the apparent surface shear viscosity is lacking. The relative deformation (shear strain) of the surface at constant angular velocity is not homogenous at all over the gap between the dish and the disc and therefore it is in fact impossible to calculate a general shear rate of the surface. Implications of this will be discussed in a forthcoming paper [31]. The results reported here are obtained using the procedures reported by other authors (e.g. [22,24-26]).

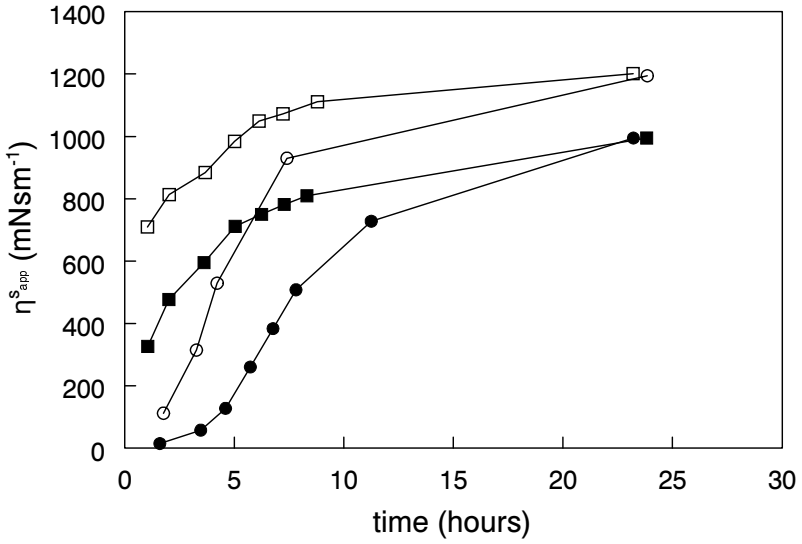

Figure 2.7 Surface shear viscosity as a function of ageing time for glycinin, measured at an angular velocity of 1.27 x 10^{-3} rad/s; (●) pH 6.7, 0.01 g/l; (ο) pH 6.7, 0.1 g/l; (■) pH 3, 0.01 g/l; (□) pH 3, 0.1 g/l)

2.3.3 Foaming properties

Due to its large size and rigid conformation glycinin pH 6.7 adsorbs only slowly at the interface and therefore it hardly adsorbs within the prevalent time scale during foam formation. Neither in the fanflutter nor in the Ledoux apparatus a good foam could be made from a glycinin pH 6.7 solution. The small amount of foam that was eventually formed was very coarse and disappeared immediately. Therefore no data are available on mean bubble size, foam drainage and drainage height for this pH. However, Yu and Damodaran [32] showed that it is possible to make foam from 11S soy protein isolate if much higher concentrations are used, e.g. 10 and 20 g/l.

In contrast, glycinin pH 3, is a very good foaming agent. Foam was made at 4 different concentrations (0.01, 0.1, 0.3 and 1 g/l). A freshly made foam can be described as stiff; it had very fine bubbles with a uni-modal size distribution. No

coalescence occurred within 30 minutes. After half an hour the foam had drained and the bubble size distribution became bi-modal; the foam was very stiff and brittle and can be described as meringue-like.

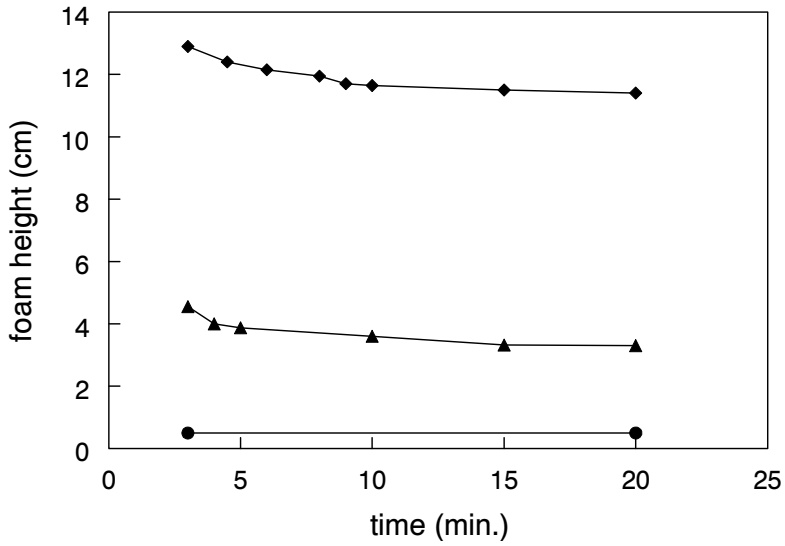

Figure 2.8 Foam height (=total height-liquid height) of glycinin (pH 3) foam made by the Ledoux apparatus as a function of ageing time; (●) 0.01 g/l, (▲) 0.1 g/l, (♦) 0.3 g/l))

In Figure 2.8 the foam height (=total height-liquid height) is given as a function of time. The height of the foam depends very much on the concentration used. Above 0.3 g/l, the concentration did not matter that much anymore. Identical results were obtained for 1 g/l as for 0.3 g/l. Foams made with 0.3 g/l and 1 g/l were very stable; there was hardly any decrease in foam height during half an hour. Results obtained for the equivalent mean bubble size are presented in Table 2.2. For both methods used the foam became coarser upon ageing. However, there is a difference upon ageing: although the fanflutter gives a smaller bubble size at the beginning, more disproportionation occurs during ageing of the foam.

Table 2.2 Mean bubble size of foam from glycinin, prepared with the Ledoux apparatus and the fanflutter

	time (s)	d_{21} (Ledoux)	d_{21} (fanflutter)
0.1 g/l	100	88	73
	2500	101	115
0.3 g/l	100	100	75
	2500	117	99

2.4 General discussion

Since different amounts of the 3S, 7S and 11S form are present at different pH, a different behaviour of the protein solutions with varying pH was to be expected. According to Wolf *et al.* (1958) at pH 6.7 (I=0.5 M) glycinin was in the 3S, 7S and 11S form for 0%, 3% and 57%, respectively (30% was present in a larger form than the 11S) and at pH 3 (I=0.01 M) for 70%, 27% and 0%, respectively. Experiments performed by us on FPLC [33] show that in a glycinin solution at pH 6.7 (30 mM) mainly the 11S form was present. This means that at pH 3 a mixture of the 3S and 7S forms will be present and at pH 6.7 mainly the 11S form. The ionic strength does not have a large influence on the conformation of glycinin in the 11S form at pH 6.7 so results for I=0.5 M can be compared with the ionic strength used in this report [34].

After short ageing times a large difference was observed in the interfacial rheological properties which can be explained mostly by the difference in adsorption behaviour. It is clear that this is due to the different molecular structure of glycinin present at different pH having different molecular size and affinity to adsorb at the air/water interface. The 3S/7S form gives a lower surface tension, a higher adsorbed amount, a higher dilational modulus and a higher apparent surface shear viscosity after shorter ageing times. However, after longer adsorption times the differences between the 3S/7S form and the 11S form seem to disappear. Wagner *et al.* [11] found that the equilibrium surface tension (after longer ageing times) was the same for all forms of glycinin despite the degree of deamidation/reduction. In Figure 2.3 the surface tensions of different glycinin solutions tend to go to the same value as well. More time is needed for pH 6.7, 0.01 g/l to retrieve the same surface tension. Looking at the adsorbed amount (Figure 2.4), Γ at pH 6.7 and concentration of 0.01 g/l is still increasing meaning that the end value has not been reached yet. The other protein solutions gave more or less the same Γ, although Γ at pH 3 and pH 6.7 (both 0.1 g/l) is still slowly increasing. This might be an indication for multi-layer formation. While the layer thickness of the pH 3 solutions and of pH 6.7 (0.01 g/l) stayed more or less the same after 1 hour, the layer thickness at pH 6.7, 0.1 g/l increased significantly from 8.3 nm at t=1 hour to 12 nm at t=5 hours.

Both adsorbed amount and apparent surface shear viscosity measurements were determined over long ageing times. The conclusion from these measurements is that the difference in behaviour of the different glycinin solutions disappears with ageing time. The apparent surface shear viscosity (see Figure 2.7) was almost the same for the 3S/7S and the 11S form after 24 hours whereas after shorter ageing time it differed clearly. The adsorption rate might play a role at the start of the measurement but the adsorbed amount reached a pseudo-equilibrium at around five hours. The apparent surface shear viscosity was then still increasing meaning that it is not the adsorbed amount alone that is important for the apparent surface shear

viscosity: both the 3S/7S and the 11S form are able to produce a network held together by interactions between the molecules. These interactions can be electrostatic or hydrophobic bonds or maybe even disulphide bridges. It seems that it is only a matter of time for the 11S form to create a network as strong as the 3S/7S form: enough protein has to adsorb at the interface and the protein needs to have time to unfold and rearrange itself.

To support our findings we propose a schematic model for the conformation of adsorbed glycinin at the air/water interface after short and long ageing times. In the beginning, the adsorbed AB subunits at pH 3 are probably evenly distributed along the surface. After longer ageing times, more molecules become adsorbed; the adsorbed amount and the layer thickness became more or less constant only after 4-5 hours. The layer thickness for the 3S/7S form found at the pseudo equilibrium of the adsorbed amount was 8.6 nm (±0.5 nm) and 7.7 nm (±0.5 nm) for concentrations of 0.1 and 0.01 g/l, respectively. A layer thickness of around 8 nm coincides with the diameter of an A and B unit together (see Figure 2.1A). This could mean that a kind of layer of AB subunits perpendicular to the surface is formed. It is not known whether the A or B subunit has a higher affinity to adsorb at the interface and therefore it is only speculative to say that primarily the more hydrophobic basic subunits will be at the interface.

The 11S form (at short ageing times) could adsorb in two different ways at the interface, with the hexameric rings perpendicular (thickness of molecule ~11 nm) or parallel (layer thickness of the molecule ~ 7.5 nm) to the surface. The layer thickness (concentration 0.1 g/l) increases from 8.3 (t=1 hour) to 12 nm (t=5 hours). Comparing these numbers to the size of the 11S form (see Figure 2.1A) this could mean that at short ageing times the molecule is situated with the hexameric rings parallel to the surface whereas later on the hexameric rings have moved to a perpendicular position. The reason why the 3S/7S and the 11S forms show similar behaviour after longer ageing times could be that then the adsorbed layers consist of close packed subunits. The rearrangement and the formation of intermolecular bonds just takes more time for the 11S form.

Though both the 3S/7S and the 11S form are able to form a network of comparable strength after longer ageing times, the protein films behave differently when characterising them more precisely. With the apparent surface shear viscosity measurements it was observed that on ageing the stress needed to fracture the 3S/7S protein film increased while its relative deformation at fracture was about constant; for the 11S form both the stress and the relative deformation at the fracture point increased [31]. This means that at pH 3 the protein film became more brittle upon ageing but at pH 6.7 it became more tough/viscous.

2.5 Conclusions

Various interfacial rheological techniques show a difference in interfacial behaviour between the 3S/7S form and the 11S form of glycinin. These differences are most clear after short ageing times. The differences tend to disappear after longer ageing times. Due to the smaller molecular size and higher ability to unfold, the 3S/7S form adsorbs faster, has a higher surface concentration, a higher dilational modulus and a higher apparent surface shear viscosity after short ageing times. After long ageing times however, the apparent surface shear viscosity and the surface concentration are more or less the same for the 3S/7S form and the 11S form.

Concerning foaming properties, it can be concluded that with the protein concentrations used here, it is not possible to make foam with glycinin at pH 6.7. At pH 3 however, glycinin behaves as a good foaming agent. Because of the ability to form a strong network at the interface the 3S/7S form gives a foam which is stable against coalescence and drainage (especially at high concentrations), though disproportionation still occurs.

Acknowledgements

The authors would like to thank Reinhard Miller and Dimitri Grigoriev from the Max Planck Institute in Golm (Germany) for help with the ellipsometry measurements performed at their institute. Katja Grolle is kindly acknowledged for performing all the foaming experiments and for preparing other experiments and Erik ten Grotenhuis for help with developing the light transmission method.

References

1. Utsumi, S.; Matsumura, Y.; Mori, T. In: *Food proteins and their applications*; Ed. S. Damodaran and A. Paraf, Dekker; 1997.
2. Badley, R.A.; Atkinson, D.; Hauser, H.; Oldani, D.; Green, J.P.; Stubbs, J.M. *Biochim. Biophys. Acta* **1975**, *412*, 214-228.
3. Wolf, W.J. *J. Agric.Food Chem.* **1993**, *41*, 168-176.
4. Peng, I.C.; Quass, D.W.; Dayton, W.R.; Allen, C.E. *Cereal Chem.* **1984**, *61(6)*, 480-490.
5. Wolf, W.J.; Briggs, D.R. *Arch. Biochem. Biophys.* **1958**, *76*, 377-393.
6. Plietz, P.D., G.; Muller, J.J., Schwencke, K. *Eur. J. Bioch.* **1983**, *130*, 315-320.
7. Lakemond, C.M.M.; de Jongh, H.H.J.; Hessing, M.; Gruppen, H.; Voragen, A.G.J. *J. Agric.Food Chem.* **2000**, *48*, 1985-1990.
8. Kinsella, J.E. *J. Am. Oil Chem. Soc.* **1979**, *56*, 242-258.
9. Kim, S.H. **1985** PhD-thesis, Cornell University, USA.
10. Kim, S.H.; Kinsella, J.E. *J. Food Sci.* **1987**, *52*, 128-131.

11. Wagner, J.R.; Guéguen, J. *J. Agric.Food Chem.* **1995**, *43*, 1993-2000.
12. Wagner, J.R.; Guéguen, J. *J. Agric.Food Chem.* **1999**, *47*, 2173-2180.
13. Wagner, J.R.; Guéguen, J. *J. Agric.Food Chem.* **1999**, *47*, 2181-2187.
14. Liu, M.X.; Lee, D.S.; Damodaran, S. *J. Agric.Food Chem.* **1999**, *47*, 4970-4975.
15. Tanh, V.H.; Shibasaki, K. *J. Agric.Food Chem.* **1976**, *24*, 1117-1121.
16. Benjamins, J.; Cagna, A.; Lucassen-Reynders, E.H. *Colloids Surf. A* **1996**, *114*, 245-254.
17. Cagna, A.; Esposito, G.; Rivière, C.; Housset, S.; Verger, R. (1992),*33rd International Conference on Biochemistry of Lipids, Lyon*.
18. de Feijter, J.A.; Benjamins, J.; Veer, F.A. *Biopolymers* **1978**, *17*, 1759-1772.
19. Bergink-Martens, D.J.M. **1993** PhD-thesis, Wageningen Agricultural University, The Netherlands.
20. Boerboom, F.J.G. **2000** PhD-thesis, Wageningen University, The Netherlands.
21. Prins, A.; Boerboom, F.J.G.; van Kalsbeek, H.K.A.I. *Colloids Surf. A* **1998**, *143*, 395-401.
22. Dickinson, E.; Murray, B.S.; Stainsby, G. *J. Coll. Interface Sci.* **1985**, *106*, 259-262.
23. Dickinson, E.; Murray, B.S.; Stainsby, G. *Int. J. Biol. Macrom.* **1987**, *9*, 302-304.
24. Murray, B.S. **1987** PhD-thesis, University of Leeds, United Kingdom.
25. Ogden, L.G.; Rosenthal, A.J. *J. Coll. Interface Sci.* **1997**, *191*, 38-47.
26. Burgess, D.J.; Sahin, N.O. *J. Coll. Interface Sci.* **1997**, *189*, 74-82.
27. Ronteltap, L. **1989** PhD-thesis, Wageningen University, The Netherlands.
28. Durian, D.J.; Weitz, D.A.; Pine, D.J. *Science* **1991**, *252*, 686-688.
29. Bos, M.A.; Grolle, K.; Kloek, W.; van Vliet, T. **2002**, accepted for publ. in Langmuir.
30. Roth, S.; Murray, B.S.; Dickinson, E. *J. Agric.Food Chem.* **2000**, *48*, 1491-1497.
31. Martin, A.H.; Bos, M.A.; Cohen Stuart, M.A.; van Vliet, T. *Langmuir* **2002**, *18*, 1238-1243.
32. Yu, M.; Damodaran, S. *J. Agric.Food Chem.* **1991**, *39*, 1563-1567.
33. Bos, M.; Martin, A.; Bikker, J.; van Vliet, T. In: *Food Colloids, Fundamentals of Formulation*; Ed. E. Dickinson and R. Miller, Royal Society of Chemistry; 2001, 223-232.
34. Lakemond, C.M.M.; de Jongh, H.H.J.; Hessing, M.; Gruppen, H.; Voragen, A.G.J. *J. Agric.Food Chem.* **2000**, *48*, 1991-1995.

3 Conformational aspects of proteins at the air/water interface studied by Infra-Red Reflection Absorption Spectroscopy

AH Martin, MBJ Meinders, MA Bos, MA Cohen Stuart & T van Vliet
Langmuir (2003) accepted for publ.

ABSTRACT

From absorption spectra obtained with Infra Red Reflection Absorption Spectroscopy (IRRAS) it is possible to obtain information on conformational changes at a secondary folding level of proteins adsorbed at the air/water interface. In addition, information on protein concentration at the interface can be retrieved by means of spectral simulation. In this paper we studied the adsorption behaviour of β-casein, β-lactoglobulin and (soy) glycinin at the air/water interface and the conformational changes that may take place during adsorption. The adsorbed amount was determined as a function of time and the values found for the three proteins agree well with ellipsometry data. Only limited conformational changes in terms of secondary structure were found. Upon adsorption at the air/water interface loss of β-sheet structure was observed for β-lactoglobulin whereas the amount of unordered structure increased. For glycinin (pH 3) aggregation at the interface was observed by the appearance of an absorption band at 1630 cm^{-1}, which involves the formation of β-sheet structures. For β-casein no conformational changes were observed at all. By comparison of IRRAS spectra of adsorbed and spread protein layers it was found that spreading of protein at an air/water interface leads to a conformational state that is somewhat different from that when adsorbed from solution.

3.1 Introduction

Protein adsorption can contribute in different ways to the stabilisation of colloidal systems such as foams and emulsions. In addition to surface tension reduction, steric and electrostatic interactions and the formation of a visco-elastic film, also conformational changes or structural rearrangements are thought to be relevant for the stabilisation of interfaces. The latter, however, have been studied to a much lesser extent. Moreover, information on conformational changes are mostly deduced from adsorption experiments relating surface excess, surface pressure and protein layer thickness to protein molecular dimensions [1-3]. These studies suggest that adsorption of globular proteins at the air/water interface results in partial unfolding of the protein structure. However, no conclusions could be drawn about the extent to which protein unfolding takes place in terms of secondary or tertiary structures.

The degree of conformational change will depend on the protein and its local environment. Also, the type of interface appears to have considerable effects on denaturation of adsorbed protein layers [4]. Only a few studies report on direct measurement of protein conformational changes upon adsorption at solid interfaces [4-6], the oil/water interface [6,7] or the air/water interface [8-10]. It is suggested from adsorption studies that proteins are more unfolded at the oil/water interface than at the air/water interface, but this has not been confirmed yet by direct measurements [1,11]. For solid interfaces major differences in conformational changes were found depending on whether the surface was hydrophilic or hydrophobic [4].

In the studies mentioned above, the techniques most commonly used to directly study conformational changes of proteins upon adsorption are Fourier Transform InfraRed in combination with Attenuated Total Reflection spectroscopy (FTIR-ATR) or InfraRed Reflection Absorption Spectroscopy (IRRAS) with or without Polarisation Modulation (PM-IRRAS). ATR and transmission IR spectroscopy, in combination with band shape analysis of the amide I region of the absorption spectra, have already been used extensively to study protein conformations in terms of secondary and tertiary structure [4,5,7,12]. In the past IRRAS has been applied to monolayers containing fatty acids [13], lipids [14] and proteins [6,10,14-19]. Recently, Meinders *et al*. [9] showed that in combination with spectral simulation it is also possible to determine the protein concentration and conformation in thicker adsorbed interfacial layers. The advantage of IRRAS over FTIR-ATR is that one can obtain information online on protein conformation and insight in the molecular structure of the layer, as shown recently by Meinders *et al*. [9] and Martin *et al*. [19]. In combination with spectral simulation it is possible to determine the protein concentration and conformation in an adsorbed layer at the interface.

As discussed above, most studies focus either on the adsorption properties or on the conformational changes of proteins at interfaces. We aim to determine these properties simultaneously using IRRAS. The purpose of this study is to compare the adsorption properties of β-casein, β-lactoglobulin and (soy) glycinin and the conformational changes that may take place during adsorption at an air/water interface. This combination of measuring surface pressure, determining the adsorbed amount and recording IRRAS spectra simultaneously has not been used before. In addition to adsorbed protein layers, also spread layers will be studied in order to determine whether the difference in behaviour between adsorbed and spread films lies in the degree of unfolding of the protein in the surface as postulated by literature [1,20].

3.2 Material & Methods

3.2.1 Materials

β-Lactoglobulin was purified according to the method of de Jongh *et al*. [21]; β-casein was purified from acid-precipitated casein following the method described by Swaisgood [22]. Glycinin was isolated from soybeans according to Tanh and Shibasaki [23] and further prepared as described by Martin *et al*. [24].

The purified proteins were dissolved in a phosphate buffer of pH 6.7 (ionic strength 30 mM). Glycinin was also studied at pH 3 (citric acid/phosphate buffer). The chemicals used for the buffer, Na_2HPO_4, NaH_2PO_4 and $C_6H_8O_7 \cdot H_2O$ were purchased from Merck (Darmstadt, Germany, analytical grade). All solutions were made with doubly distilled water and stirred for 1 h before use. Temperature was kept at 23°C. For both the IRRAS and the ellipsometry measurements a protein concentration of 0.1 g/l was used.

3.2.2 IRRAS

Experimental

IRRAS spectra were acquired using an Equinox 55 Fourier Transform InfraRed (FTIR) spectrometer (Bruker) attached to an IRRAS accessory (XA500) equipped with a broadband MCT detector by collecting the external reflected light beam. The IRRAS accessory contained a Langmuir trough (NIMA Technology) consisting of two separate compartments, one for the buffer (length × width = 26 × 5 cm) and the other for the protein solution (length × width = 26 × 10 cm). The volumes of the buffer and protein solutions were 200 ml and 400 ml, respectively. The spectrometer was continually purged with dry air.

FTIR-spectra were acquired from 1000 cm^{-1} to 5000 cm^{-1} using s-polarised light. Data were collected at 2 cm^{-1} resolution; typically 100 scans (scanning velocity 20 kHz) were averaged. The angle of incidence was 30°. Buffer was used as

background and the IRRAS spectrum was corrected (if necessary) for water vapour contributions by subtracting a water vapour spectrum. After data acquisition and water subtraction the spectrum was smoothed to 8 cm^{-1} resolution.

ATR spectra were collected on a Biorad FTS6000 equipped with a broadband MCT detector using a Ge crystal (45°, trapezoid, six internal total reflections).

Measurements were performed at room temperature. The Langmuir-trough and IRRAS equipment were placed in a Perspex box to keep out the dust and to create a constant atmosphere. Spectra were acquired every 15 minutes for a period of 8 hours.

For the experiments with adsorbed protein layers, the protein solution was poured into the Langmuir trough and before a measurement was started the surface was cleaned by suction of the compressed surface. Spread protein layers were made according to the method as described by Trurnit [25,26]. About 200 μl of a 0.1 g/l protein solution was applied to the top of a roughened and wetted glass rod (diameter 1 cm) protruding 10 cm from the buffer solution. According to Trurnit these conditions should give an optimum spreading result.

Spectral simulations

The reflectivity of a sample R is defined as the ratio of the specularly reflected light intensity I_R and the incident intensity I_0, ($R=I_R/I_0$). It is a function of the wavenumber, the angle of incidence, the polarisation of the incoming light and the optical properties of the material measured. The latter is described by the complex refractive index $\hat{n}$, which consists of a real part, the refractive index n, and an imaginary part, the extinction coefficient k. The extinction coefficient is related to the absorption coefficient $\alpha = 4\pi \cdot k/\lambda$ (with λ the wavelength of the incoming light) which is measured in ATR and transmission experiments. The optical properties are directly related to the protein concentration, conformation and orientation [9].

IRRAS spectra are presented as $-\log (R/R_{ref})$, where R is the IR reflection spectrum of the sample (the aqueous protein solution) and R_{ref} is that of the reference (buffer). We simulated IRRAS spectra using an ATR spectrum of a dried protein film, which is proportional to the absorption coefficient α of the protein. The optical constants of H_2O were taken from literature [27]. A detailed description of the simulation method, in which a single homogeneous layer model is used, has been published by Meinders *et al.* [9]. Fit parameters are the proportionality constant relating the protein ATR spectrum and the protein absorption coefficient, the concentration of the protein in the adsorbed layer (c_1) and the sublayer (c_2) and the thickness of the adsorbed layer (d). The thickness of the sublayer is taken to be infinite (probing depth ~500 nm).

3.2.3 Ellipsometry

Ellipsometry measurements were performed at the Colloid and Interface Science Group at the Max Planck Institute (Golm, Germany). A null-ellipsometer (Optrel) was used. Calculations were done with the program 'Ellipsometry' (version 1.31, 1997) (courtesy of Plamen Petrov).

The angle of incidence used was 50° and the wavelength was set at 532 nm. From the change in ellipsometric angles Δ and Ψ the layer thickness and the refractive index were calculated supposing that the protein density profile could be described by a stratified layer model. For the refractive-index increment, dn/dc, of protein solutions 0.18 cm^3/g was taken [28].

Before measurements were started the surface was cleaned by suction of the air/water interface. As reference solution pure buffer was used. Temperature was kept constant at 22 °C.

3.2.4 Circular Dichroism

Far-UV circular dichroism (CD) spectra of protein solutions containing approximately 0.1 mg/ml of glycinin or β-lactoglobulin in phosphate buffer (pH 6.7 or pH 3) were recorded on a Jasco J-715 spectrapolarimeter (Jasco Corp. Japan) at 20°C. Quartz cells with a path length of 0.1 cm were used. The scan interval for far-UV CD was 190-260 nm. Recorded spectra are averages of 16 spectra using a scan speed of 100 nm/min, a bandwidth of 1 nm, a response time of 125 ms and a step resolution of 0.5 nm. The spectra were corrected for the corresponding protein-free sample. Far-UV CD spectra were analysed for α-helix and β-sheet content of the proteins using a non-linear least squares fitting procedure as described previously by de Jongh *et al*. [29].

3.3 Results & Discussion

Adsorption kinetics

IRRAS spectra were recorded as a function of time for adsorbed layers of β-casein (pH 6.7), β-lactoglobulin (pH 6.7) and glycinin (both at pH 3 and pH 6.7). In Figure 3.1 IRRAS spectra are displayed from 1900 to 1300 cm^{-1} for β-lactoglobulin (0.1 g/l); in this region the amide I and amide II bands are present. The amide I band (1600-1700 cm^{-1}) represents the C=O bond in the protein and from the shape the geometry of the backbone of the polypeptide chain can be determined; the amide II band (1500-1600 cm^{-1}) is a combination of C-N and N-H bonds [12]. At t=0 the surface was cleaned; no protein was present, resulting in a zero intensity of the IRRAS spectrum. The intensity of the amide I and amide II bands grew with time indicating adsorption of protein and, hence, an increase in the protein concentration

in the surface layer. After 2 hours, the intensity of the peaks hardly changed anymore indicating that the maximum adsorbed amount had been reached. For β-casein and glycinin (both pH's) similar adsorption behaviour was obtained, except that β-casein adsorbed much faster and reached a steady state in intensity in much less time. By means of spectral simulation information on the protein concentration c_1 (mg/ml) and layer thickness d (nm) can be retrieved from the IRRAS spectra. Because the wavelength used is large compared to the thickness of the protein layer, it is difficult to uncouple c_1 and d (especially at short time scales when the experimental error is large due to the low intensity). Therefore we use, as is often done in ellipsometry [28], the adsorbed amount Γ (mg/m^2), which is equal to $c_1 \times d$ and can be determined accurately. At longer time scales the accuracy of c_1 and d increases and reasonable values could be found for both c_1 and d [19].

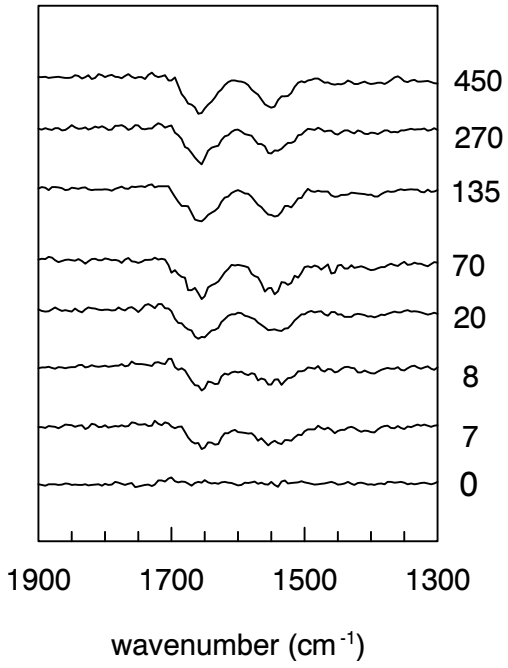

Figure 3.1 Experimental IRRAS spectra in the amide I and amide II region of β-lactoglobulin (0.1 g/l, pH 6.7) at the air/water interface as a function of time (indicated in minutes); offsets are given for clarity

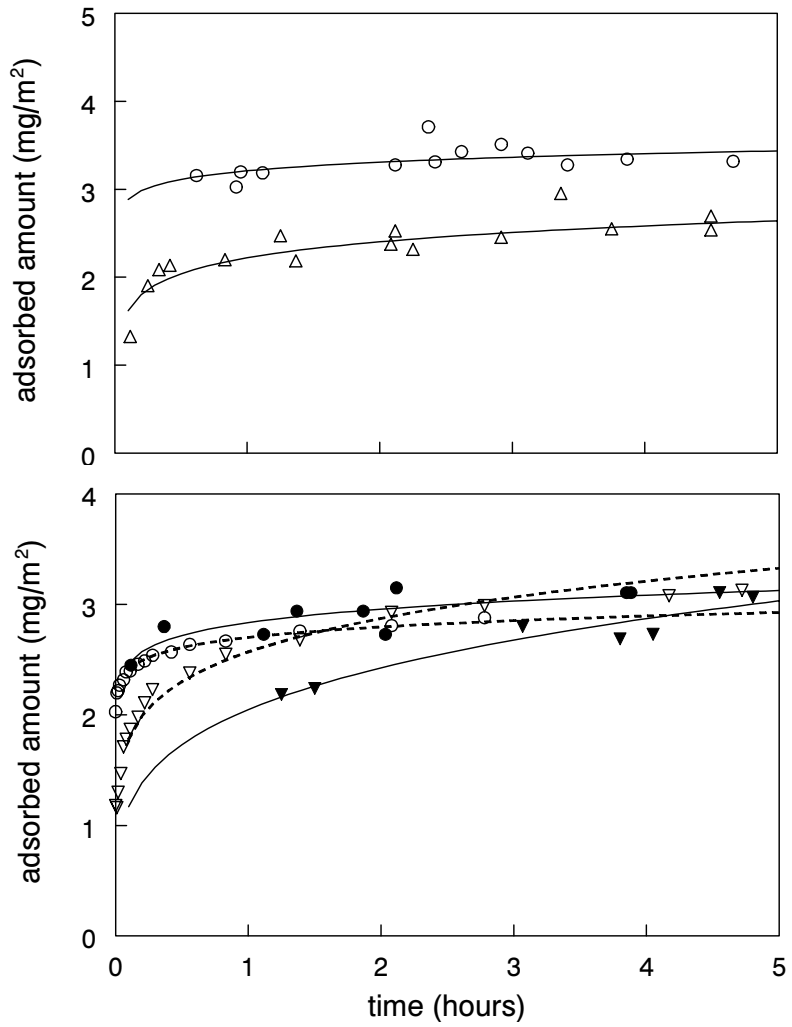

Figure 3.2 Upper panel: Adsorbed amount Γ (mg/m^2) as a function of time for ($\circ$) β-casein (0.1 g/l) and (Δ) β-lactoglobulin (0.1 g/l) ; Lower panel: a comparison between IRRAS (closed symbols) and ellipsometry (open symbols) of the adsorbed amount (mg/m^2) for glycinin (0.1 g/l); (∇) glycinin (pH 6.7), ($\circ$) glycinin (pH 3)

In Figure 3.2 (upper panel) Γ is shown as a function of time for β-casein and β-lactoglobulin as determined by IRRAS; in the lower panel Γ is compared with values determined by ellipsometry for glycinin (pH 3 and pH 6.7). Generally, the rate of initial increase in Γ increased in the following order: glycinin (pH 6.7) < β-lactoglobulin < glycinin (pH 3) < β-casein. This order coincides more or less with the order of decreasing protein molecular mass, which is 350, 37 (dimer at pH 6.7), 44, and 24 kDa for glycinin (pH 6.7), β-lactoglobulin, glycinin (pH 3) and β-casein, respectively. It also agrees with the order of increasing adsorption rate as determined by the rates of decrease in surface tension as shown previously by Martin *et al*. [30]. For glycinin (pH 3) Γ corresponds very well for the different

methods used; for pH 6.7 the values determined with IRRAS were lower than with ellipsometry at short time scales but at longer time scales similar adsorbed amounts were found. Moreover, at long time scales the adsorbed amount for pH 3 and pH 6.7 is about the same. Various interfacial rheological techniques show differences in behaviour of glycinin pH 3 and pH 6.7 at short time scales but similar behaviour after longer ageing times [24]. The adsorbed amounts obtained for β-casein and β-lactoglobulin correspond well to data obtained with neutron reflection and ellipsometry [31-33].

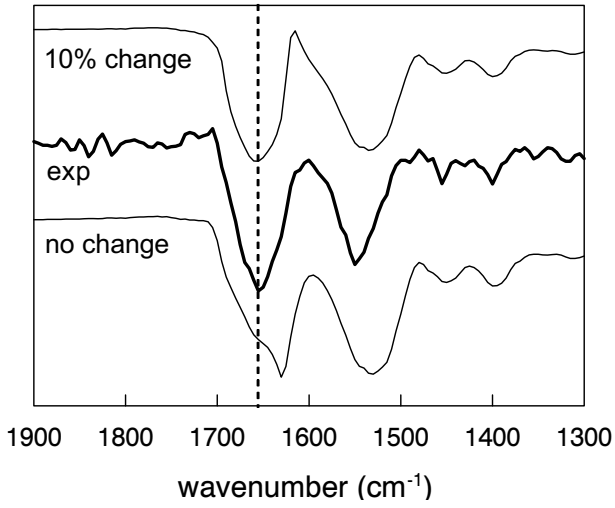

Figure 3.3 Experimental IRRAS spectrum (exp) in the amide I and II region of β-lactoglobulin (0.1 g/l, pH 6.7) and simulated spectra with (upper curve) and without (lower curve) taking a conformational change into account; conformational change is 10 ± 3% β-sheet to random coil

Conformational changes

In addition to information on the adsorption properties, IRRAS is able to give information on protein conformational state on a secondary folding level. We followed the change in conformation during adsorption of β-casein, β-lactoglobulin and glycinin at the air/water interface. For β-casein, a random-coiled protein, no conformational changes on a secondary folding level were detected nor upon adsorption nor as a function of time. For β-lactoglobulin, however, we detected a change in the shape of the amide I band which indicates structural changes in secondary protein structure. Spectral simulation reveals that only limited conformational changes take place: upon adsorption at the air/water interface a conformational change of $10 \pm 3\%$ from β-sheet to random coil was found. In Figure 3.3, an experimental IRRAS spectrum of

β-lactoglobulin is shown together with two simulated spectra taking into account either no conformational change or a change of 10 ± 3% β-sheet to random coil. The best fit was obtained when the conformational change was taken into account. This is in good agreement with data of Meinders *et al*. [34] However, whereas these authors measured adsorbed protein layers only in a steady state, we followed the change in conformation as a function of time. We found that the entire conformational change already took place before t=7 minutes. This change in conformation did not alter during the time scale of the experiment (~8 hours). Moreover, after 2-3 hours the surface pressure, Π, and Γ reached stationary values and did not change upon further ageing meaning that no extensive rearrangements had taken place after an (apparent) steady state set in. It is not known if and to what extent conformational changes occur at longer time scales (> 8 hours) although various authors assume that conformational changes are slow processes [1,7,25,35]. For example, Fang *et al*. [7] followed the change in conformation for β-lactoglobulin upon adsorption at an oil/water interface by FTIR for over 72 hours and observed ongoing changes in secondary structure over the whole duration of the experiment. Similar to our results they found a loss in β-sheet structure and an increase in disordered structure. The extent to which conformational changes take place may depend on the type of interface as well as on the protein concentration in solution. It is expected that proteins are more unfolded at an oil/water interface than at the air/water interface [1,11], but this has not been confirmed experimentally yet. At relatively low protein solution concentration, more protein denaturation could take place, whereas at excess of protein there is little deformation from the native structure [7]. It is likely that the protein conformational state may differ between individual proteins; moreover, this will depend on the protein solution concentration. Meinders *et al*. [36] measured different concentrations of β-lactoglobulin and found that for a concentration of 10 mg/ml (and higher) no clear change in conformation could be distinguished on basis of the spectra, as was the case for a 0.1 g/l protein solution. Probably the interface is full rapidly and the proteins have no place or time to adopt a favourable conformational state. There were no reports, unfortunately, on concentrations lower than 0.1 g/l.

Glycinin (both pH 3 and 6.7) did not show such a change in conformation from β-sheet to random coil upon adsorption at the air/water interface. Ovalbumin, however, did behave similarly to β-lactoglobulin [8,37] and also showed a change of 10 ± 3% β-sheet to random coil upon adsorption at the air/water interface. In Table 3.1, the secondary structures of β-casein, β-lactoglobulin and glycinin are compared. Both β-lactoglobulin and ovalbumin contain a large amount of β-sheets and therefore the secondary structure of these proteins is probably more rigid than those of β-casein and glycinin. To adopt a favourable conformational state at the

air/water interface ovalbumin and β-lactoglobulin change secondary structure whereas the other proteins do not.

Unfortunately there is little or no information on changes in tertiary structure of proteins upon adsorption at the air/water interface. However, it is reasonable to expect that the change in tertiary structure will generally be considerably larger than the change in secondary structure upon adsorption at an air/water interface. It is believed that upon adsorption at the air/water interface probably no protein tertiary structure remains, although the conformation on secondary level is largely maintained [1,7].

Table 3.1 Secondary structures of β-casein, β-lactoglobulin [20,38], glycinin (pH 3 and pH 6.7) [39] and ovalbumin [37,40] in solution, determined by CD; α = α-helix, β = β-sheet, rc = random coil, turn = β-turn

	α	β	rc	turn
β-lactoglobulin	15%	55%	20%	10%
β-casein	10%	13%	60%	-
glycinin (pH 3)	41%	-	51%	8%
glycinin (pH 6.7)	67%	-	16%	17%
ovalbumin	35%	47%	-	-

For glycinin (pH 3), a very different change in the secondary structure was found. In the experimental IRRAS spectra of adsorbed glycinin (pH 3) layers, an absorbance band was found at 1630 cm^{-1}, which is assigned to the formation of intermolecular β-sheet structures. The appearance of the band at 1630 cm^{-1} is an indication for protein aggregation at the interface, probably induced by intermolecular β-sheet formation. Robert *et al*. [41] observed the appearance of the same absorbance band at 1620-1630 cm^{-1} upon heating of glycinin solutions at pH 7.6. After longer times of heating this absorbance band grew in intensity indicating the development of aggregates in the gel through intermolecular β-sheets. Work on interfacial gelation of proteins showed that glycinin (pH 3) forms much stronger networks at the air/water interface than for example β-lactoglobulin or ovalbumin [30]. Almost directly after adsorption a strong network is formed which can also be observed visually. Moreover, in foams made from a glycinin (pH 3) solution large aggregates were found as determined by Fast Protein Liquid Chromatography (FPLC) [42]. In Figure 3.4, an experimental IRRAS spectrum of an adsorbed layer of glycinin (pH 3) is shown in the amide I band region together with two simulated

spectra. The experimental data could be fitted very well by taking into account a conformational change of 10 ± 3% random coil to β-sheet. At pH 6.7 no β-sheet peak was found for glycinin. This could be related to the fact that glycinin forms a less strong network or interfacial gel at pH 6.7 than at pH 3 as confirmed by rheological experiments [24,30]. We did not observe a significant effect of ageing time of the adsorbed glycinin (pH 3) layer on intensity of the β-sheet peak. Recently, Renault and co-workers [8] found similar β-sheet formation for ovalbumin and correlated the development of an intermolecular β-sheet network with surface rheological properties. They questioned whether β-sheet formation was specific for ovalbumin; our data indeed show that this is also observed for glycinin (pH 3).

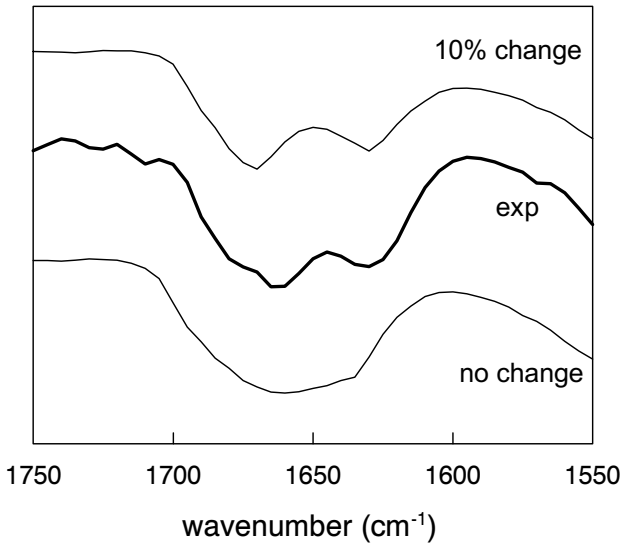

Figure 3.4 Experimental IRRAS spectrum (exp) in the amide I region of an adsorbed glycinin layer (0.1 g/l, pH 3) and simulated spectra taking into account no conformational change (no change) and a change of 10 ±3 % random coil to β-sheet (10% change)

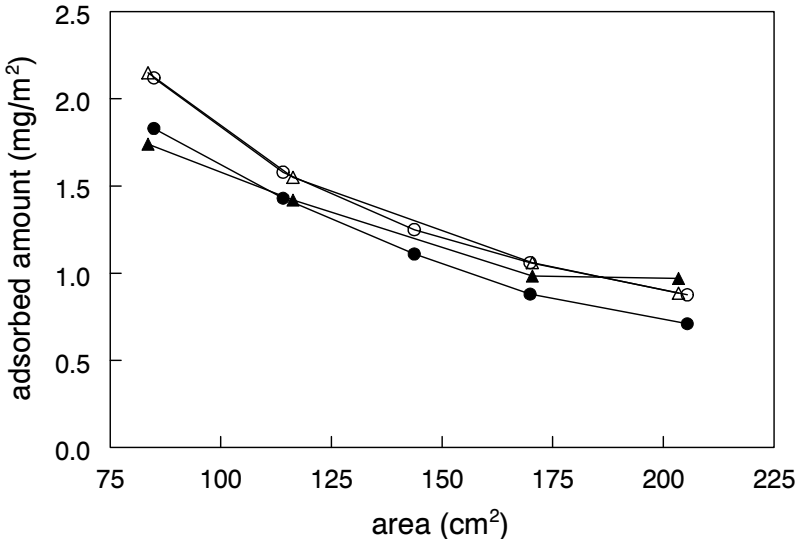

Figure 3.5 Adsorbed amount Γ (mg/m^2) as a function of area (cm^2) of a spread β-lactoglobulin layer (measured in duplo (▲), (●)); open symbols represent Γ_{spread}, the amount of protein spread on the surface; closed symbols represent $\Gamma_{simul.}$, the amount of protein simulated from the IRRAS spectra

Comparison of spread and adsorbed protein layers

Spread layers of β-lactoglobulin, β-casein and glycinin (pH 3) were made at a surface area of ~205 cm^2 by using the method described by Trurnit [26]. IRRAS spectra were recorded, and Γ was determined as a function of area. It was possible to acquire a good IRRAS spectrum at Γ as low as 0.9 mg/m^2 although the intensity of the amide I and II bands was very low. Upon compression of the surface the intensity of both the (negative-oriented) amide I and II bands and the (positive-oriented) water band at 3600 cm^{-1} increased. The increase in the amide I and II bands is due to an increase in protein concentration in the surface layer; the increase in the water band can be explained by the fact that the spectrum of the protein sample is measured relative to that of the protein free sample. It illustrates the depletion of water from the interface by the volume occupied by the protein. In Figure 3.5 we present Γ as determined by simulation of the IRRAS spectrum ($\Gamma_{simul.}$) as well as Γ calculated from the amount of protein spread on the surface (Γ_{spread}); both are given as a function of area, and for two different spread layers of β-lactoglobulin. It appears that $\Gamma_{simul.}$ is consistently 10-20% lower than Γ_{spread}. We assume that during spreading some protein went into solution because the spreading behaviour varies with the kind of protein studied. For glycinin (pH 3) the difference between Γ_{spread} and $\Gamma_{simul.}$ was somewhat larger than for β-lactoglobulin and β-casein. Anyhow, simulation of IRRAS

spectra from spread protein layers shows that IRRAS is able to measure quite low quantities of protein present at the air/water interface.

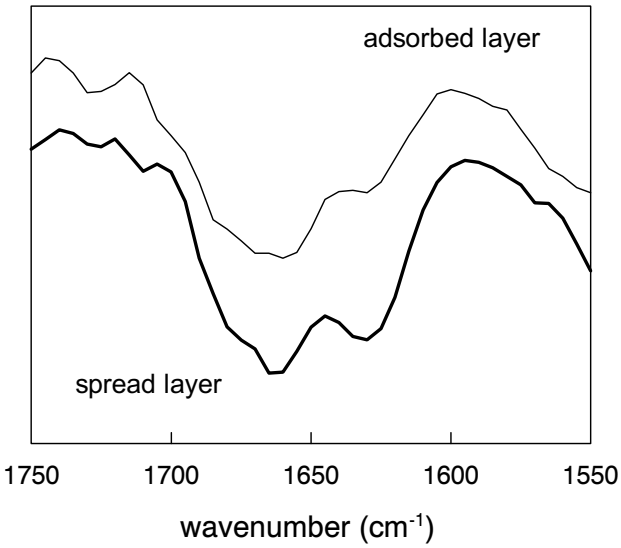

Figure 3.6 Experimental IRRAS spectrum of an adsorbed glycinin layer (pH 3, 0.1 g/l) and a spread glycinin layer (pH 3); in both cases the adsorbed amount is 2.5 mg/m ^{2}

Whereas spread protein layers have to be compressed to reach a Γ of ~2.5 mg/m^2, adsorbed layers can usually attain similar adsorbed amounts without compression. In Figure 3.6 experimental IRRAS spectra are given for a spread and an adsorbed glycinin (pH 3) layer. Both layers contain the same amount of protein (Γ~2.5 mg/m^2) but Π is higher for the compressed, spread layer than for the adsorbed layer. In both spectra, a β-sheet peak at 1630 cm^{-1} is present, but the intensity in the spread layer is higher. Figure 3.4 already shows that glycinin (pH 3) forms β-sheet structures when adsorbed at the air/water interface. The conformational change obtained by spectral simulation was 10 ± 3% random coil to β-sheet. For a spread layer the IRRAS spectrum was best fitted taking into account a conformational change of 15 ± 3% from random coil to β-sheet. Since these changes in conformation are generally relatively small, a difference of 5% is considerable. The difference in β-sheet formation between spread and adsorbed layers could be related to the compression of the spread layer. However, upon compression of an adsorbed layer of glycinin (pH 3) no further increase in the intensity of the absorption band at 1630 cm^{-1} was observed whereas the intensity in amide I and II did increase. This is in spite of the fact that upon compression of either a spread or an adsorbed layer Π (mN/m) reached similar values. Apparently, glycinin (pH 3) in spread layers is in a

conformational state somewhat different from that in adsorbed layers, even though Γ is the same for both layers. To check whether the formation of β-sheets was reversible upon expansion, three compression-expansion cycles were performed. It appeared that during this cycle the absorption band at 1630 cm^{-1} remained, meaning that the formation of β-sheet structures is not reversible upon expansion of the surface.

Neither β-lactoglobulin nor β-casein showed any form of aggregation at the interface upon compression for either spread or adsorbed layers: no β-sheet formation due to aggregation was found for these proteins. However upon compression of a spread β-lactoglobulin layer, we observed clear shifts in the amide I band. Performing a stepwise compression we observed that at a certain area (and therefore at a certain Π) the amide I band shifts to lower wavenumber. In Figure 3.7 experimental IRRAS spectra are shown of (A) an adsorbed β-lactoglobulin layer, (S) a spread layer at an area of ~205 cm^2 and (C) a compressed, spread layer at an area of ~125 cm^2. Upon compression of the spread layer the maximum of the amide I band is shifted from 1660 to 1650 cm^{-1}. By means of spectral simulation it was found that β-lactoglobulin is ~5% less unfolded in a compressed spread layer (Γ ~ 1.4 mg/m^2) than in an uncompressed spread layer (Γ ~ 0.9 mg/m^2). The maximum of the amide I band for an adsorbed layer (Γ ~ 2.5 mg/m^2) is found at 1655 cm^{-1} (thus at lower wavenumber than for a spread layer). The difference between a spread and an adsorbed layer could indicate that β-lactoglobulin is less condensed in a spread layer than when adsorbed from solution. This might, however, depend on the protein concentration used. Upon compression of the adsorbed layer no shift in amide I band was observed. In conclusion, it appears that the conformational state of β-lactoglobulin differs between spread and adsorbed layers like that of glycinin (pH 3). Likely, β-lactoglobulin is somewhat more unfolded in a dilute spread layer but upon compression the protein rearranges itself again. Upon expansion (followed by a compression-expansion cycle) no changes were found in the position and shape of the amide I band, meaning that the rearrangement that took place during the first compression (see Figure 3.7) of a spread β-lactoglobulin layer is not reversible.

Our results agree very well with what is postulated in literature by Graham and Phillips [1]. They expected that the difference in behaviour between adsorbed and spread films lies in the degree of unfolding of the protein in the surface.

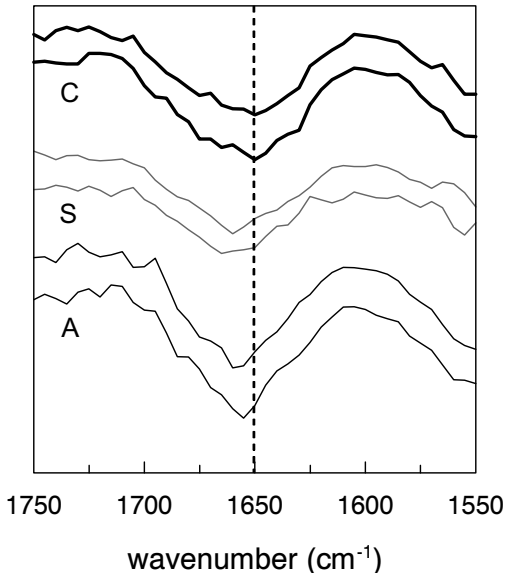

Figure 3.7 Experimental IRRAS spectra (duplicate measurements) in the amide I region of (A) adsorbed β-lactoglobulin layers, (S) spread β-lactoglobulin layers at an area of ~205 cm^2 and (C) spread β-lactoglobulin layer after compression to an area of ~125 cm^2

3.4 Conclusions

The combination of measuring surface pressure, determining the adsorbed amount and recording IRRAS spectra simultaneously has not been studied before. It can be concluded that this gives new insight in the adsorption process of proteins at the air/water interface. IRRAS spectra not only reveal changes in protein conformation upon adsorption at the air/water interface but also give access to the protein concentration at the interface by means of spectral simulation. Differences were found in the adsorption rate among β-casein, β-lactoglobulin and glycinin (pH3 and pH 6.7). These results agree well with our own ellipsometry data and with other data from literature, thus showing that IRRAS is able to determine the adsorbed amount correctly.

The conformational change was found to be limited to only 10-15% in terms of secondary protein structure. For β-lactoglobulin a change of 10 ± 3 % β-sheet to random coil was detected upon adsorption at the air/water interface whereas β-casein and glycinin (pH 3 or pH 6.7) showed no such change in conformation. For adsorbed glycinin (pH 3) layers, β-sheet formation was observed indicating aggregation of the protein at the interface. This agrees with the formation of a strong protein network that one detects interfacial rheological experiments. At pH 6.7 no β-sheet formation was observed for glycinin and this may be related to the fact that glycinin has poorer network forming properties at pH 6.7. From comparison of

adsorbed layers of β-casein, β-lactoglobulin and glycinin in terms of conformational changes, it can be concluded that each protein behaves differently depending on its flexibility and internal structure.

Spreading of protein at an air/water interface (at low Π) leads to a conformational state that is somewhat different from that obtained by adsorption from solution. For β-lactoglobulin a difference in the position of the maximum peak of the amide I band was observed between a spread layer, a compressed spread layer and an adsorbed layer. It was found that upon spreading β-lactoglobulin assumes an unfolded state; upon compression, however, the protein rearranges itself to a less unfolded state. In an adsorbed layer, the conformational state of β-lactoglobulin is intermediate between that of a spread and a compressed spread layer meaning that β-lactoglobulin is less unfolded than in a spread layer. For glycinin (pH 3) differences in state of aggregation were found between a compressed spread layer and an adsorbed layer while both layers had similar adsorbed amounts. Upon compression of a spread layer more β-sheet structures were found indicating a more aggregated protein layer. This means that before compression the spread layer contained glycinin (pH 3) in such a conformational state that it was possible to form more intermolecular β-sheet structures upon compression. Moreover, upon compression of an adsorbed glycinin (pH 3) layer no further increase in β-sheet formation was found in comparison with the original adsorbed layer.

Acknowledgements

The authors would like to thank Harmen de Jongh and Peter Wierenga (Wageningen Centre for Food Sciences) for valuable discussions. Also Dimitri Grigoriev and Reinhard Miller (Max Planck Institute, Golm, Germany) are kindly acknowledged for their help with the ellipsometry measurements.

References

1. Graham, D.E.; Phillips, M.C. *J. Coll. Interface Sci.* **1979**, *70*, 427-439.
2. Lu, J.R.; Su, T.J.; Thomas, R.K.; Penfold, J.; Webster, J. *J. Chem.Soc.Far.Trans.* **1998**, *94*, 3279-3287.
3. Clark, D.C.; Smith, L.J.; Wilson, D.R. *J. Coll. Interface Sci.* **1988**, *121*, 136-147.
4. Green, R.J.; Hopkinson, I.; Jones, R.A.L. *Langmuir* **1999**, *15*, 5102-52110.
5. Ball, A.; Jones, R.A.L. *Langmuir* **1995**, *11*, 3542-3548.
6. Zangi, R.; de Vocht, M.L.; Robillard, G.T.; Mark, A.E. *Biophys. J.* **2002**, *83*, 112-124.
7. Fang, Y.; Dalgleish, D.G. *J. Coll. Interface Sci.* **1997**, *196*, 292-298.
8. Renault, A.; Pezennec, S.; Gauthier, F.; Vié, V.; Desbat, B. *Langmuir* **2002**, *18*, 6887-6895.

9. Meinders, M.B.J.; van den Bosch, G.G.M.; de Jongh, H.H.J. *Eur. Bioph. J.* **2000**, *30*, 256-267.
10. de Vocht, M.L.; Scholtmeijer, K.; van der Vegte, E.W.; de Vries, O.M.H. *Biophys. J.* **1998**, *74*, 2059-2068.
11. Murray, B.S. *Colloids Surf. A* **1997**, *125*, 73-83.
12. Goormaghtigh, E.; Cabiaux, V.; Ruysschaert, J.-M. In: *Physicochemical methods in the study of biomembranes*; Ed. H.J. Hilderson and G.B. Ralston, Plenum Press; 1994, 329-450.
13. Dluhy, R.A.; Cornell, D.G. *J. Phys. Chem.* **1985**, *89*, 3195-3197.
14. Flach, C.R.; Prendergast, F.G.; Mendelsohn, R. *Biophys. J.* **1996**, *70*, 539-546.
15. Lavoie, H.; Desbat, B.; Vaknin, D.; Salesse, C. *Biochemistry* **2002**, *41*, 13424-13434.
16. Gallant, J.; Desbat, B.; Vaknin, D.; Salesse, C. *Biophys. J.* **1998**, *75*, 2888-2899.
17. Gericke, A.; Flach, C.R.; Mendelsohn, R. *Biophys. J.* **1997**, *73*, 492-499.
18. Boncheva, M.; Vogel, H. *Biophys. J.* **1997**, *73*, 1056-1072.
19. Martin, A.H.; Meinders, M.B.J.; Bos, M.A.; Cohen Stuart, M.A.; van Vliet, T. In: *Food Colloids, Biopolymers & Materials*; Ed. E. Dickinson and T. van Vliet, Royal Society of Chemistry; 2003.
20. Mackie, A.R.; Gunning, A.P.; Wilde, P.J.; Morris, V.J. *J. Coll. Interface Sci.* **1999**, *210*, 157-166.
21. de Jongh, H.H.J.; Gröneveld, T.; de Groot, J. *J. Dairy Sci.* **2001**, *84*, 562-571.
22. Swaisgood, H.E. In: *Developments in Dairy Chemistry-1*; Ed. P.F. Fox, Applied Science Publ.; 1982, 1-57.
23. Tanh, V.H.; Shibasaki, K. *J. Agric.Food Chem.* **1976**, *24*, 1117-1121.
24. Martin, A.H.; Bos, M.A.; van Vliet, T. *Food Hydrocoll.* **2002**, *16*, 63-71.
25. van Aken, G.A.; Merks, M.T.E. *Colloids Surf. A* **1996**, *114*, 221-226.
26. Trurnit, H.J. *Journal of Colloid Science* **1960**, *15*, 1.
27. Bertie, J.E.; Ahmed, M.K.; Eysel, H.H. *J. Phys. Chem.* **1989**, *93*, 2210-2218.
28. de Feijter, J.A.; Benjamins, J.; Veer, F.A. *Biopolymers* **1978**, *17*, 1759-1772.
29. de Jongh, H.H.J.; Goormaghtigh, E.; Killian, J.A. *Biochemistry* **1994**, *33*, 14521-14528.
30. Martin, A.H.; Grolle, K.; Bos, M.A.; Cohen Stuart, M.A.; van Vliet, T. *J. Coll. Interface Sci.* **2002**, *254*, 175-183.
31. Atkinson, P.J.; Dickinson, E.; Horne, D.S.; Richardson, R.M. *J. Chem.Soc.Far.Trans.* **1995**, *91*, 2847-2854.
32. Benjamins, J. **2000** PhD-thesis, Wageningen University, the Netherlands.
33. Harzallah, B.; Aguié-Béghin, V.; Douillard, R.; Bosio, L. *Int. J. Biol. Macrom.* **1998**, *23*, 73-84.
34. Meinders, M.B.J.; de Jongh, H.H.J. *Biospectroscopy* **2002**, *67*, 319-322.
35. MacRitchie, F. In: *Proteins at Liquid Interfaces*; Ed. D. Möbius and R. Miller, Elsevier; 1998, 149-177.
36. Meinders, M.B.J.; van den Bosch, G.G.M.; de Jongh, H.H.J. *Trends in Food Sci. Techn.* **2000**, *11*, 218-225.
37. Kudryashova, E.V.; Meinders, M.B.J.; Visser, A.J.W.G.; van Hoek, A.; de Jongh, H.H.J. *submitted.*

38. Razumovsky, L.; Damodaran, S. *Langmuir* **1999**, *15*, 1392-1399.
39. Lakemond, C.M.M.; de Jongh, H.H.J.; Hessing, M.; Gruppen, H.; Voragen, A.G.J. *J. Agric.Food Chem.* **2000**, *48*, 1991-1995.
40. Dong, A.; Meyer, J.D.; Brown, J.L.; Manning, M.C.; Carpenter, J.F. *Arch. Biochem. Biophys.* **2000**, *338*, 148-155.
41. Robert, P.; Mangavel, C.; Renard, D. *Appl. Spectrosc.* **2001**, *55*, 781-787.
42. Bos, M.; Martin, A.; Bikker, J.; van Vliet, T. In: *Food Colloids, Fundamentals of Formulation*; Ed. E. Dickinson and R. Miller, Royal Society of Chemistry; 2001, 223-232.

4 Stress-strain curves of adsorbed protein layers at the air/water interface measured with surface shear rheology

AH Martin, MA Bos, MA Cohen Stuart & T van Vliet
Langmuir (2002) 18: 1238-1243

ABSTRACT

Interfacial shear properties of adsorbed protein layers at the air/water interface were determined using a Couette-type surface shear rheometer. Such experiments are often used to determine a steady state ratio between stress and rate of strain, which is then denoted as 'surface shear viscosity'. However, by measuring the stress on the protein layer as a function of time at a fixed shear rate, more information on the mechanical properties of the protein layers can be obtained. The development of the stress exerted on the inner disc with time was recorded. Initially the stress increased steadily with time, then it went through a maximum and next attained a steady-state value from which the surface shear viscosity is usually determined. Stress-strain curves can be calculated from the data obtained. Differences in the stress-strain curve were observed for the proteins studied (ovalbumin, β-lactoglobulin, and glycinin) and the shape of the stress-strain curve is discussed. The maximum in the stress-strain curve can be regarded as a kind of fracture/yield stress. This implies that the strain at the maximum is a fracture strain and the decrease in stress reflects a kind of breakdown of the protein film structure.

4.1 Introduction

Interfacial shear rheology of adsorbed protein layers is considered to be a useful technique to obtain information about the structural state of adsorbed layers of proteins and/or surfactants. Various authors assume that surface shear properties play an important role in the formation and stability of foams and emulsions [1-3]. The mechanical properties of adsorbed protein layers may have a substantial influence on the kinetics of processes such as coalescence, disproportionation or film rupture. Experiments have been reported which suggest that by creating a gel-like adsorbed film with a high resistance against shear around an emulsion droplet, droplet deformation and break-up are suppressed and droplet coalescence is retarded [4]. However, the evidence is not at all conclusive; there are also contrary results from experiments in which break-up of drops covered with β-lactoglobulin was not at all hindered by any resistance in shear [5].

Surface shear rheology of adsorbed protein layers appears to be very sensitive to the detailed macromolecular structure and to the nature of intermolecular interactions in the adsorbed layer. For example, modifying β-lactoglobulin by cleaving and blocking its disulphide bridges, leads to different surface shear rheological properties. The surface shear viscosity seems to be dependent on the type of interactions than can take place at the interface [6]. Heating of β-lactoglobulin after its adsorption onto an oil/water interface resulted in an increase in surface shear viscosity because heating accelerates the process of (disulphide) cross-link formation [1].

In literature various methods to determine shear properties of adsorbed layers have been described. Examples are the Couette-type viscometers [1,4,6-9] and double concentric ring viscometers [4,10] where the surface is continuously deformed at a constant shear rate. Other methods are the canal viscometer [11], a torsion pendulum apparatus designed by Krägel *et al.* [12], an interfacial stress rheometer with a magnetised floating rod constructed by Brooks *et al.* [13] and a Langmuir-trough method from Petkov and Gurkov [14]. It appears that there is no standardisation of the method. This makes data comparison difficult, all the more because not only different kinds of materials have been used for the disc or ring (e.g. glass [15], gold [16], platinum [10,16], stainless steel [1,9]), but also the discs or rings have different shapes (straight side or biconical), and the geometry of the apparatus varies.

Generally, two parameters are determined with surface shear rheology: the apparent surface shear viscosity, η^s_{app} (mN·s/m), and the surface shear modulus, G^s (mN/m). The apparent surface shear viscosity is usually determined by applying a constant shear rate to the adsorbed film, while the shear modulus is most frequently determined by oscillatory deformation or free oscillation. The advantage of the latter

methods is that only very small deformations of the surface are needed such as with the shear rheometer of Krägel *et al.* [12] and Benjamins [17]. This is in contrast with most methods determining surface shear viscosity.

In this work a Couette-type shear rheometer was used with a stainless steel disc and a glass dish in which the protein solution was contained. The purpose of this work was initially to determine the apparent surface shear viscosity of different adsorbed protein layers using a procedure described by other authors [8,10,18,19]. However, by measuring the stress exerted on the protein network as a function of time during which shear is applied (instead of taking the steady state stress value at the end of a shearing period only), we found that more information can be retrieved from these measurements than only η^s_{app}. The purpose of this paper is therefore also to discuss transients in surface shear experiments and the meaning of stresses and strains involved. The quantity referred to as 'surface shear viscosity' seems in many cases not to be a real (apparent) viscosity.

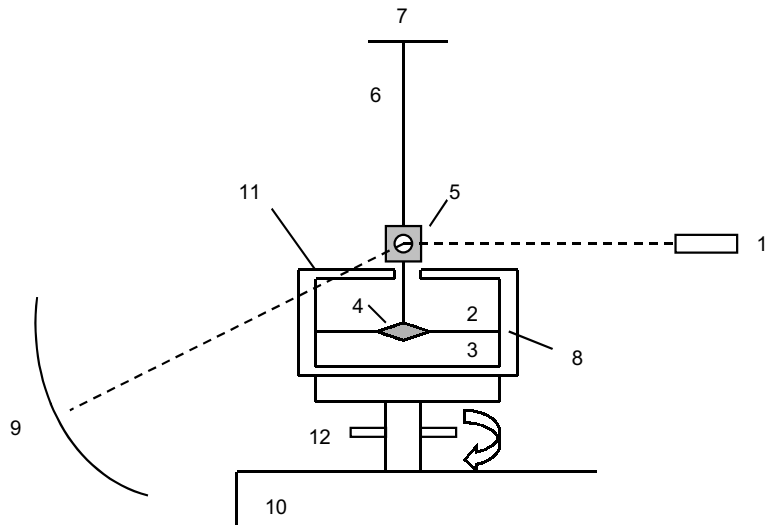

Figure 4.1 The set-up of the surface shear rheometer; 1, light source; 2, air; 3, protein solution; 4, biconical disc; 5, mirror; 6, torsion wire; 7, support for wire; 8, thermostatted water in water jacket; 9, circular scale; 10, vibration-free bench; 11, perspex lid; 12, coq for attachment to motor

4.2 Materials & Methods

4.2.1 The apparatus

The instrument used was a two-dimensional Couette-type interfacial viscometer described by Murray *et al.* (see Figure 4.1) [18-20]. Originally, a stainless steel biconical disc (diameter 30 mm) was used that was suspended from a (stainless steel) torsion wire with its edge in the plane of the air/water interface formed by the

protein solution and the air phase which were contained in a thermostated glass dish (diameter 145 mm, T=23°C). In addition, another (biconical) disc was used made of stainless steel and with a diameter of 55 mm. Moreover, in some of the experiments a smaller dish was used with a diameter of 78 mm. The additional disc and dish were used in the experiments to determine the shear modulus (see Results & Discussion).

By rotating the glass dish at a known angular velocity the liquid (surface) exerts a force on the edge of the disc so that it starts to rotate to an extent depending on the system being measured. On top of the disc there is a mirror on which a laser beam is projected. The reflected light beam is projected on a circular scale with a radius of 600 mm. The glass dish is driven by a stepper motor connected to a computer by which the rotational speed can be set.

4.2.2 Calculation of the data

The equations used for calculating surface shear viscosity were published by Murray [19]. On moving the dish with a certain speed, a torque τ will be exerted on the disc causing the disc to rotate over a certain angle:

$$\tau = \mathrm{K} \cdot \Theta_i \tag{4.1}$$

where K is the torsion wire constant and Θ_i (rad) is the angle of rotation of the disc. The torsion wire constant depends on the thickness, the elasticity of the material and the length of the wire used ($K \propto 1/L$). The torsion wire thickness used was 0.15 mm and its length was 740 mm.

The apparent interfacial shear viscosity, η^s_{app}, can be calculated as follows:

$$\eta^s_{app} = \frac{\tau}{4 \cdot \pi \cdot \Omega} \cdot \left(\frac{1}{R_i^2} - \frac{1}{R_o^2} \right) \tag{4.2}$$

where R_i en R_o are the radius of the disc and the dish, respectively; Ω is the angular velocity (rad/s) of the dish.

4.2.3 Measurements

For determining the stress exerted on the protein film, the film was subjected to intermittent shear at a steady state dish rotation speed of 1.27×10^{-3} rad/s until a steady-state stress was obtained, usually after 10-20 minutes. The angle of rotation of the bob was determined from the light beam reflected onto the scale. The deflection on the scale was determined every 10 seconds for 10-20 minutes. From the angle (Θ_i) the torque was calculated using eq. (4.1). According to Whorlow [21] the stress exerted on the disc is calculated as follows

$$\sigma = \frac{\tau}{2 \cdot \pi \cdot R_i^2} \tag{4.3}$$

Measurements were performed over an ageing period of 24 hours.

4.2.4 Reproducibility

Surface shear viscosity measurements are very sensitive to the history of the protein film and the way the film is prepared. The film was set up using a separatory funnel with a bent spout to easily let the protein solution flow in from the wall of the dish and therefore preventing foam formation. The dish is filled just until the surface touches the bob. In this way the experimental error for η^s_{app} is generally 5-10%.

4.2.5 Materials

β-Lactoglobulin was purified according to the method of de Jongh *et al.* [22]. Ovalbumin was obtained from Sigma (grade V). The proteins were dissolved in a phosphate buffer with pH 6.7. Glycinin (soy) was measured at pH 3 and prepared as described by Martin *et al.* [23]. The chemicals used for the buffer, Na_2HPO_4 and NaH_2PO_4, were purchased from Merck (Darmstadt, Germany, analytical grade). All solutions were made with doubly distilled water and stirred for 1 hour before bringing them into the apparatus. Temperature was kept at 23°C.

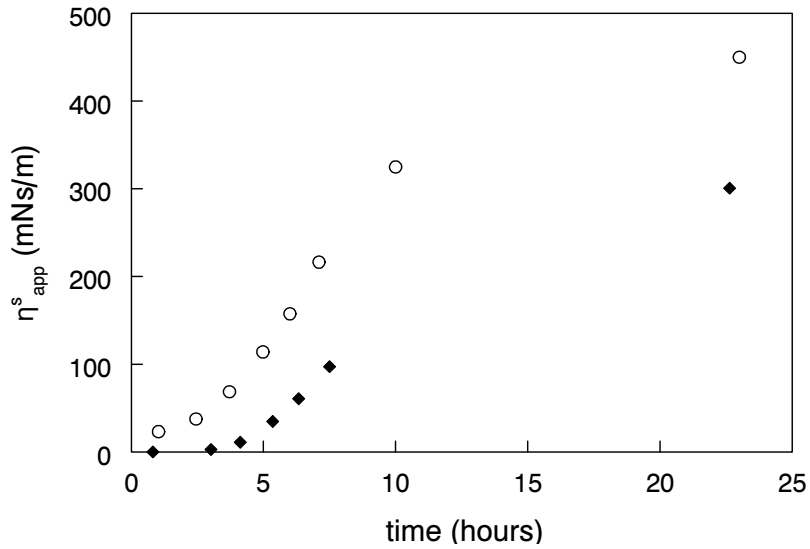

Figure 4.2 Apparent surface shear viscosity (mNs/m) of ovalbumin (0.1 g/l) and β-lactoglobulin (0.1 g/l) measured at pH 6.7 (I=30 mM); η^s_{app} was determined from the steady state stress value according to literature; (♦) ovabumin, (o) β-lactoglobulin

4.3 Results & Discussion

The apparent surface shear viscosity was determined according to the procedure described in literature [8,10,18,19]. Following the rotation of the disc with time, the angle of rotation reaches a steady state value after 10-20 minutes and from this value the apparent surface shear viscosity was calculated using eq. (4.2). In

Figure 4.2 η^s_{app} is given as a function of ageing time for β-lactoglobulin (0.1 g/l) and ovalbumin (0.1 g/l) at the air/water interface. For both proteins η^s_{app} increases during ageing of the protein network. Literature is not very extensive on surface shear viscosity data for adsorbed protein layers. Roth *et al.* [1] measured β-lactoglobulin (0.01 g/l) at different interfaces, also at the air/water interface and found η^s_{app} = 200 mN·s/m after 24 hours of ageing at this interface. Graham & Phillips [9] and Izmailova [15] also studied at the air/water interface but used other proteins than β-lactoglobulin and ovalbumin. Generally, η^s_{app} is lower at air/water interfaces than at oil/water interfaces. Because of the high concentrations used in this study, our results are comparable with those of the authors mentioned above.

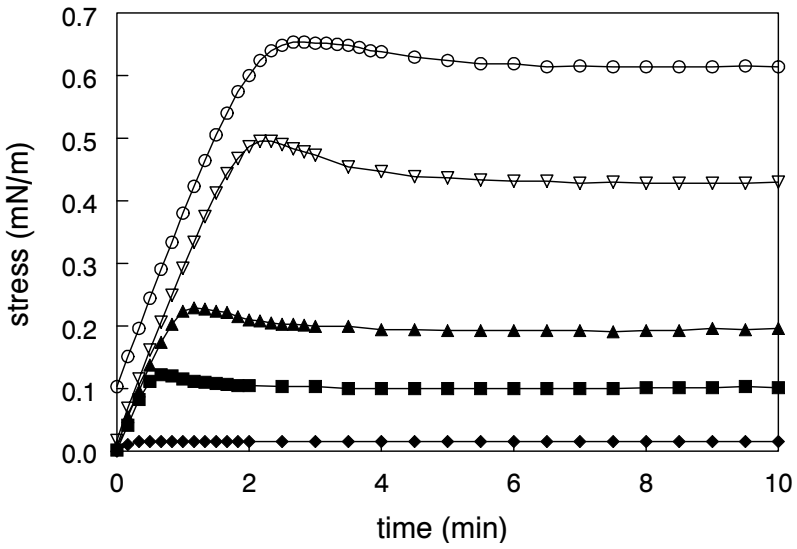

Figure 4.3 Development of stress exerted on the disc as a function of shearing time for β-lactoglobulin (0.1 g/l; pH 6.7, 30 mM) at different ageing times of the protein film; (♦) t=0h53, (■) t=2h30, (▲) t=3h53, (∇) t=5h53, (o) t=7h07

So far only the steady state stress value (used to determine η^s_{app}) was found to be important to characterise a protein network. However, when following the stress exerted on the disc with time, the following results are obtained. In Figure 4.3 the stress exerted on the disc for β-lactoglobulin is given as a function of time during which shear is applied, at five different ageing times of the protein layer. After 2-3 minutes a very well reproducible maximum is observed in the stress although the value of the stress at the maximum may vary somewhat (±10%). In bulk rheology such a maximum, known as a stress-overshoot, is also quite often observed for comparable experiments. A higher maximum stress represents a higher strength

of the protein layer; during ageing the protein film becomes stronger. After the maximum, the stress decreases slightly to a constant value.

For a further analysis of the curves, the stress development with time has been recalculated to a stress-strain curve. Both stress and strain, γ, were calculated at the inner disc. The stress is given by eq. (4.3). Assuming that the surface is homogeneously deformed, the strain can be calculated according to Whorlow [21]:

$$\gamma = \frac{2 \cdot R_o^2}{(R_o^2 - R_i^2)} \cdot (\Theta_o - \Theta_i) \qquad (4.4)$$

where Θ_o and Θ_i are the angles of rotation of the dish and disc, respectively. In Figures 4.4 and 4.5 stress-strain curves are given for β-lactoglobulin and ovalbumin, respectively. As can be seen the stress developed in the film is about the same for β-lactoglobulin and ovalbumin, but the shape of the curve is different. The strain at which the maximum occurs for β-lactoglobulin is much lower than for ovalbumin. Another difference between the data sets is the absence of the maximum for ovalbumin.

The stress-strain curves (Figures 4.4 and 4.5) can be characterised by four parameters: (1) the (initial) slope, (2) the maximum, (3) the decrease in stress after the maximum and (4) the steady-state stress value. These characteristics depend on the protein used. Izmailova [15] also described these phenomena. She interpreted the maximum as the ultimate strength of the protein layer and related this to its elastic properties; the steady state stress value was seen as the equilibrium shear stress in stationary flow characterising the viscous properties of the protein layer. Upon changing the shear rate the curves as shown in Figures 4.4 and 4.5 change (data not shown). By decreasing the shear rate to a low enough value, the maximum disappeared. Increasing the shear rate led to a higher maximum and a steeper decrease of the stress after the maximum. The maximum itself shifted to the left, to lower strain (shorter time scales). A similar effect of shear rate was observed by Izmailova [15].

Below, we discuss the four characteristics of stress-strain curves. As an example the observed differences between β-lactoglobulin and ovalbumin will be discussed. The experimental error of the stress-strain curves is around 10%, somewhat higher than for η^s_{app} alone. However, the goal of the stress-strain curve is to show trends in the behaviour of protein films when subjected to shear; the reproducibility of these trends is very good.

(1) The (initial) slope

The shear modulus, G^s, was calculated from stress-strain curves determined in a set-up using the smaller dish (R_0 = 39 mm) and the larger disc (R_i = 27.5 mm) than in the standard set-up; the gap width is then 11.5 mm instead of 57.5 mm. The latter

gap width would result in a difference between the strain occurring at the inner disc and the outer dish by a factor 23 making it problematic to calculate G^s from the slope of these curves. A gap width of 11.5 mm is about the same as the one used by Benjamins (~11 mm) [4].

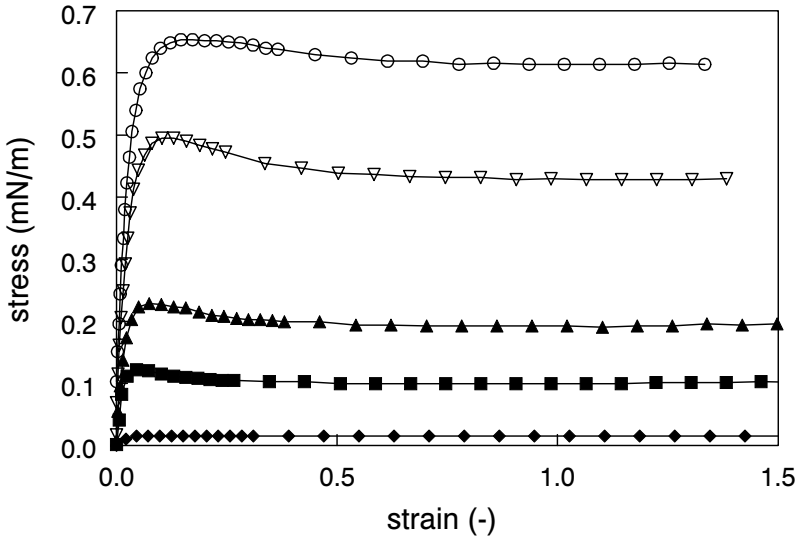

Figure 4.4 Stress-strain curve for β-lactoglobulin (0.1 g/l, pH 6.7, 30 mM) at different ageing times of the protein film; (♦) t=0h53, (■) t=2h30, (▲) t=3h53, (∇) t=5h53, (o) t=7h07

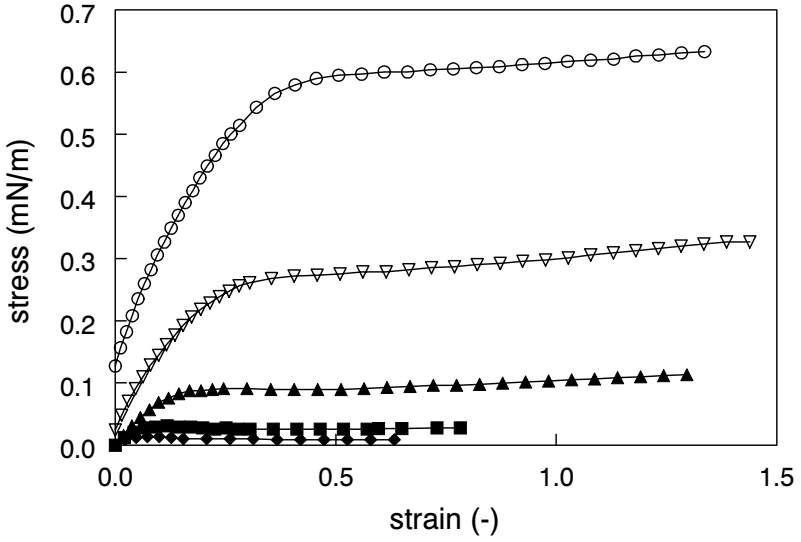

Figure 4.5 Stress-strain curve for ovalbumin (0.1 g/l, pH 6.7, 30 mM) at different ageing times of the protein film; (♦) t=1h32, (■) t=3h15, (▲) t=5h09, (∇) t=7h14, (o) t=9h48

The difference in strain between the disc and the dish is now reduced to a factor 2, which is still relatively large. Using an even smaller gap width will result in a curved surface between the inner disc and the outer dish. From the initial part of the stress-strain curves G^s (= σ/γ) was calculated using the stress and strain at the inner disc. Note that the difference between Θ_o and Θ_i should not be too small otherwise the measured strain becomes very small and therefore inaccurate. For ovalbumin G^s increases from 0.16 mN/m to 2 mN/m during ageing of the protein film over 10 hours, while for β-lactoglobulin G^s increases from 2 to 2.8 mN/m.

In literature different methods have been used to determine the shear modulus and the values for G^s differ with the method used. Roth *et al.* [1] and Murray [19] used the large gap width (=57.5 mm) and determined G^s by measuring the elastic response of the disc after a known, rapid rotation of the dish. Roth *et al.* [1] measured a shear modulus for β-lactoglobulin (0.01 g/l) at an oil-water interface of 0.12 mN/m and at the air/water interface of 0.08 mN/m after an ageing time of 24 hours. Boyd *et al.* [24] determined the shear modulus of a spread β-lactoglobulin layer (at the air/water interface) with a creep method and found a modulus varying from 5 to 10 mN/m. The low values found by Roth *et al.* can not be due to using a strain which was too large. Maximum shear strains used were in the order of 1%, which lies definitely within the range where the stress is linear with the strain. According to our measurements for β-lactoglobulin (0.1 g/l) the linear region extends up to 4%.

By using an oscillatory method Benjamins [4] found G^s = 19 mN/m and G^s = 40 mN/m for ovalbumin at concentrations of 0.1 g/l and 0.3 g/l, respectively; G^s was 20 mN/m (0.3 g/l) when he calculated G^s from a stress-strain curve as is done here. His values are somewhat higher than the values found by us (Benjamins performed his measurements at pH 6.7 as well but the ionic strength was not given).

(2) The maximum

The question arises what actually happens at the observed maximum in the stress-strain curve and what kind of property of the layer is measured after the maximum. The deformation of the surface after starting the rotation of the dish was followed by bringing a straight line of talcum powder on the surface from the centre of the disc to the side of the dish. At t=0 when no shear is applied the line is straight. When shear is applied, the line is displaced in the direction of the shear component. At a certain threshold stress the line breaks near the disc (see Figure 4.6A and 4.6B). This breaking phenomenon corresponds with the maximum in the measured stress-strain curves. Applying shear for a longer time (see Figure 4.6C) the disc does not move any further (constant deflection/stress) while the line on the surface keeps moving as a straight line of constant length. This indicates that the protein film rotates

as a whole without being further deformed. This is observed for all proteins used, also at small gap width and at a concentration of 0.01 g/l.

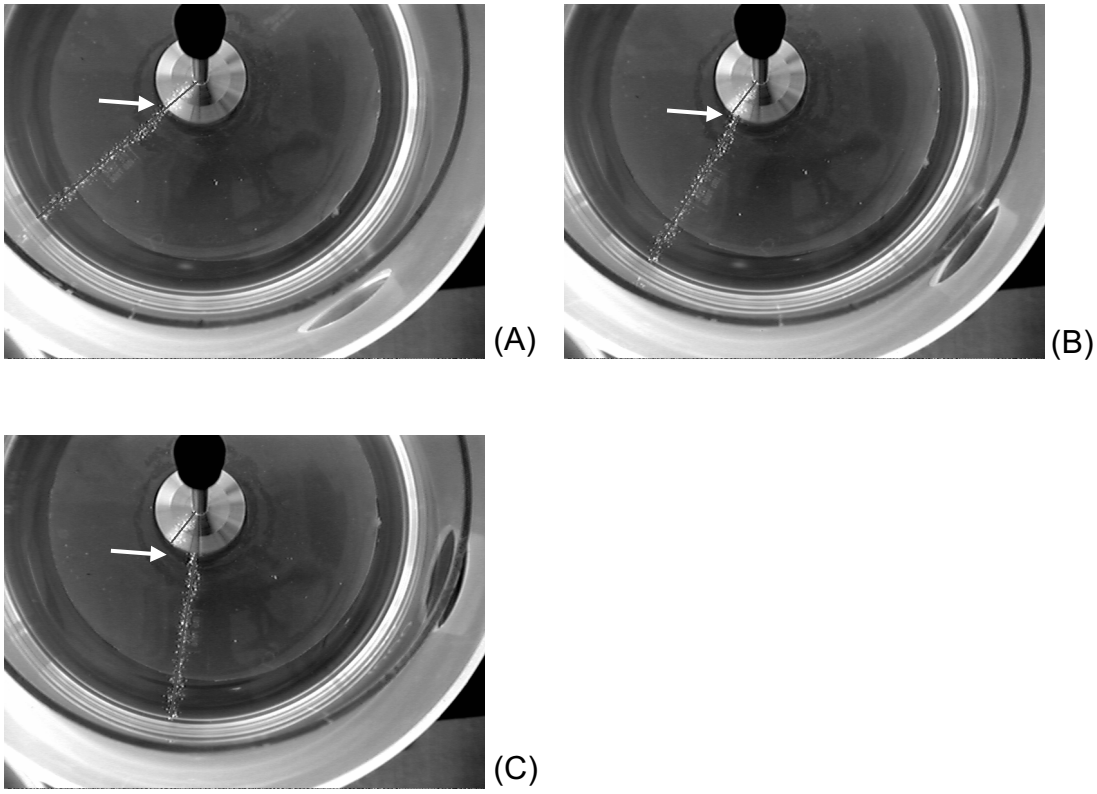

Figure 4.6 Deformation of the protein film by shear by rotating the outer dish: prove for fracture/slip at the inner disc (β-lactoglobulin, 0.1 g/l, pH 6.7, 30 mM); A represents t=0 when no shear is applied; B represents the situation after 2-3 minutes of shearing (=maximum in stress-strain curve); C is situation after ten minutes of shear deformation. Arrows indicate the contact point between the talcum powder line on the surface and on the inner disc (A) and the place where fracture occurs (B and C)

The breaking of the talcum powder line implies that fracture of the protein film and/or slip between the protein layer and the disc occurred. Graham and Phillips [9] did a comparable experiment to determine whether the maximum value found for the elastic and viscous components at saturated monolayer coverage was a yield value for the surface monolayer. They made a distinction between two types of yielding: (1) at the place of contact between the disc and the protein film and (2) at points within the protein film. By means of a lycopodium powder line deposited radially from the disc across the protein film, they observed yielding due to effect (2) only, implying that the maximum shear parameters can be regarded as intrinsic functions of the protein layers. It is not clear whether yielding at points within the protein network as

described by Graham & Phillips can be defined as fracture. If fracture does occur at points within the protein film, the quantity ‘surface shear viscosity’ would cease to be a well-defined monolayer property.

At first sight our results are opposite to those of Graham and Phillips which may be due to the fact that they used much lower concentrations. However, in one single experiment we also observed yielding of the talcum powder line within the protein network at some distance of the disc. This was observed for a very weak (and probably inhomogeneous) protein network. Indeed, the monolayer was so weak that the disc did not move at all when shear was applied. Different talcum powder lines ruptured at different distances from the disc, indicating a very inhomogeneous network. It thus seems that Graham and Phillips had very weak films in all their experiments.

According to Figure 4.6 the breaking of the talcum powder line is due to fracture (between points within the protein film) and/or slip (between disc and protein film). Obviously, fracture occurs close to the disc, which is not unexpected because the exerted stress is highest there (see eq.(4.3)). Fracture between the protein network and the disc would occur when the interaction between the protein and the material of the disc is smaller than the protein-protein interaction. In most publications on surface shear rheometry, the aspect of slip is not discussed at all explicitly. A way to check if slip occurs is by using different materials for the disc. This aspect is not dealt with either in literature as far as we know.

To check whether slip occurs Teflon and Perspex discs were used. With a Teflon disc it was obvious that slip occurred. The disc did not move at all upon shearing the protein layer, no matter what kind of protein or what protein concentration was used. The Perspex disc did move when shear was applied to the protein film. However, the angle of rotation of the disc was not as high as when a stainless steel disc was used, which implies that the stresses exerted on the disc were not as high, likely due to slip.

To avoid slip in bulk rheology, the inner cylinder or spindle is often grooved or covered by sandpaper. In the same vein, a new disc was created having the same geometry as the original stainless steel disc. The roughened edge of the disc was grooved in such a way that the diameter of the disc (=30 mm) was not altered. Using this roughened disc the contact area between the protein network and the disc was enlarged. Benjamins [4] also used roughened glass rings in his concentric ring surface shear rheometer in order to suppress slip.

No differences were found concerning the apparent surface shear viscosity and the fracture behaviour between measurements using the normal disc and the roughened disc. The apparent surface shear viscosity and the stress and strain at the maximum were within the range of reproducibility; fracture of the talcum powder line

occurred near the disc. This means that it is very likely that true slip does not occur between the steel disc and the protein network. Fracture probably occurs within the protein film such that a small layer of protein remains adsorbed on the disc.

Upon inspection of the stress-strain curves of β-lactoglobulin and ovalbumin one notices a difference in the shape of the curves, especially around the maximum. Whereas the maximum for β-lactoglobulin is clearly visible, ovalbumin does not show such a clear maximum but a more gradual process of breakdown and flow of the protein film. The strain at which the maximum occurs for β-lactoglobulin is much lower (~0.15 at t_{age}=7 hours) than for ovalbumin (strain~0.35 at t_{age}=7 hours) meaning that ovalbumin can be much further deformed before fracture occurs. Ovalbumin exhibits more a yielding behaviour. A similar difference in fracture strain between ovalbumin and β-lactoglobulin was also found in bulk rheology [25,26].

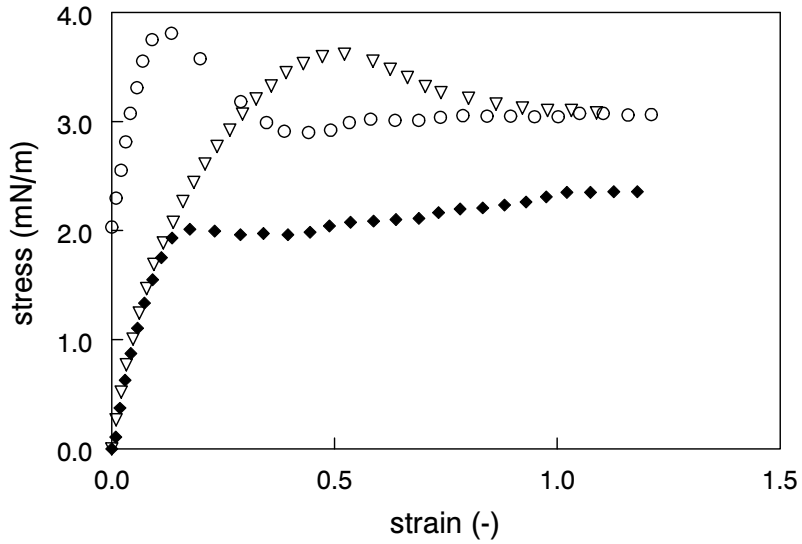

Figure 4.7 Stress-strain curve for glycinin (0.1 g/l, pH 3, 30 mM) showing the history dependence of the protein film; (♦) t=1 hour, (o) t=6 hours (same protein film as (♦) but also subjected to shear at t = 2, 3½ and 5 hours), (∇) t=6 hours (new protein film, first time shear is applied)

Another protein that shows a distinct maximum in the stress-strain curve is glycinin at pH 3. In Figure 4.7 two glycinin films at t_{age}=6 hours, are compared: one that has been sheared several times and another that has not been sheared before. It appears that although the steady state stress (and therefore η^s_{app}) is the same for both proteins, the maximum occurs at different strain even if a correction was made for the strain by extrapolating the stress to zero and taking that point as the zero

strain. It has to be noted that the difference in stress at a strain of zero between the two measurements at t_{age}=6 hours is due to the experimental procedure. For glycinin it appeared that after applying shear at t_{age}=1 hour the stress did not return to zero: a part of the stress remained on the disc being the starting position for the next shearing period. Apparently the two films show different behaviour depending on the way the surface was aged; the steady state stress seems to be less history dependent.

Some authors [4,12] claim that conventional methods such as the Couette-type surface shear viscometer are not appropriate for characterising protein layers while such layers are visco-elastic; continuous deformation at constant shear rate will at least partly destroy the protein network. This phenomenon is expected to lead to inhomogeneity of the monolayer [4]. Indeed, with the method used in this paper it is not possible to determine the elastic and viscous components in the resistance against deformation. However, at small strains reliable data can be obtained for G^s. At large strains inhomogeneous deformation followed by fracture will occur but that is an inherent property of adsorbed protein layers and may also occur using other types of instruments. In fact, inhomogeneous deformation hinders the calculation of a meaningful η^s_{app} (see below).

Fracture properties measured with the surface shear rheometer can be compared to fracture properties measured in expansion with the overflowing cylinder [27]. In the overflowing cylinder the fracture strength for ovalbumin is about 3×10^5 Pa; while σ (mN/m) exerted on the disc (t=6 hours) is 2.2×10^{-4} mN/m. Taking for the adsorbed protein layer thickness ~5 nm, the fracture strength in the surface shear rheometer becomes 4.4×10^4 Pa. For β-lactoglobulin comparable values for the fracture strength were obtained for both techniques. Taking into account that the used techniques are completely different and the applied deformation as well, the values for the fracture strength are strikingly similar.

(3) The decrease in stress after the maximum

If the maximum can be seen as the ultimate strength of the interfacial layer, the decrease in stress represents a kind of structure breakdown of the protein network after failure. It resembles to some extent thixotropic structure breakdown in bulk rheology of soft solids. The stress decreases until there is a steady state with balanced formation and breaking of bonds, or a constant friction between the two protein layers moving along each other. For ovalbumin there is no decrease in stress indicating a gradual breakdown of the network structure while β-lactoglobulin shows a small but reproducible decrease in stress. The difference between ovalbumin and β-lactoglobulin could indicate a transition from a predominantly yielding behaviour to

a more fracture behaviour. Other proteins (e.g. glycinin at pH 3 (see Figure 4.7)) show even stronger fracture behaviour than β-lactoglobulin.

(4) The steady state stress value

From the steady state stress value the apparent surface shear viscosity was determined. For β-lactoglobulin the steady-state stress was reached relatively quickly whereas for ovalbumin the stress keeps on slowly increasing suggesting a build-up of a transient network during shearing. For other proteins it has been observed that the stress is not going to a steady state stress value either; the stress keeps on increasing and decreasing. Murray [19] had to wait almost an hour for gelatine to get a steady state value in deflection. The steady-state stress can be seen as the condition under which the rate of bond breakage due to shearing must be balanced by the rate of bond formation. The fluctuation in the steady-state stress could also be due to friction of pieces of fractured protein layer passing each other meaning that the protein film is not homogeneous anymore. Or even, the filling up of the 'cracks' caused by the fracture process with protein from the bulk solution could lead to irregularities in the stress.

Therefore, the quantity 'apparent surface shear viscosity' is clearly not a well defined material property now that it has become clear that in most systems local yielding or fracture occurs at some maximum stress, after which a very inhomogeneous deformation remains, thus deferring the use of a properly defined rate of strain. Moreover, Figure 4.7 shows that even though the steady state stress (and therefore the calculated η^s_{app}) is the same independent of the history of the protein film, the curve preceding the steady state stress may be largely different. This implies that the steady state stress alone is not enough to characterise a protein network because it leaves out information that can be obtained when using full stress-strain curves.

4.4 Conclusions

Measurements with a surface shear rheometer may give more information on the mechanical behaviour of adsorbed proteins layer than just the apparent surface shear viscosity and shear modulus usually given in literature. By plotting the shear stress versus (average) shear strain in the protein film, clear differences can be observed between proteins. A maximum in such a stress-strain curve can be regarded as a fracture stress, the accompanying strain as a fracture strain and the decrease in stress as a kind of structure breakdown of the protein film.

Ovalbumin and β-lactoglobulin show different behaviour. This is reflected by the strain that can be applied to the protein layer before it fractures and by the way the steady-state stress is reached. The fracture strain of an adsorbed ovalbumin layer is

much larger than that for a β-lactoglobulin film. Also the way the stress changes after the maximum differs between the proteins. These differences show that the mechanical properties of the layer vary from one protein to another; the interfacial strength and homogeneity of such films are therefore different. After all, it appears that η^s_{app} is less suitable to characterise adsorbed protein layers than full stress-strain curves.

References

1. Roth, S.; Murray, B.S.; Dickinson, E. *J. Agric.Food Chem.* **2000**, *48*, 1491-1497.
2. Dickinson, E. *Colloids Surf. B* **1999**, *15*, 161-176.
3. Coke, M.; Wilde, P.J.; Russell, E.J.; Clark, D.C. *J. Coll. Interface Sci.* **1990**, *138*, 489-504.
4. Benjamins, J. **2000** PhD-thesis, Wageningen University, the Netherlands.
5. Williams, A.; Janssen, J.J.M.; Prins, A. *Colloids Surf. A* **1997**, *125*, 189-200.
6. Dickinson, E.; Rolfe, S.E.; Dalgleish, D.G. *Int. J. Biol. Macrom.* **1990**, *12*, 189-194.
7. Murray, B.S. *Colloids Surf. A* **1997**, *125*, 73-83.
8. Ogden, L.G.; Rosenthal, A.J. *J. Coll. Interface Sci.* **1997**, *191*, 38-47.
9. Graham, D.E.; Phillips, M.C. *J. Coll. Interface Sci.* **1980**, *76*, 240-250.
10. Burgess, D.J.; Sahin, N.O. *J. Coll. Interface Sci.* **1997**, *189*, 74-82.
11. Joly, M. In: *Surface and Colloid Science*; Vol.5; Ed. E. Matijevic, Wiley-Interscience; 1972, 1-193.
12. Krägel, J.; Siegel, S.; Miller, R.; Born, M.; Schano, K.-H. *Colloids Surf. A* **1994**, *91*, 169-180.
13. Brooks, C.F.; Fuller, G.G.; Frank, C.W.; Robertson, C.R. *Langmuir* **1999**, *15*, 2450-2459.
14. Petkov, J.T.; Gurkov, T.D. *Langmuir* **2000**, *16*, 3703-3711.
15. Izmailova, V.N. *Progr. Surf. Membr. Sci.* **1979**, *13*, 141-209.
16. Biswas, B.; Haydon, D.A. *Progr. R. Soc. A* **1963**, *271*, 296.
17. Benjamins, J.; van Voorst Vader, F. *Colloids Surf.A* **1992**, *65*, 161-174.
18. Dickinson, E.; Murray, B.S.; Stainsby, G. *J. Coll. Interface Sci.* **1985**, *106*, 259-262.
19. Murray, B.S. **1987** PhD-thesis, University of Leeds, United Kingdom.
20. Dickinson, E.; Murray, B.S.; Stainsby, G. *Int. J. Biol. Macrom.* **1987**, *9*, 302-304.
21. Whorlow, R.W. Rheological Techniques; Ellis Horwood Limited; New York; 1992.
22. de Jongh, H.H.J.; Gröneveld, T.; de Groot, J. *J. Dairy Sci.* **2001**, *84*, 562-571.
23. Martin, A.H.; Bos, M.A.; van Vliet, T. *Food Hydrocoll.* **2002**, *16*, 63-71.
24. Boyd, J.V.; Mitchell, J.R.; Irons, L.; Musselwhite, P.R.; Sherman, P. *J. Coll. Interface Sci.* **1973**, *45*, 478-483.
25. Stading, M.; Hermansson, A.-M. *Food Hydrocoll.* **1991**, *5*, 339-352.
26. van Kleef, F.S.M. *Biopolymers* **1986**, *25*, 31-59.
27. Bos, M.A.; Grolle, K.; Kloek, W.; van Vliet, T. **2002**, accepted for publ. in Langmuir.

5 Network forming properties of various proteins adsorbed at the air/water interface in relation to foam stability

AH Martin, K Grolle, MA Bos, MA Cohen Stuart & T van Vliet
J of Colloid and Interface Science (2002) 254: 175-183

ABSTRACT

A series of proteins was studied with respect to their ability to form a network at the air/water interface and their suitability as foaming agents and foam stabilisers. Proteins were chosen with a range of structures from flexible to rigid/globular: β-casein, β-lactoglobulin, ovalbumin and (soy) glycinin. Experiments were performed at neutral pH except for glycinin, which was studied at both pH 3 and at pH 6.7. The adsorption process was followed with an Automated Drop Tensiometer (ADT). Network forming properties were assessed in terms of surface dilational modulus (determined with the ADT), the critical falling film length (L_{still}) and flow rate (Q_{still}) below which a stagnant film exists (as measured with the overflowing cylinder technique) and the fracture stress and fracture strain measured in surface shear. It was found that glycinin (pH 3) can form an interfacial gel in a very short time, whereas β-casein has very poor network forming properties. Hardly any foam could be produced at the chosen conditions with glycinin (pH 6.7) and with ovalbumin, whereas β-casein, β-lactoglobulin and glycinin (pH 3) were good foaming agents. It seems that adsorption and unfolding rate are most important for foam formation. Once the foam is formed, a rigid network might favour stabilising the foam.

5.1 Introduction

Water-soluble proteins accumulate strongly at liquid interfaces. Upon adsorption interfacial protein layers are formed with a visco-elastic character. The rheological properties of these layers are of interest for the formation and stabilisation of emulsions and foams. The role of proteins in the stabilisation and formation of emulsions and foams has been extensively reviewed by Walstra [1], Dickinson [2] and Wilde [3] among others. A key factor that determines whether or not emulsions and foams can be formed and are stable is the response of an interfacial protein film to expansion and compression of the interface [4].

Two kinds of surface deformation are important: area changes (dilation/compression) and shape changes (shear). Dilation is associated with adsorption/desorption of the surface-active agent, together with relaxation processes at constant surface concentration and with the internal cohesion of and interactions between protein molecules. Interactions between proteins, however, are better probed by deformation in shear. Another factor of impact in shear rheology (in addition to internal cohesion and protein interactions) is the surface density of the proteins present at the surface [5,6].

Both types of interfacial deformation are relevant for emulsions and foams. The majority of studies on protein solutions have focussed on either surface rheology or on foaming behaviour, but only a few studies have attempted to relate the observed foaming behaviour explicitly to the dynamic properties of protein films in dilation as well as in shear [7].

Foams are subjected to destabilisation processes like disproportionation, drainage and coalescence. Disproportionation can be slowed down by a gel-like adsorbed film with a finite yield stress [8,9]. It has been suggested that a kind of skin slows down gas transport because of lack of gas solubility in this skin [8]. During film drainage surface shear rheological properties seem to be important because a correlation was found between surface rheological properties and foam properties: the higher the apparent surface shear viscosity, the slower drainage and the more stable the foam [7,10]. A surface tension gradient is a prerequisite for stability against coalescence during foaming because coalescence requires film rupture and the rate of rupture depends on the film thickness and on its mechanical properties, in particular on the stress at which the film breaks [3,11-13].

Various interfacial properties are claimed to have some sort of influence on foamability and foam stability but what the influences are, is not clear. The purpose of this paper is therefore to study the relation between the rheological behaviour of some selected proteins (each with a different tertiary structure and molecular size) and their foaming behaviour. For each protein we studied adsorption kinetics, surface dilational modulus, fracture behaviour and coarsening rate of the foam. Fracture

behaviour was assessed using surface shear measurements from which stress-strain curves were derived as described elsewhere [14]. The four selected proteins form a series in which the structure varies: β-casein, β-lactoglobulin, (soy) glycinin and ovalbumin. The milk proteins β-casein and β-lactoglobulin have been extensively studied by various authors using different methods [15-20] but ovalbumin and glycinin have been investigated to a lesser extent [21-24].

All proteins were studied at pH 6.7 except for glycinin, which was also investigated at pH 3. At pH 3 glycinin is present as a monomer (M~44 kDa) and at pH 6.7 it exists as a hexamer (M~350 kDa). This change in quaternary structure has great impact on the rheological properties of both interfacial films and solutions [21,25].

5.2 Materials & Methods

5.2.1 Materials

Proteins studied were β-lactoglobulin, β-casein, ovalbumin and glycinin. β-Lactoglobulin was purified according to the method of de Jongh *et al.* [26]. Ovalbumin was obtained from Sigma (grade V). Glycinin was isolated from soybeans according to the fractionation scheme given by Tanh and Shibasaki [27] and further prepared as described by Martin *et al.* [21]. β-Casein was obtained from Eurial (Nantes, France, ref. CBG 312/3).

Proteins were dissolved in a phosphate buffer with pH 6.7. For the measurements at pH 3 (glycinin) a citric acid/phosphate buffer was used. The chemicals used for the buffers, Na_2HPO_4, NaH_2PO_4 and $C_6H_8O_7 \cdot H_2O$ were purchased from Merck (Darmstadt, Germany, analytical grade). All solutions were made with doubly distilled water and stirred for 1 h. Temperature was kept at 23°C.

5.2.2 Methods

The Automated Drop Tensiometer

An Automated Drop Tensiometer (ADT) [28,29] was used to measure the interfacial tension between liquid and air. The interfacial tension was determined by means of drop shape analysis of a bubble formed within a cuvette containing the protein solution. The bubble was illuminated by a uniform light source and its profile was imaged and digitised by a CCD-camera and a computer. The profile was used to calculate the interfacial tension using Laplace's equation. All experiments were performed in the rising drop configuration.

During the measurements the decrease in surface tension of a newly formed bubble was followed; the dilational modulus was obtained by dynamic oscillation of the bubble area at 100 s after bubble formation and at the end of each measurement. The bubble volume used was 4 μl and the area change during oscillation was

approximately 8%. This change in area was within the linear region. Temperature was kept constant at 22°C.

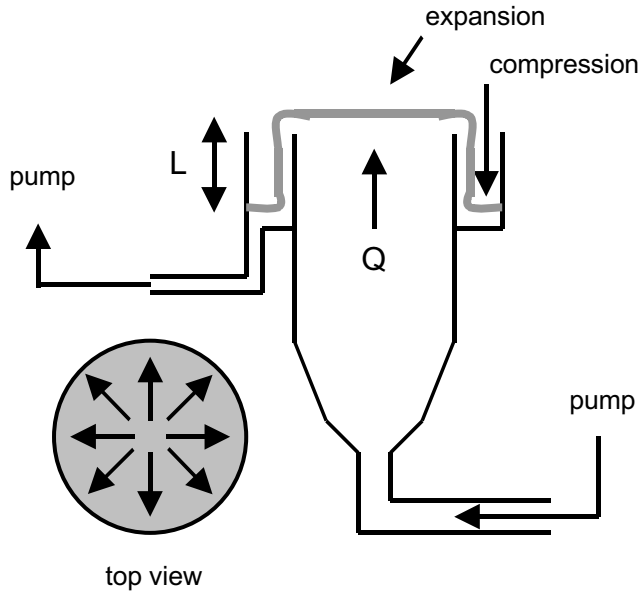

Figure 5.1 Schematic representation of the overflowing cylinder; L is the length of the falling film, Q is the flow rate (cm^3/s)

The overflowing cylinder

The overflowing cylinder technique used in this study has been described by Bergink-Martens [30] and Boerboom [31]. The overflowing cylinder consists of an inner cylinder through which the liquid is pumped at a constant flow rate (see Figure 5.1). Liquid flows over the upper rim of the inner cylinder along the inner cylinder wall into the circular container formed by the inner and outer cylinder. From this vessel the liquid is pumped back to the inner cylinder. The height difference between the level of the liquid in the outer cylinder and the rim is called the falling film length, L [31]. At the top of the inner cylinder the surface expands radially at a constant relative expansion rate dlnA/dt. For water dlnA/dt is independent of the falling film length while for surfactant solutions it is not. By increasing the length L of the falling film, dlnA/dt of an aqueous surfactant solution increases beyond the value for pure water, whereas below a certain value of L the expansion rate is lower than that of pure water. By decreasing L below a threshold value the surface expansion stops completely. The critical falling film length at which this first occurs is called L_{still} (dlnA/dt~0). L_{still} depends strongly on the nature of the surfactant used [32] and characterises the ability of a surfactant to build up a network preventing the surface

from flowing. Whether the surface expands or not and whether or not a network is formed depends not only on L but also on the flow rate Q and on the age of the surface (time). The flow rate (at fixed L) for which dlnA/dt~0 is called Q_{still}. Going from high to low Q at a certain L, Q_{still} can be determined. Hence, a stagnant protein film is formed at a certain combination of L_{still} and Q_{still}; increasing L or Q will rupture the film. Therefore, measuring dlnA/dt going from high to low Q or L can be interpreted as stagnant film formation whereas going from low to high Q or L is related to fracture of the protein layer.

The flow rate varied from 0 to 68 cm^3/s and L from 0.5 and 3 cm. Temperature was kept constant at 26°C.

Surface shear rheometer

Stress-strain curves were determined with a two-dimensional Couette-type interfacial viscometer as described previously [14]. A stainless steel biconical disc (diameter 30 mm) was suspended by a torsion wire such that the disc edge was in the plane of the air/water interface. The protein solution was contained in a thermostated circular glass dish (diameter 145 mm). The thickness of the torsion wire was 0.20 mm (glycinin), 0.15 mm (β-lactoglobulin, ovalbumin) and 0.10 mm (β-casein); the torsion wire length was 740 mm. Stress-strain curves were made as a function of ageing time of the protein layer. Stress was exerted on the inner disc by rotating the outer dish at a fixed shear rate until a steady state stress was observed, usually after 10-20 minutes. The stress, σ, is calculated according to Whorlow [33]:

$$\sigma = \frac{K \cdot \Theta_i}{2 \cdot \pi \cdot R_i^2} \tag{5.1}$$

where K represents the torsion wire constant, Θ_i (rad) the rotation of the disc and R_i the radius of the disc. Assuming that the surface is homogeneously deformed, the strain, γ, is equal to [33]:

$$\gamma = \frac{2 \cdot R_o^2}{(R_o^2 - R_i^2)} \cdot (\Theta_o - \Theta_i) \tag{5.2}$$

where Θ_o is the angle of rotation of the dish and R_o the radius of the dish.

At intervals of 1 hour, the measurement procedure was repeated; the starting position of a subsequent measurement is determined by the position accomplished after stress relaxation of the previous measurement. Temperature was kept constant at 23°C.

Continuous expansion measurements

The dynamic surface tension in steady state expansion was determined using a Langmuir trough with an endless caterpillar belt with moving barriers [34]. The

dimensions of the trough were 400 × 190 × 30 mm. Six Teflon barriers were mounted on the endless belt. Measurements were performed going from highest to lowest expansion rate (dlnA/dt varies from around 10^{-3} to 10^{-1} s^{-1}). The surface tension was measured by use of the Wilhelmy-plate method. Measurements were performed at 23°C.

Foam experiments

Foams were made using a 'fanflutter' (high speed, single fan at the bottom of the cylinder, diameter of fan = 4.6 cm) and a whipping apparatus (Ledoux b.v., Dodewaard, the Netherlands; medium speed, double beaters, diameter of each beater = 4 cm). With the 'fanflutter' 100 ml of protein solution was mixed at 3000 rpm for 2 minutes. The sample container was a volumetric cylinder 11 cm high and 6.2 cm of diameter. With the Ledoux, the protein solution (200 ml) was mixed for 2 minutes at 450 rpm; the cylindrical sample container was 14 cm high and had a diameter of 9.2 cm. Protein concentration was varied between 0.01 and 3 g/l.

Foam drainage and drainage height were monitored for a period of 20 minutes in the sample container in which the foam was made. From the foam a sample was taken (with a pipette with an opening of 3 mm in diameter) to determine the mean bubble size, d_{21}, by using laser light transmission. The light transmission through the cuvette filled with foam was measured at a set height at intervals of 30 s during a period of 15 min. The laser beam passes through the foam during 3 s per interval to avoid heating up of the foam.

The amount of light transmission was correlated to the mean bubble size d_{21} determined by light microcsopy. This size parameter was chosen because the relation between d_{21} and light transmission is linear as shown by Durian *et al.* [35]. A more detailed description of the technique has been given by Martin *et al.* [21].

5.3 Results

5.3.1 Adsorption behaviour

The adsorption of various proteins at the air-water interface (concentration 0.1 g/l) was followed by measuring the decrease in surface tension γ (mN/m) with time (Figure 5.2). The adsorption rate of the proteins increased in the order glycinin (pH 6.7) < ovalbumin < glycinin (pH 3) < β-lactoglobulin < β-casein. This order in adsorption rate coincides with the order in protein molecular size, which is 24, 18, 44, 45 and 350 kDa for β-casein, β-lactoglobulin, glycinin (pH3), ovalbumin and glycinin (pH 6.7), respectively. At pH 6.7 however, β-lactoglobulin is known to self-associate into a dimer with a molecular weight of 37 kDa [36]. Not only protein molecular size but also protein structure and hydrophobicity appear to influence the adsorption rate. Disordered, small and flexible proteins are more surface active than ordered, rigid

and larger proteins [37,38]. β-Casein is a flexible, random-coil protein whereas ovalbumin and glycinin are compact globular proteins that are likely to unfold more slowly at an interface. Although glycinin (pH 3) and ovalbumin have more or less the same molecular size, their adsorption rate is rather different: ovalbumin adsorbs more slowly at the air/water interface than glycinin (pH 3) (see Figure 5.2). This difference in adsorption behaviour is probably due to a difference in molecular functional properties such as for example the exposed hydrophobicity.

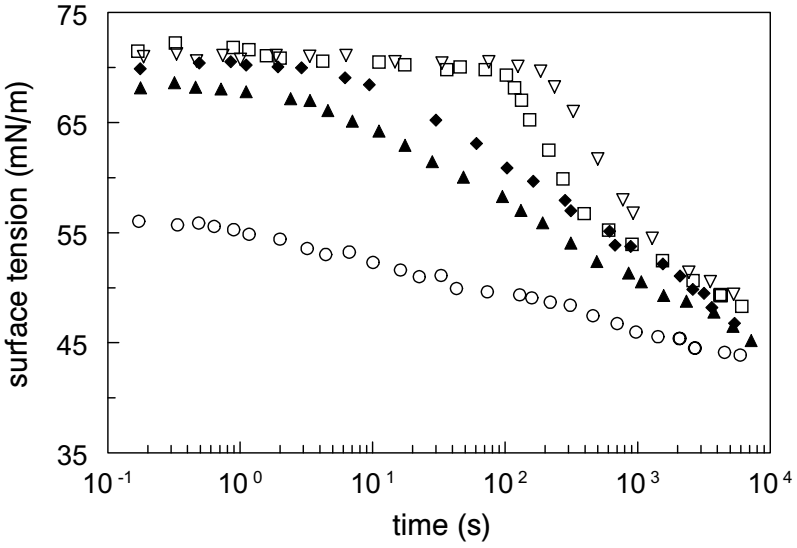

Figure 5.2. Surface tension as a function of time for different proteins at the air/water interface (protein concentration 0.1 g/l) measured with the ADT; (o) β-casein, (▲) β-lactoglobulin, (□) ovalbumin, (∇) glycinin, (♦) glycinin pH 3

At a static interface the decrease in surface tension continues over a long time due to protein adsorption and unfolding. At a continuously expanding interface however, the surface tension quickly reaches a steady state (γ_{ss}) at which protein adsorption to the expanded interface just compensates with the two-dimensional dilution of the adsorbed amount at the expanding interface. For a continuously expanding interface (as created with the Langmuir trough with caterpillar belt) the decrease in surface tension compared to water depends on the expansion rate (the rate at which the interface is diluted). Figure 5.3 shows γ_{ss} at an expanding interface for five 'different' proteins. At high expansion rates ovalbumin and glycinin were unable to adsorb in quantities sufficient to lower γ; glycinin (pH 3) and β-lactoglobulin reduced γ only to some extent whereas β-casein is able to reduce γ very well.

Decreasing the expansion rate increases the ability for all proteins to adsorb in sufficient quantities at the interface to lower γ. At low expansion rates all proteins are able to lower γ; however, the extent to which they lower γ differs a lot. In general, smaller (and flexible) proteins can lower γ at relatively higher expansion rates than larger (and compact) proteins, because the adsorption rate of the former is higher. Conclusively, adsorption at an expanding interface is similar to adsorption at a static interface as both methods result in the same order in protein adsorption.

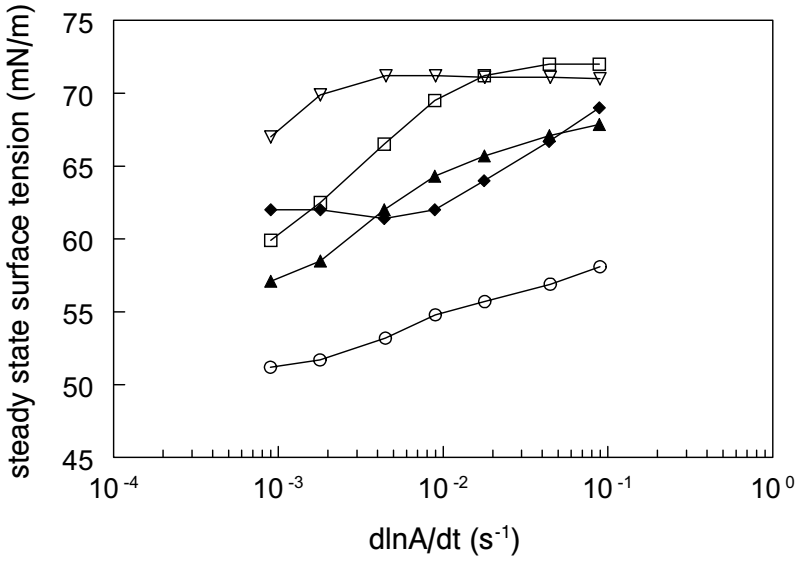

Figure 5.3 Steady state surface tension of a continuously expanding interface determined by using a Langmuir trough with caterpillar belt versus expansion rate dlnA/dt (protein concentration 0.1 g/l); (o) β-casein, (▲) β-lactoglobulin, (□) ovalbumin, (▽) glycinin, (♦) glycinin pH 3

5.3.2 Properties of the adsorbed layer

The dilational modulus E (mN/m) was measured with the ADT, both at 100 s after bubble formation, and after 1.7 h. In Table 5.1 E is given for the series of proteins studied. At an ageing time of 100 s the value of E is very low for glycinin (pH 6.7) and ovalbumin because hardly any protein has adsorbed at t=100 s (see Figure 5.2). β-Lactoglobulin, β-casein and glycinin lowered γ to different extents proportional to their adsorption rate. E however, is not proportional to the adsorbed amount: E increases in the order β-casein < β-lactoglobulin < glycinin (pH 3), whereas the increase in adsorption rate is in reverse order. After ageing of the protein film for 1.7 h all proteins lowered γ to about the same value indicating roughly similar adsorbed amounts. Now, differences in E mainly represent the difference in

rigidity of the protein molecules and its response to changes in area and not a difference in adsorbed amount. At an ageing time of 1.7 h E increased in the order β-casein < glycinin (pH 6.7) < glycinin (pH 3) < β-lactoglobulin < ovalbumin.
Remarkable is the difference in ratio $E_{t=100\ s}$ / $E_{t=1.7\ h}$, which is low for ovalbumin and glycinin (pH 6.7). This is due to the rather slow adsorption rate of ovalbumin and glycinin (pH 6.7).

Table 5.1 Dilational modulus E (mN/m) measured with the ADT for different proteins (protein concentration 0.1 g/l, pH 6.7)

	E (mN/m) t=100 s	E (mN/m) t=1.7 h
β-casein	11	20
β-lactoglobulin	38	63
ovalbumin	5	75
glycinin	3	43
glycinin (pH 3)	47	60

Below a certain falling film length in the overflowing cylinder, proteins are able to slow down the motion of the surface drastically. The radial surface expansion is completely counteracted at and below L_{still} due to the formation of a network; below L_{still} the surface does not expand anymore at a measurable rate (dlnA/dt ~0). L_{still} is therefore a measure for network formation under rough circumstances. At a flow rate of 31.4 cm^3/s and a protein concentration of 0.1 g/l L_{still} increases in the order β-casein < glycinin (pH 6.7) < β-lactoglobulin < ovalbumin < glycinin (pH 3) with 1.8, 2.0, 2.25, 2.4 and 2.5 cm, respectively. Increasing L (from L_{still} on) leads to protein film rupture; L_{still} can therefore also be seen as a measure of the yield/fracture stress of the adsorbed layer [39]. Keeping L at a constant value, network formation and fracture can also be established by decreasing or increasing Q. This yields the parameter Q_{still} at given length L.

In Figure 5.4 L_{still} is given as a function of Q_{still} for different proteins at a concentration of 0.01 g/l. The combination of L_{still} and Q_{still}, at which a stagnant film is formed, is assessed by decreasing L at constant Q or decreasing Q at constant L until the surface does not expand anymore. Decreasing L or Q even further leads to no change in the formed network whereas increasing L or Q leads to film rupture. From Figure 5.4 it appears that at low concentrations (0.01 g/l) glycinin (pH 3) and

β-lactoglobulin form a network at a combination of higher L and Q than ovalbumin, glycinin (pH 6.7) and β-casein. Logically, a higher stress is needed to fracture a glycinin (pH 3) or β-lactoglobulin film again. From experiments at higher concentrations it is known that glycinin (pH 6.7) and ovalbumin are also capable to form a stagnant layer at larger L_{still}. At a protein concentration of 0.01 g/l however, protein adsorption at the expanding interface is not sufficient to form a stagnant film as strong as glycinin (pH 3) and β-lactoglobulin. β-Casein does adsorb rapidly but does not form a rigid network at all.

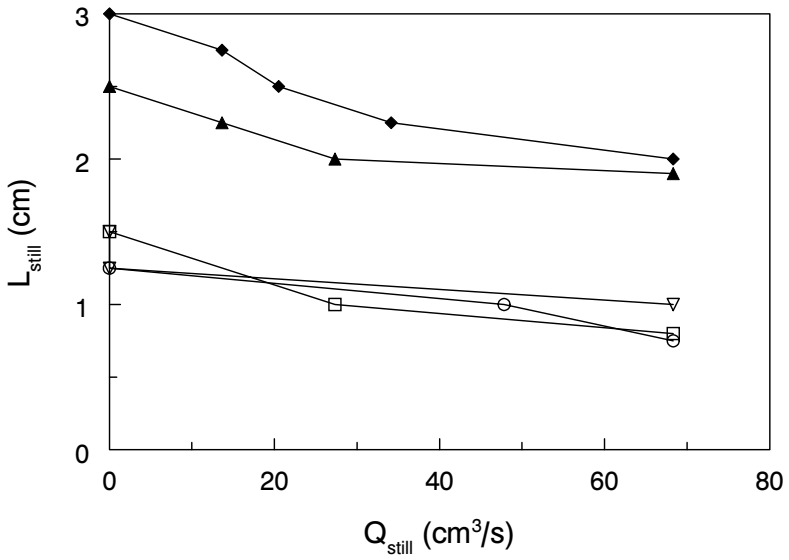

Figure 5.4 L_{still} versus Q_{still} measured with the overflowing cylinder (protein concentration 0.01 g/l): above the line no protein network is formed on top of the cylinder surface; (o) β-casein, (▲) β-lactoglobulin, (□) ovalbumin, (∇) glycinin, (♦) glycinin pH 3

Interfacial shear rheology of adsorbed protein films is considered to be very sensitive to the macromolecular structure and to the nature of intermolecular interactions in the adsorbed layer. As shown previously [14], information on the adsorbed protein layer can be best retrieved from the stress-strain curves calculated from the stress versus angular deformation of the inner disc. In Figure 5.5 an example is given of stress-strain curves for glycinin (pH 3) at different ageing times of the protein film. Stress-strain curves for ovalbumin and β-lactoglobulin are given elsewhere [14].

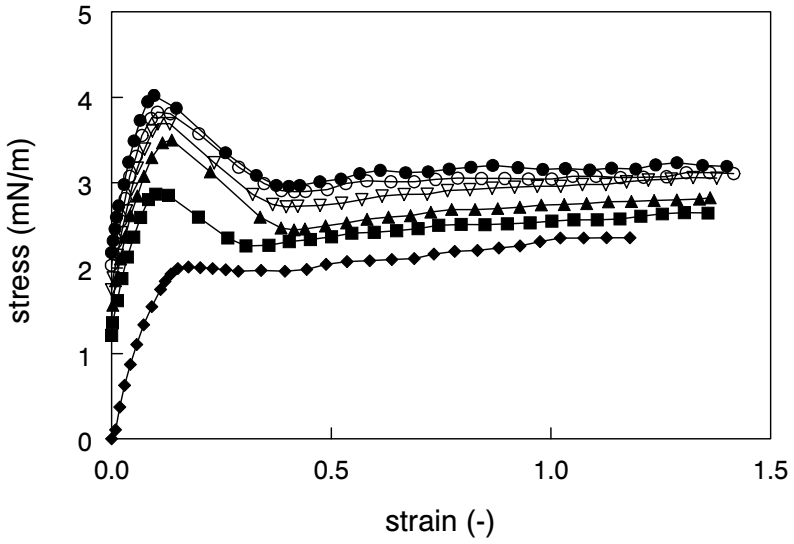

Figure 5.5 Stress-strain curves for glycinin (pH 3, 0.1 g/l) at different ageing times of the protein film; (♦) t=1h02, (■) t=2h02, (▲) t=3h41, (▽) t=5h01, (o) t=6h08, (●) 7h13

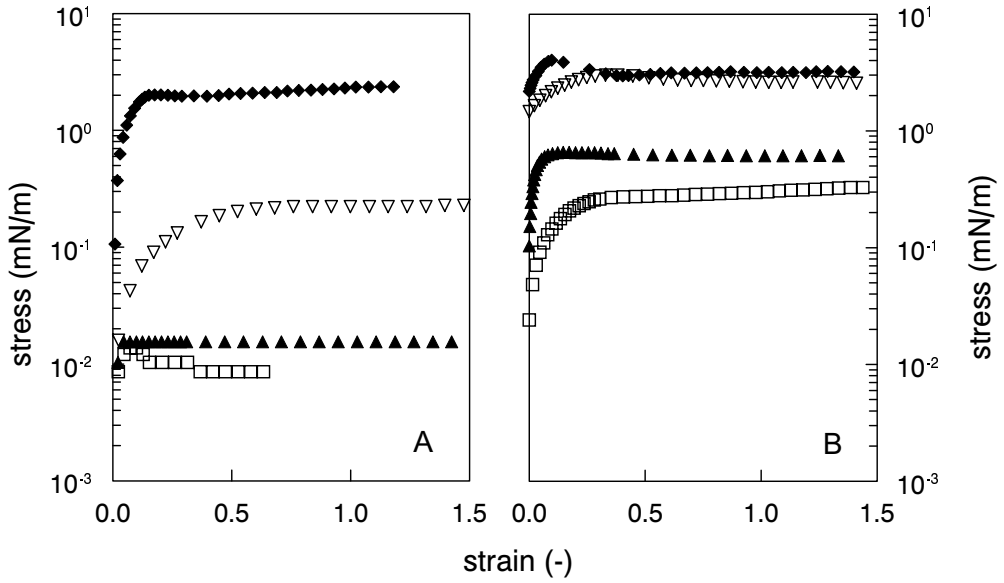

Figure 5.6 Stress-strain curves for various proteins (concentration 0.1 g/l) at two different ageing times; (▲) β-lactoglobulin, (□) ovalbumin, (♦) glycinin (pH 3) and (▽) glycinin (pH 6.7); A: t_{age}=1 hour, B: t_{age}=8 hours

Four characteristics of the stress-strain curves were distinguished [14]: (1) the initial slope, (2) the maximum stress, σ_f, (3) the decrease in stress after the maximum and (4) the steady state stress, σ_{ss} from which the apparent surface shear viscosity

can be determined as often done by Dickinson, Murray and co-workers [40-42]. In Figure 5.6 stress-strain curves are given for β-lactoglobulin, ovalbumin and glycinin (both pH) at ageing times of 1 and 8 h. Because there is a large difference in stress between the proteins studied, σ is given on a log scale. As a result of this however, the four characteristics of a stress-strain curve are less visible. For β-casein it was not possible to determine stress-strain curves; the protein network was too weak to give sufficient deflection of the disc even with a very thin torsion wire.

Table 5.2 Surface shear rheological properties of different proteins determined from stress-strain curves (conc. 0.1 g/l, pH 6.7)

	t_{age} ~ 1 h			t_{age} ~ 8 h		
	σ_{ss} (mN/m)	σ_f (mN/m)	γ_f (-)	σ_{ss} (mN/m)	σ_f (mN/m)	γ_f (-)
β-casein	0.001	-	-	0.002	-	-
β-lactoglobulin	0.01	0.015	0.05	0.6	0.65	0.15
ovalbumin	0.01	0.01	0.12	0.5	0.5	0.4
glycinin	0.2	0.2	0.6	2.6	3	0.35
glycinin (pH 3)	2	2	0.2	3.2	4.1	0.1

σ_{ss} = steady state stress, σ_f = fracture stress at maximum, γ_f = fracture strain at maximum

Clear differences can be observed between the proteins studied. While glycinin (pH 3) for example has a much higher σ_{ss} than β-lactoglobulin, it fractures at smaller strain (γ_f). The rapid decrease in stress after fracture (fracture occurs at σ_f) is also much larger for glycinin (pH 3) than for β-lactoglobulin. The maximum was not evident for all proteins; ovalbumin and glycinin (pH 6.7) showed more a kind of yielding behaviour rather than fracture. Figure 5.6 shows that, for glycinin (pH 6.7) and ovalbumin, σ grows more steadily with increasing strain while β-lactoglobulin and glycinin (pH 3) give a steeper rise in σ. However, visually it was observed that also for glycinin (pH 6.7) and ovalbumin the adsorbed layer does not yield homogeneously but only in a very small region close to the inner disc resulting in two protein layers moving along each other [14]. In Table 5.2 a summary is given for some of the characteristics for all proteins studied at ageing times of 1 and 8 h, respectively. Glycinin (at both pH values) gave a very high σ_f compared to other proteins: at t_{age} ~ 8 h σ_f was 3 and 4.1 mN/m at a pH of 6.7 and 3, respectively. The smaller subunits of glycinin at pH 3 gave a stiffer network and more brittle behaviour whereas the hexamers at pH 6.7 behaved more like a liquid. Ovalbumin behaved similarly. Differences between glycinin at pH 3 and pH 6.7 have been discussed by

Martin *et al.* [21] and van Vliet *et al.* [25] and are due to the difference in quaternary structure. Comparing β-lactoglobulin and ovalbumin, σ_{ss} and σ_f are more or less the same at t_{age} ~ 8 h. However, γ_f shows that the structure of the protein layer is quite different; β-lactoglobulin fractured at lower strain than ovalbumin.

5.3.3 Foam formation and stability

Whether or not a good foam can be produced depends on the amount of protein present and on the experimental technique with which the foam is produced. Comparing, for example, whipping, shaking and gas sparging, the amount of protein required for foam production is less for gas sparging and shaking than for whipping [12]. At low concentrations (0.01-0.1 g/l) a reasonable foam could be formed with β-casein, β-lactoglobulin and glycinin (pH 3) whereas producing foam with ovalbumin and glycinin (pH 6.7) solutions only resulted in few very coarse bubbles.

Increasing the protein concentration (1-3 g/l) enlarged the amount of foam formed for β-casein, β-lactoglobulin and glycinin (pH 3), but at a certain concentration the amount of foam formed remained the same. For ovalbumin and glycinin (pH 6.7) the concentration had to be at least 10 g/l to create some foam. The differences in ability to produce foam between the various protein solutions can be explained by the differences in adsorption rate observed at either a static (Figure 5.2) or an expanding interface (Figure 5.3) but also by the structure of the protein. Because of their high molecular weight and rigid structure, ovalbumin and glycinin (pH 6.7) cannot adsorb and unfold at the interface within the time-scale of the foam experiment to sufficiently lower γ, hence, no foam is formed.

In general, with the whipping apparatus (a low energy input mixer) more foam was created than with the fanflutter (a high energy input mixer). The initial amount of foam increased in the order glycinin (pH 6.7) < ovalbumin < β-lactoglobulin < glycinin (pH 3) < β-casein (both with the fanflutter and whipping apparatus, for a concentration of 0.1 g/l).

The foam height (total height - liquid height) was recorded as a function of time. A normalised foam height, H_t/H_0, was calculated as a function of time where H_0 is the initial foam height and H_t the foam height at a time t. It appears that after ageing for 20 min H_t/H_0 was the same for β-casein, β-lactoglobulin and glycinin (pH 3) provided that at t=0 the sample container was almost completely filled with foam (no liquid present). However, this is only the case at and above different threshold concentration, which were 0.3, 1 and 3 g/l for β-casein, glycinin (pH 3) and β-lactoglobulin, respectively. At and above these concentrations the foams initially drained very fast, followed by a more gradual increase of the liquid height and finally

a steady state. Drainage was dependent on the amount of foam and not directly on the protein type.

Table 5.3 Mean bubble size d_{21} (μm) of different proteins foams made with the fanflutter at 3000 rpm

	t = 0		t = 20 min.	
	0.3 g/l	1 g/l	0.3 g/l	1 g/l
β-casein	69	66	115	115
β-lactoglobulin	78	69	165	145
glycinin (pH 3)	75	69	100	100

The mean bubble size, d_{21}, was determined using light transmission. Above a certain concentration the protein type had no large effect on the initial d_{21} anymore; the size distribution however, differed between the proteins studied. The initial d_{21}, and the d_{21} after 20 min, for the foams made with the fanflutter are given in Table 5.3 for two protein concentrations. At a concentration of 1 g/l β-casein, β-lactoglobulin and glycinin (pH 3), all had the same initial d_{21}. The whipping apparatus produced foams with a larger d_{21}, but also for this apparatus d_{21} was more or less the same (d_{21} ~ 98 μm) for all proteins at a concentration of 1 g/l. Ageing of the foams lead to drainage and disproportionation, the latter resulting in an increase of d_{21} (no coalescence was observed for either foaming method or protein provided that the concentration was high enough). The increase of d_{21} with time is reflected in the coarsening rate ($d(d_{21})/dt$). In Figure 5.7 the coarsening rate is given as a function of protein concentration for different protein foams made with the fanflutter and with the whipping apparatus. Foams made with glycinin (pH 3) had the lowest coarsening rate (d_{21} increases less with time). These foams were therefore most stable with respect to disproportionation. The coarsening rate depended on the way the foam was produced. The coarsening rate was lower with the whipping apparatus because the initial d_{21} was higher and upon ageing the bubble size changed relatively little. The difference in coarsening rate between β-lactoglobulin and β-casein was larger for foams made with the fanflutter than for foams made with the whipping apparatus. A clear explanation cannot be given at the moment.

Differences were also observed in the appearance of the foams, in particular in the dryness and stiffness of the foam. A β-casein foam was quite stiff; it had a normal bubble size distribution but the foam was not very dry. Glycinin (pH 3) formed also a rather stiff foam but the bubble size distribution was bi-modal. Moreover, the foam was very brittle and dry, although the volume fraction of air, Φ_{air}, was a little lower

than for a β-casein foam. Foams made with β-lactoglobulin were not stiff, though a little brittle; they had a normal bubble size distribution. For all proteins addition of Tween increased the coarsening rate except for glycinin (pH 3) where Tween diminishes the brittleness of the glycinin foam but not the stiffness (results not shown).

In theory, disproportionation can be stopped for purely elastic adsorbed protein layers namely if the relation $E > \gamma/2$ is satisfied [9]. However, disproportionation still occurs in protein foams and this is in agreement with the theoretical prediction because protein films are visco-elastic causing E to be time dependent. Moreover, $E > \gamma/2$ is only valid for gas bubbles of similar size. For a 3-d system of gas cells E has to be larger than $\sim 2 \cdot \gamma$ to stop disproportionation [43]. Comparing the coarsening rate of β-casein and glycinin with their respective dilational moduli, it can be said that glycinin (having a higher E than β-casein) is more stable to coarsening.

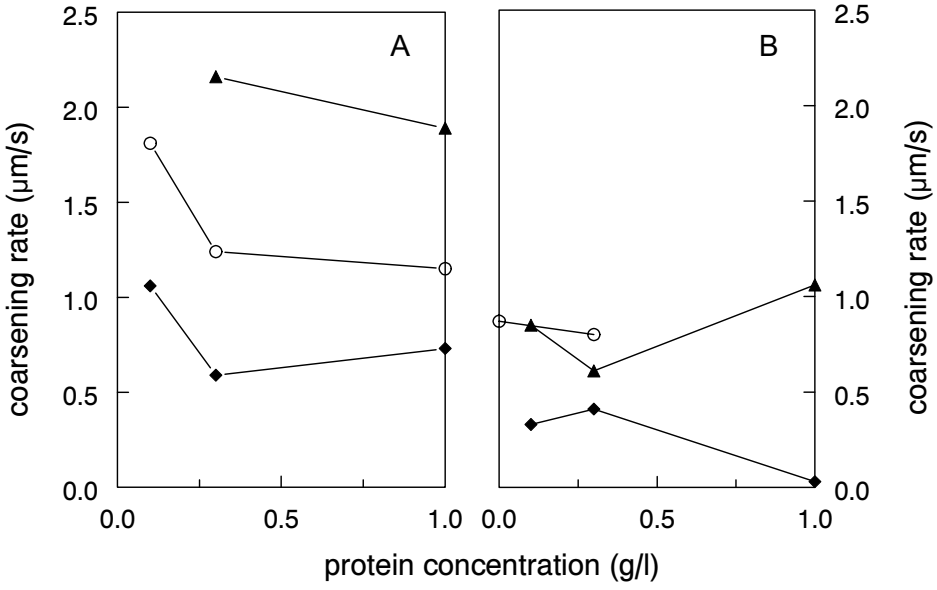

Figure 5.7 Coarsening rate (μm/s) of different proteins foams (0.1 g/l) made with the fanflutter (A, 3000 rpm) and the whipping apparatus (B, 450 rpm); (o) β-casein, (▲) β-lactoglobulin, (♦) glycinin pH 3

5.4 Discussion

5.4.1 Foam formation

Our results show that foam formation is strongly correlated to the rate at which γ can be lowered. If a protein cannot adsorb in a sufficient amount within the time scale of foam production, no foam is formed. Hence, the most important factor for foam formation is the adsorption rate. The adsorption rate depends on (i) the protein concentration, (ii) the molecular weight of the protein, (iii) protein structure and solution conditions such as (iv) pH. At concentrations of 0.1-1 g/l hardly any foam was produced with ovalbumin and glycinin (pH 6.7) whereas β-casein, β-lactoglobulin and glycinin (pH 3) behaved as good foaming agents. The adsorption of glycinin (pH 6.7) and ovalbumin to an expanding interface in order to stabilise gas cells is in the first place limited by the concentration: increasing the concentration up to 10 g/l resulted in foam formation. Secondly, glycinin (pH 6.7) has a molecular weight of 350 kDa, which is quite large with respect to the other proteins. The molecular weight of ovalbumin is similar to that of glycinin (pH 3) but due to a different protein structure the adsorption rate is lower for ovalbumin. The influence of the pH is visualised in the behaviour of glycinin, which associates at pH 6.7, leading to a larger molecule that adsorbs more slowly.

The adsorption behaviour of proteins can be described more quantitatively by the penetration theory for mass transport of surfactants by diffusion [9,44]. It estimates a time t (s), as a function of surfactant concentration, in which surfactant diffuses to the interface over a distance Γ / c yielding $t = \Gamma^2 / \pi \cdot c^2 \cdot D$ (where D is the diffusion coefficient). For high-molecular weight surfactants such as proteins the penetration theory is also valid but an additional time is needed in order for the proteins to find a proper conformation to 'attach' to the interface. The penetration theory can then be written as:

$$t \approx \frac{1}{c^2 \cdot D \cdot A^2 \cdot \beta} \qquad (3)$$

where c is the protein concentration (mol/m^3), A is the area of the adsorbed protein ($A \sim M^{2/3}$), D the diffusion coefficient (m^2/s) and β is the adsorption probability. If only diffusion of protein to the interface would be important for foam formation, then for all proteins the foaming capacity would be nearly equal since the diffusion coefficient only varies with a factor 2 at the most. However, foam formation is not only driven by diffusion of protein to the interface, the protein also needs time to adsorb/attach at the interface. This is represented by the parameter β. This parameter can be estimated if we suppose that the time available for foam formation is only determined by the foam production method and thus the same for all proteins, provided that we take the protein concentration at which a certain minimum amount of foam is formed.

In eq. (5.3), $D \sim M^{-1/3}$ and $A^2 \sim M^{4/3}$ resulting in $(D \times A^2) \sim M$. If for β-casein β is taken 1, then β can be calculated for the other proteins with respect to β-casein:

$$\frac{\beta_{\beta-cas}}{\beta_{protein}} \approx \frac{c^2_{protein} \cdot M_{protein}}{c^2_{\beta-cas} \cdot M_{\beta-cas}} \tag{5.4}$$

In Table 5.4 the minimum amount of protein needed for foam formation, the molecular weights and β are given for various proteins with respect to β for β-casein. The adsorption probability decreases in the order β-casein > β-lactoglobulin > glycinin (pH 3) > ovalbumin > glycinin (pH 6.7). This agrees with the order in lag time, i.e. the time after which the surface tension starts to decrease from 72 mNm^{-1}. Comparing the foaming properties of for example β-casein and ovalbumin the minimum protein concentration needed for foam formation differs by a factor 100. On the basis of diffusion only, increasing the protein concentration from 0.1 g/l (β-casein) to 10 g/l (ovalbumin) would lead to much shorter time scales for adsorption at the interface but this is not observed experimentally. Apparently, ovalbumin has much more difficulty to establish a stable contact with the interface than β-casein. This is reflected in its low adsorption probability.

Table 5.4 Adsorption probability β calculated for the minimum protein concentration needed for foam formation

	M (kDa)	protein conc. (g/l)	β
β-casein	24	0.1	1
β-lactoglobulin	37	0.3	0.073
ovalbumin	45	10	5.3×10^{-5}
glycinin (pH 6.7)	350	20	0.17×10^{-5}
glycinin (pH 3)	44	0.3	0.06

It is suggested that also the amount of SH/SS groups in a protein has an influence on the amount of foam formed. The volume of the foam formed was found to decrease with increasing amount of SS/mol protein; this indicates that it is important for protein molecules to be flexible enough to spread out at the interface to stabilise fresh air cells, thus preventing collapse of foams during foam formation [38]. The foaming capacity improves upon cleaving the SS-bridges using DTT [45]. Cleavage facilitates unfolding at the interface, which increases protein adsorption and hence foaming properties, possibly because of an increased number of points of contact with the interface. The role of thiol/disulphide bond interactions is protein

dependent [12]. It seems that for the formation of stable ovalbumin foams the essential factor is not the formation of intermolecular disulphide bonds, because disrupting them did not affect foam stability. Probably other non-covalent interactions play a role here [12].

5.4.2 Foam stability

Destabilisation mechanisms that occur in foams are drainage, disproportionation and coalescence. The foams made with β-casein, β-lactoglobulin and glycinin (pH 3) were studied for their stability against drainage and disproportionation. Coalescence was hardly observed in the foams studied. With respect to drainage of the three different foams we observed that all protein foams drained at the same rate provided that the sample container was initially completely filled with foam. This happens at different protein concentrations for β-casein, glycinin (pH 3) and β-lactoglobulin (namely at 0.3, 1 and 3 g/l, respectively). For drainage, the main factors are the film thickness, which is related to the amount of foam, and the mobility of the surface of the films between the gas bubbles. At high protein concentrations, coupled with a high volume fraction of gas, the film thickness will be more or less the same for all the proteins studied. Apparently, under the low shear and dilational stress conditions during film drainage the adsorbed protein layer behaves as rigid for all three proteins [9].

Stability against disproportionation was best correlated with a high E at the relevant ageing time (0-20 min) in agreement with theoretical predictions by Kloek *et al.* [43]. Experimentally, glycinin (pH 3) has a higher E and is also more stable to coarsening than β-casein.

5.4.3 Mechanical properties in relation to foam stability

It has been suggested that the formation of an interfacial protein gel layer is important for the stability of foams. Most likely, globular proteins with a strong internal structure and preferably free SH-groups have the highest ability to form a gel-like network at the interface. Globular proteins give high dilational moduli and shear viscosities and are difficult to be displaced from the surface by low-molecular-weight surfactants [3,18].

The ability to form a network is reflected in the interfacial properties, in particular in L_{still}, L_{still} versus Q_{still}, E, σ_{ss} and σ_f. For all of these parameters, except E after ageing, glycinin (pH 3) turns out to form the strongest interfacial gel and β-casein has the weakest network. Both proteins adsorb rapidly both at static and at expanding interfaces, and they form stable foams. This means that although β-casein has poor network forming capacities and glycinin (pH 3) forms strong interfacial films, their foam formation and stabilising properties against drainage are more or less equal. An

important factor with respect to stability against drainage is that the adsorbed layers are mobile or immobile under prevalent conditions; in general, all protein layers behave immobile [9]. Coalescence will be absent because of the large disjoining pressure for protein films. With respect to the stability against disproportionation the mechanical properties do have an influence: glycinin is more stable to coarsening than β-casein (see Table 5.3). Conclusively, the measured differences in mechanical properties of adsorbed protein layers only play a role in this study regarding a specific instability mechanism and are less important for other instability mechanisms. Moreover, besides their differences in mechanical properties there are also other differences between β-casein and glycinin (pH 3) such as flexibility, unfolding upon adsorption, the adsorbed amount or volume fraction of protein at the surface. It is not clear how these parameters influence the different mechanisms causing foam instability exactly.

The network forming properties of glycinin (pH 3) might be related to the possibility of SH/SS interactions. Whereas in solution only monomers were present, at the air/water interface (in foam) glycinin (pH 3) formed large aggregates upon ageing of the foam and these could be detected with FPLC [46]. β-Casein does not form similar aggregates. Whether or not the formation of intermolecular SS-bridges plays a role in the properties of surface films, foam formation and stability, is not yet clear, though several authors have speculated about this. Ovalbumin and β-lactoglobulin form strong films once they are adsorbed partly because of the possibility of forming SS-bridges.

The appearance of the foams can be correlated with the mechanical properties of the interface. Glycinin (pH 3) forms a very brittle and stiff foam. The brittleness can be related to the very low fracture stain and the stiffness to the high L_{still} and σ_{ss}. A β-lactoglobulin foam is also somewhat brittle and displays a low fracture strain. In contrast, the β-casein foam is much softer and fluid-like, as expected from film properties.

5.5 Conclusions

Various interfacial rheological techniques show that glycinin (pH 3) forms an interfacial protein gel layer in much shorter time-scales than β-casein, β-lactoglobulin, ovalbumin and glycinin (pH 6.7). Although ovalbumin and β-lactoglobulin have a higher E after ageing for 1.7 h, experiments with the overflowing cylinder and surface shear rheometer show that glycinin (pH 3) is more resistant to shear and to dilation under dynamic conditions.

Concerning foaming properties, no foam could be formed at the chosen conditions with ovalbumin and glycinin (pH 6.7) whereas β-casein, β-lactoglobulin

and glycinin (pH 3) behaved as good foaming agents. The rate at which d_{21} increases with time increased in the order glycinin (pH 3) < β-casein < β-lactoglobulin. Whereas glycinin forms strong interfacial films and β-casein has poor network forming properties, they both form reasonable amounts of foam. The most important factor for foam formation is therefore the adsorption rate and ability to unfold at the interface. Only for stability against disproportionation surface rheological properties were found to play a role. Due to a higher E, glycinin (pH 3) is more stable to coarsening than β-casein. Regarding the results shown in this paper it appears that the relation between surface rheological properties and foam stability is more subtle as has been suggested in literature and likely depends on the prevalent instability mechanisms of the foam involved.

References

1. Walstra, P. In: *Encyclopedia of emulsion technology*; Ed. P. Becher, Marcel Dekker; 1996, 2-62.
2. Dickinson, E. *J. Chem.Soc.Far.Trans.* **1998**, *94*, 1657-1669.
3. Wilde, P.J. *Curr. Op. Coll.Interface Sci.* **2000**, *5*, 176-181.
4. Murray, B.S. *Colloids Surf. A* **1997**, *125*, 73-83.
5. Murray, B.S.; Faergemand, M.; Trotereau, M.; Ventura, A. In: *Food Emulsions and Foams; Interfaces, Interactions and Stability*; Ed. E. Dickinson and M.J. Rodriguez Patino, Royal Society of Chemistry; 1999, 223-235.
6. Benjamins, J. **2000** PhD-thesis, Wageningen University, the Netherlands.
7. Prins, A.; van Kalsbeek, H.K. *Curr. Op. Coll.Interface Sci.* **1998**, *3*, 639-642.
8. Gandolfo, F.G.; Rosano, H.L. *J. Coll. Interface Sci.* **1997**, *194*, 31-36.
9. Prins, A. In: *Adv. Food Emulsions and Foams*; Ed. E. Dickinson and G. Stainsby, Elsevier; 1988, 91-122.
10. Prins, A. *Colloids Surf. A* **1999**, *149*, 467-473.
11. Dickinson, E. *Colloids Surf. B* **1999**, *15*, 161-176.
12. German, J.B.; Phillips, L. In: *Protein Functionality in Food Systems*; Ed. N.S. Hettiarachchy and G.R. Ziegler, IFT Basic Symposium Series; 1991, 181-208.
13. Izmailova, V.N.; Yampolskaya, G.P.; Tulovskaya, Z.D. *Colloids Surf. A* **1999**, *160*, 89-106.
14. Martin, A.H.; Bos, M.A.; Cohen Stuart, M.A.; van Vliet, T. *Langmuir* **2002**, *18*, 1238-1243.
15. Wüstneck, R.; Krägel, J.; Miller, R.; Fainerman, V.B.; Wilde, P.J.; Sarker, D.K.; Clark, D.C. *Food Hydrocoll.* **1996**, *10*, 395-405.
16. Boerboom, F.J.G.; de Groot-Mostert, A.E.A.; Prins, A.; van Vliet, T. *Netherlands Milk and Dairy Journal* **1996**, *50*, 183-198.
17. Chen, J.; Dickinson, E. *J. Sci.Food Agric.* **1993**, *62*, 283-289.

18. Mackie, A.R.; Gunning, A.P.; Wilde, P.J.; Morris, V.J. *J. Coll. Interface Sci.* **1999**, *210*, 157-166.
19. Nylander, T.; Wahlgren, N.M. *J. Coll. Interface Sci.* **1994**, *162*, 151-162.
20. Williams, A.; Prins, A. *Colloids Surf. A* **1996**,
21. Martin, A.H.; Bos, M.A.; van Vliet, T. *Food Hydrocoll.* **2002**, *16*, 63-71.
22. Wagner, J.R.; Guéguen, J. *J. Agric.Food Chem.* **1999**, *47*, 2173-2180.
23. Pezennec, S.; Gauthier, F.; Alonso, C.; Graner, F.; Croguennec, T.; Brulé, G.; Renault, A. *Food Hydrocoll.* **2000**, *14*, 463-472.
24. Benjamins, J.; van Voorst Vader, F. *Colloids Surf.A* **1992**, *65*, 161-174.
25. van Vliet, T.; Martin, A.; Renkema, M.; Bos, M. In: *Plant Biopolymer Science, Food and Non Food Applications*; Ed. D. Renard, G. Della Valle and Y. Popineau, Royal Society of Chemistry; 2002, 241-252.
26. de Jongh, H.H.J.; Gröneveld, T.; de Groot, J. *J. Dairy Sci.* **2001**, *84*, 562-571.
27. Tanh, V.H.; Shibasaki, K. *J. Agric.Food Chem.* **1976**, *24*, 1117-1121.
28. Benjamins, J.; Cagna, A.; Lucassen-Reynders, E.H. *Colloids Surf. A* **1996**, *114*, 245-254.
29. Cagna, A.; Esposito, G.; Rivière, C.; Housset, S.; Verger, R. (1992),*33rd International Conference on Biochemistry of Lipids, Lyon*.
30. Bergink-Martens, D.J.M. **1993** PhD-thesis, Wageningen Agricultural University, The Netherlands.
31. Boerboom, F.J.G. **2000** PhD-thesis, Wageningen University, The Netherlands.
32. Prins, A.; Boerboom, F.J.G.; van Kalsbeek, H.K.A.I. *Colloids Surf. A* **1998**, *143*, 395-401.
33. Whorlow, R.W. Rheological Techniques; Ellis Horwood Limited; New York; 1992.
34. Lyklema, J. Fundamentals of Interface and Colloid Science, Volume III: Liquid-Fluid Interfaces; Academic Press; London; 2000.
35. Durian, D.J.; Weitz, D.A.; Pine, D.J. *Science* **1991**, *252*, 686-688.
36. McKenzie, H.A.; Sawyer, W.H. *Nature* **1967**, *214*, 1101.
37. Graham, D.E.; Phillips, M.C. *J. Coll. Interface Sci.* **1979**, *70*, 427-439.
38. Townsend, A.-A.; Nakai, S. *J. Food Sci.* **1983**, *48*, 588-594.
39. Bos, M.A.; Grolle, K.; Kloek, W.; van Vliet, T. **2002**, accepted for publ. in Langmuir.
40. Dickinson, E.; Murray, B.S.; Stainsby, G. *J. Coll. Interface Sci.* **1985**, *106*, 259-262.
41. Murray, B.S. **1987** PhD-thesis, University of Leeds, United Kingdom.
42. Roth, S.; Murray, B.S.; Dickinson, E. *J. Agric.Food Chem.* **2000**, *48*, 1491-1497.
43. Kloek, W.; van Vliet, T.; Meinders, M.B.J. *J. Coll. Interface Sci.* **2001**, *237*, 158-166.
44. Ward, A.F.H.; Tordai, L. *J. Chem. Phys.* **1946**, *14*, 453-461.
45. Kim, S.H.; Kinsella, J.E. *J. Food Sci.* **1987**, *52*, 128-131.
46. Bos, M.; Martin, A.; Bikker, J.; van Vliet, T. In: *Food Colloids, Fundamentals of Formulation*; Ed. E. Dickinson and R. Miller, Royal Society of Chemistry; 2001, 223-232.

6 Mechanical behaviour of protein films at the air/water interface in relation to the protein molecular properties

AH Martin, MA Cohen Stuart, MA Bos & T van Vliet
in preparation (2003)

ABSTRACT

The relation between mechanical film properties of various adsorbed protein layers at the air/water interface and molecular properties of the corresponding proteins is discussed. Mechanical film properties were determined by surface deformation in shear and dilation. In shear, fracture stress σ_f and strain γ_f were determined as well as the relaxation behaviour after macroscopic fracture. The dilational measurements were performed in a Langmuir-trough equipped with an Infra-Red Reflection Absorption Spectroscopy (IRRAS) accessory. During compression and relaxation of the surface, the surface pressure Π and adsorbed amount Γ (determined from the IRRAS spectra) were determined simultaneously. In addition, IRRAS spectra revealed information on conformational changes in terms of secondary structure. Possible correlations between macroscopic film properties and molecular properties of the proteins in terms of molecular dimensions and secondary structure were determined and discussed. Molecular properties involved, among others, the area per protein molecule at Π~0 mN/m (A_0), A_0/M (M = molecular weight), the maximum slope of the Π-Γ curves ($d\Pi/d\Gamma$) and the volume fraction ϕ of the protein in the 'interfacial' gel. The differences observed in mechanical properties and relaxation behaviour indicate that the behaviour of a protein film subjected to large deformation may vary widely from predominantly viscous (yielding) to more elastic (fracture). The transition from viscous to elastic behaviour can be related to the density of the protein layers. Layers with low ϕ and higher A_0/M have a high γ_f and behave more viscously whereas protein films characterised by high ϕ, low A_0/M have a low γ_f and behave more elastically.

6.1 Introduction

In systems like emulsions and foams proteins are known to often form a cohesive visco-elastic film around oil droplets and air cells which appears to stabilise them against flocculation, coalescence or disproportionation. The process of network formation of proteins at the interface can be viewed as a three-step process, namely, the adsorption and initial anchoring of the protein at the interface, the accompanying conformational change and subsequent rearrangement of the adsorbed protein and the formation of a protein network with specific mechanical properties [1,2]. Adsorption of proteins at the air/water interface has been fairly well studied and the molecular factors affecting the initial anchoring are partly understood [3-7]. The conformational changes that take place upon adsorption at the air/water interface have been studied to a much lesser extent. Information on conformational changes has been frequently deduced from indirect evidence, namely by relating surface excess, surface pressure and protein layer thickness to protein molecular dimensions [8-10]. Recently, however, Meinders *et al.* [11], Renault *et al.* [12] and Martin *et al.* [13] have reported on in situ measurement of structural changes in terms of secondary structure of proteins upon adsorption at the air/water interface using Infra-Red Reflection Absorption Spectroscopy (IRRAS). Relatively small changes in secondary structure were observed, but no conclusions could be drawn about the extent to which tertiary structure changes.

Conformational changes of proteins at the interface permit the formation of intermolecular bonds and partly as a result of this visco-elastic protein films are formed. These films can be mechanically characterised by deformation in shear (shape changes) or in dilation (area changes) as has often been done in literature [2,14-16]. The results of these studies show differences in mechanical strength for various proteins, but a molecular explanation for the differences is not really available. The relation between protein molecular properties, such as secondary structure or hydrophobicity, and adsorption properties was earlier discussed by Razumovsky *et al.* [1], but they did not deal with visco-elastic properties of protein films. The aim of this study is therefore to relate *mechanical* properties of protein films to protein molecular properties. Protein molecular properties are defined in terms of molecular dimensions and secondary structure. Molecular dimensions may involve those of single proteins, e.g. the area occupied by one film forming protein (A_0) or those of the interfacial protein network. In the latter case the adsorbed protein layer is seen as a 3-dimensional gel in which the dimension perpendicular to the interface is relatively small (< 0.01 μm) [17].

As a rule the molecules in ‘interfacial’ and bulk gels interact cohesively, i.e. they form physical, sometimes even chemical, intermolecular bonds. Examples of intermolecular bonding are hydrophobic interactions or disulphide bridging; the latter

was found to be normally of less importance at air/water interfaces [18]. Both Renault *et al.* [12] and Martin *et al.* [13] reported on the possibility to measure one type of intermolecular aggregation at the interface, i.e. the formation of anti-parallel β-sheets by ovalbumin and (soy) glycinin, respectively. Intermolecular β-sheet formation due to hydrogen bonding between protein molecules was observed and this is probably one of the reasons that ovalbumin and glycinin form a cohesive protein film. It indicates that changes in secondary structure may be related to the formation of a strong protein network at the interface.

In this paper we look for correlations between the mechanical properties of adsorbed protein films and the molecular properties of the corresponding proteins. The mechanical properties are derived from force measurements on films under shear and dilation and from the relaxation behaviour after exposure to shear/dilation. Particularly the latter served to assess the extent of elasticity of a protein film. IRRAS spectra were simultaneously recorded of the surfaces exposed to dilation. These spectra provide information on the adsorbed amount and on the level of secondary structure changes [13]. From Π-Γ curves, A_0 and the maximum slope of the curve ($d\Pi/d\Gamma$) can be derived. These two properties would seem to reflect the molecular flexibility and compressibility of the protein film. The relation between mechanical properties and molecular dimensions or even secondary protein structure would give a deeper insight into the behaviour of the protein molecule itself.

6.2 Materials & Methods

6.2.1 Materials

β-Lactoglobulin was purified according to the method of de Jongh *et al.* [19]; β-casein was purified from acid-precipitated casein following the method described by Swaisgood [20]; ovalbumin was obtained from Sigma (grade V). Glycinin was isolated from soybeans according to the fractionation scheme given by Tanh and Shibasaki [21] and further prepared as described by Martin *et al.* [22].

Proteins were dissolved in a phosphate buffer of pH 6.7 (ionic strength 30 mM). Glycinin was also measured at pH 3 (I=30 mN) and for those measurements a citric acid/phosphate buffer was used. The chemicals used for the buffers, Na_2HPO_4, NaH_2PO_4 and $C_6H_8O_7{\cdot}H2O$ were purchased from Merck (Darmstadt, Germany, analytical grade). All solutions were made with doubly distilled water and stirred for 1 hour. Temperature was kept at 23°C.

6.2.2 Surface shear rheometer

Stress-time curves were determined using a two-dimensional Couette-type interfacial viscometer as described previously [23]. A stainless steel biconical disc

(diameter 30 mm) was suspended by a torsion wire such that the disc edge was in the plane of the air/water interface. The protein solution was contained in a thermostated circular glass dish (diameter 145 mm). The thickness of the selected torsion wire was 0.20 mm (glycinin), 0.15 mm (β-lactoglobulin, ovalbumin) and 0.10 mm (β-casein); the torsion wire length was always 740 mm. Stress-time curves were made as a function of ageing time of the protein layer. Stress was exerted on the inner disc by rotating the outer dish at a fixed shear rate until a steady state stress, σ_{ss}, was observed, usually after 10-20 minutes. The stress at the disc edge, σ, was calculated according to Whorlow [24]:

$$\sigma = \frac{K \cdot \Theta_i}{2\pi \cdot R_i^2} \tag{6.1}$$

where K represents the torsion wire constant, Θ_i (rad) the rotation of the disc and R_i the radius of the disc. After σ_{ss} was reached the rotation of the dish was stopped and the stress relaxation was followed as a function of time. At intervals of 1 hour, the measurement procedure was repeated; the starting position of a subsequent measurement was determined by the position reached after stress relaxation of the previous measurement. Temperature was kept constant at 23°C.

6.2.3 IRRAS

Experimental

IRRAS spectra were acquired by collecting the externally reflected light beam, using an Equinox 55 Fourier Transform InfraRed (FTIR) spectrometer (Bruker) attached to an IRRAS accessory (XA500) equipped with a broadband MCT detector. The IRRAS accessory contained a Langmuir trough (NIMA Technology) consisting of two separate compartments, one for the buffer (length × width = 26 × 5 cm) and the other for the protein solution (length × width = 26 × 10 cm). The volumes of the buffer and protein solutions were 200 ml and 400 ml, respectively. The spectrometer was continually purged with dry air. A NIMA balance with a Wilhelmy-plate was used to measure the surface pressure.

FTIR-spectra were acquired from 1000 cm^{-1} to 5000 cm^{-1} using s-polarised light. Data were collected at 2 cm^{-1} resolution; typically 100 scans (scanning velocity 20 kHz) were averaged. The angle of incidence was 30°. Buffer was used as background and the IRRAS spectrum was corrected (if necessary) for water vapour contributions by subtracting a water vapour spectrum. After data acquisition and water subtraction the spectrum was smoothed to 8 cm^{-1} resolution.

Attenuated Total Reflection (ATR) spectra were collected on a Biorad FTS6000 equipped with a broadband MCT detector using a Ge crystal (45°, trapezoid, six internal total reflections).

Measurements were performed at room temperature. The Langmuir-trough and IRRAS equipment were placed in a Perspex box to keep out dust and to create a constant atmosphere. The protein solution was poured into the Langmuir trough; before a measurement was started the surface was cleaned by suction of the compressed surface. The surface pressure Π (mN/m) and adsorbed amount Γ (mg/m^2) were followed during one hour after which the surface was compressed. After compression IRRAS spectra were recorded every 10 minutes and Γ was determined simultaneously with Π. After 70 minutes the surface was expanded again.

Spectral simulations

The reflectivity of a sample R is defined as the ratio of the specularly reflected light intensity I_R and the incident intensity I_0, ($R=I_R/I_0$). It is a function of the wavenumber, the angle of incidence, the polarisation of the incoming light and the optical properties of the material measured. The latter are captured by the complex refractive index $\hat{n}$, which consists of a real part, the refractive index n, and an imaginary part, the extinction coefficient k. The extinction coefficient is related to the absorption coefficient $\alpha = 4\pi k/\lambda$ (with λ the wavelength of the incoming light) which is measured in ATR and transmission experiments. The optical properties are directly related to the protein concentration, conformation and orientation [25].

IRRAS spectra are presented as –log (R/R_{ref}), where R is the IR reflection spectrum of the sample (the aqueous protein solution) and R_{ref} is that of the reference (buffer). We simulated IRRAS spectra using an ATR spectrum of a dried protein film, which gives the absorption coefficient α of the protein. The optical constants of H_2O were taken from literature [26]. A detailed description of the simulation method, in which a single homogeneous layer model is used, has been published by Meinders *et al.* [25]. Fit parameters are the proportionality constant relating the protein ATR spectrum to the protein absorption coefficient, the concentration of the protein in the adsorbed layer (c_1) and in the subphase (c_2) and the thickness of the adsorbed layer (d). The thickness of the subphase is taken to be infinite (i.e. much larger than the probing depth of about 500 nm). The adsorbed amount Γ is determined as $\Gamma = c_1 \cdot d$.

6.3 Results & Discussion

6.3.1 Stress relaxation following deformation in shear

Adsorbed protein layers of β-casein, β-lactoglobulin and glycinin (pH 3) were subjected to deformation in shear. The stress exerted on the disc was followed as a function of time and for each protein the shape of the stress-time curve was found to be characteristic for the protein studied [23]. In Figure 6.1A a stress-time curve is given for β-lactoglobulin at different ageing times of the protein layer. At the maximum of the curve the protein layer fractures at a certain fracture strain γ_f; the accompanying stress is called the fracture stress σ_f. The stress reached at t~10 minutes is termed the steady state stress σ_{ss}. Both σ_{ss} and σ_f depend on the strength of the protein layer, which is related to the extent of cohesive interactions between the proteins at the surface. In Table 6.1 values are given for σ_{ss}, σ_f and γ_f for adsorbed layers of β-casein, β-lactoglobulin, ovalbumin and glycinin (pH 3 and pH 6.7) at ageing times of 1 and 8 hours. Differences between proteins can be observed in the magnitude of σ_{ss} and σ_f but also in the increase in these parameters as a function of time. Whereas σ_{ss} for glycinin (pH 3, high σ_{ss}) and β-casein (very low σ_{ss}) increases only to a relatively small extent as a function of ageing time, for β-lactoglobulin, ovalbumin and glycinin (pH 6.7) it increases enormously upon ageing (more than a factor 10).

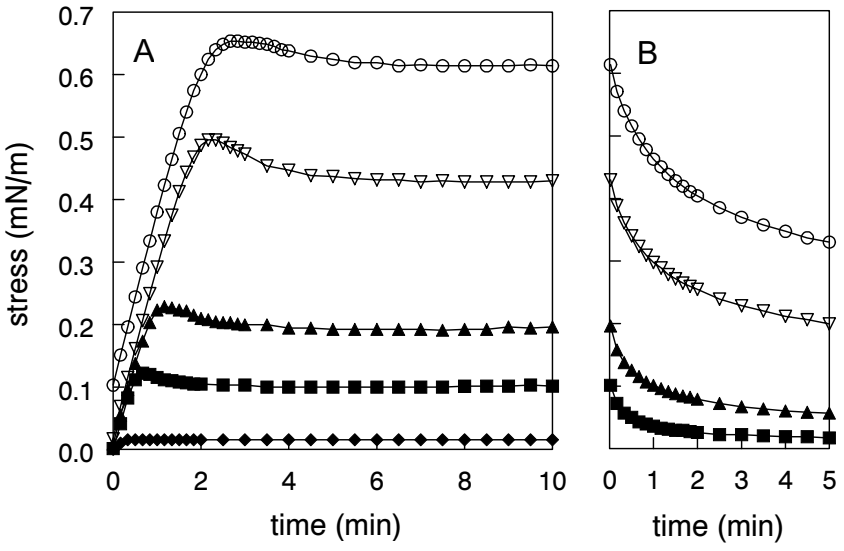

Figure 6.1 Stress-time curve for β-lactoglobulin at different ageing times of the protein film: (♦) t=0h53, (■) t=2h30, (▲) t=3h53, (∇) t=5h53, (o) t=7h07; A = deformation in shear, B = relaxation after deformation in shear

After t~10 minutes σ_{ss} is reached and at that point the deformation of the protein layer is stopped. Immediately, the stress present in the protein layer starts to decrease. In Figure 6.1B this is shown for β-lactoglobulin for different ageing times of the protein layer. At short ageing times σ goes more or less back to zero but with ageing of the protein layer σ becomes larger and the decrease in σ upon relaxation less. The stress does not return to zero but attains a new steady state value meaning that some of the stress is retained in the protein network. For glycinin (pH 3) similar results were found; however, σ_{ss} was much higher and the relative decrease less. In Figure 6.2 the relaxation behaviour of β-lactoglobulin and glycinin (pH 3) is plotted on a double logarithmic scale. For β-casein it was not possible to follow the stress with time due to the very low values of σ. Figure 6.2 shows that for glycinin the decrease in stress is much less during relaxation than for β-lactoglobulin and that both proteins give an algebraic decrease in stress as function of time. The relaxation behaviour of σ with time could be fitted to a power law: $\sigma = a \cdot t^{-b}$ where a is determined by the mechanical strength of the protein layer (stress at t=1 s) and b is a measure of the elasticity of the layer termed as 1/b. The higher 1/b, the less the stress relaxation and the more elastic the layer. The value b=0 corresponds to purely elastic behaviour. Both a and b depend on protein type and ageing time of the protein layer. For both β-lactoglobulin and glycinin (pH 3) 1/b was found to increase with ageing time of the protein layer meaning that the protein layer became more elastic as the protein network grew stronger. Upon ageing for 6 hours 1/b increased from 14 to 50 for glycinin (pH 3) and from 2 to 6 for β-lactoglobulin. A glycinin (pH 3) layer thus behaves much more elastically than a β-lactoglobulin layer, and the factor by which the elasticity increases is somewhat higher for glycinin as well.

Table 6.1 Mechanical properties of adsorbed layers of β-casein, β-lactoglobulin, glycinin and ovalbumin at the air/water interface

	t_{age} ~ 1 hour			t_{age} ~ 8 hours		
	σ_{ss} (mN/m)	σ_f (mN/m)	γ_f (-)	σ_{ss} (mN/m)	σ_f (mN/m)	γ_f (-)
β-casein	0.001	-	-	0.002	-	-
β-lactoglobulin	0.01	0.015	0.05	0.6	0.65	0.15
ovalbumin	0.01	0.01	0.12	0.5	0.5	0.4
glycinin (pH 3)	2	2	0.2	3.2	4.1	0.1
glycinin (pH 6.7)	0.2	0.2	0.6	2.6	3	0.35

σ_{ss} = steady state stress, σ_f = fracture stress at maximum, γ_f = fracture strain at maximum

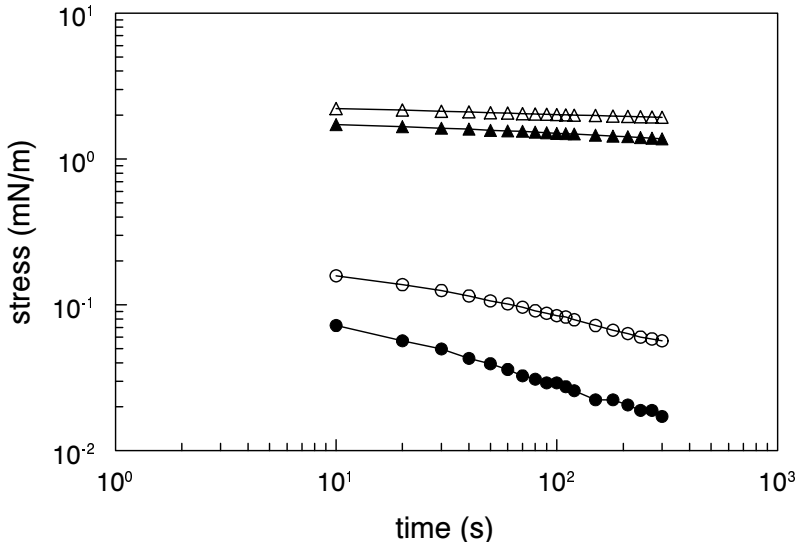

Figure 6.2 Relaxation behaviour of β-lactoglobulin and glycinin plotted on a log stress vs. log time scale at 2 different ageing times of the protein film; (o) β-lactoglobulin, (Δ) glycinin (pH 3); closed symbols t~2.5 hours, open symbols t~5 hours

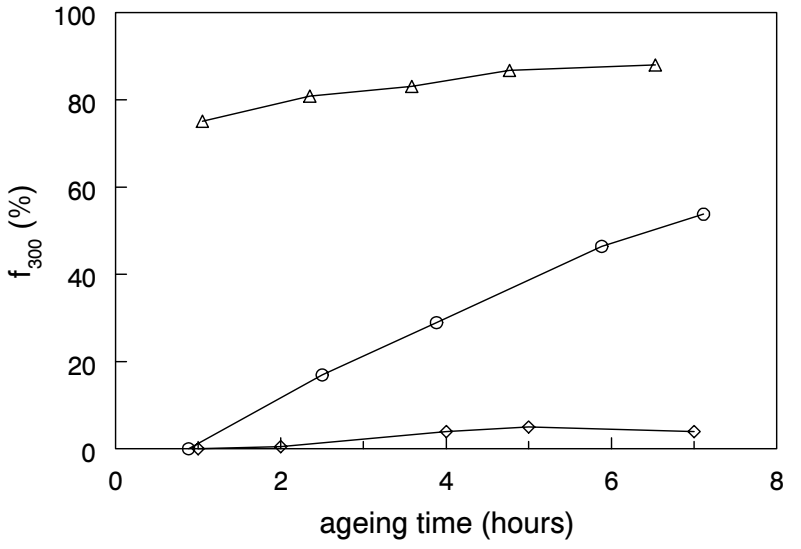

Figure 6.3. The amount of stress retained in protein layer (f_{300} = (σ_{end} / σ_{start}) * 100) as a function of ageing time; (◊) β-casein, (o) β-lactoglobulin, (Δ) glycinin (pH 3)

After relaxation a certain amount of stress is retained in the layer. The fraction of stress after 300 s, f_{300}, is calculated as follows

$$f_{300} = \frac{\sigma(t = 300s)}{\sigma(t = 0s)} * 100 \qquad (6.2)$$

In Figure 6.3 f_{300} is given as a function of ageing time of the protein layer, for β-casein, β-lactoglobulin and glycinin (pH 3) respectively. Glycinin is able to maintain ~80% of the stress whereas for β-casein the stress relaxes almost completely. Both proteins show only small changes upon ageing of the protein film. For β-lactoglobulin, f_{300} increases from 0% to 50% with ageing time meaning that the properties of a β-lactoglobulin film change considerably upon ageing. The large increase in σ_{ss} and f_{300} indicate major changes in the β-lactoglobulin layer upon ageing. These changes could be the result of further changes in conformation, disulphide bridging or other intermolecular interactions. As our IRRAS data did not show any further changes in secondary structure between ~7 minutes and 8 hours after adsorption [13], we have an indication that the increase in strength is not due to changes in secondary structure and (probably) also not in tertiary structure. With regard to disulphide bridges, the influence of the SS-interchange reaction on the network formation of proteins at the air/water interface is not unambiguous at all and is probably not the dominant mechanism of protein-protein interactions [18]. Therefore the large increase in σ_{ss} is probably due to a change in network structure or to an increase in other types of intermolecular bonding such as hydrophobic interactions.

In general, the differences in σ_{ss} and in relaxation behaviour between β-casein, β-lactoglobulin and glycinin (pH 3) indicate that mechanical properties of protein films may vary widely from predominantly viscous to predominantly elastic. One remark has to be made concerning the meaning of the steady state stress and the relaxation behaviour after deformation in shear, because these are both determined after failure of the protein layer. As stated previously [23], σ_{ss} can be seen as the condition under which the rate of bond breakage due to shearing is balanced by the rate of bond formation. For β-lactoglobulin σ_{ss} was constant in time but for glycinin σ_{ss} fluctuated, which might be due to friction between pieces of fractured protein layer passing each other. This would mean that the film was not homogeneous. Moreover, the filling up of the ‘cracks’ caused by the fracture process with fresh protein from the bulk solution might lead to irregularities in the stress. After failure, the following three processes could play a role: (1) relaxation within the protein film, (2) a repair mechanism: adsorption of protein from solution in the cracks caused by fracture and (3) friction of patches of protein films moving along each other. After failure of the protein film mechanism 3 is probably most dominant but also the repair mechanism may play a role. Similar measurements performed on spread protein layers showed more

relaxation behaviour (data not shown) meaning that it is likely that adsorption from solution plays a role. The role of mechanism 1 is almost negligible regarding the behaviour of a protein film *after* failure. Following stress relaxation *before* σ_f was reached, σ hardly decreased for glycinin (pH 3). For $\gamma \leq 0.02$ the behaviour of glycinin (pH 3) was almost purely elastic, solid-like. Upon further deformation ($0.02 < \gamma < \gamma_f$) the stress relaxation was somewhat more extensive. However, it was still much less than the stress relaxation after macroscopic fracture (data not shown).

6.3.2 Surface pressure relaxation following area changes

Adsorbed protein layers of β-casein, β-lactoglobulin and glycinin (pH 3), respectively, were subjected to compression. The surface area was first compressed from 200 to 85 cm^2 after which $\Pi(t)$ and $\Gamma(t)$ were determined. In Figure 6.4 $\Pi(t)$ and $\Gamma(t)$ are given for (a) β-casein, (b) β-lactoglobulin and (c) glycinin (pH 3). At t=130 min the surface was expanded back to 200 cm^2 and $\Pi(t)$ and $\Gamma(t)$ were measured again. Upon compression of the surface both Π and Γ always increased, while during relaxation both parameters decreased again; the extent to which this happened depended on the protein. For β-casein, which formed the most fluid film of the three proteins studied, both Π and Γ rapidly decreased during relaxation, but 1 hour was not enough to reach static values. Upon expansion Γ decreased but during relaxation it recovered to reach a higher value than before the compression. For β-lactoglobulin Γ and Π first decreased rapidly but after 30 min relaxation stopped altogether: during relaxation steady state values were obtained. Upon dilation the initial Π and Γ were recovered. Glycinin (pH 3) formed the most elastic film and behaved accordingly: during relaxation Γ changed only little and upon dilation Γ seemed to go back to its original value. The relaxation behaviour of these three proteins appeared to be quite different. For the sake of simplicity three idealised cases of $\Gamma(t)$ profiles are schematically shown in Figure 6.5: (a) a predominantly viscous behaviour, (b) a visco-elastic behaviour and (c) a completely elastic behaviour. The differences in relaxation behaviour may be related to desorption/re-adsorption behaviour of (segments of) proteins, packing density of the molecules at the surface and the extent of elasticity of the protein layer. Such effects can be studied by looking at the IRRAS spectra taken during compression and relaxation. In Figure 6.6A experimental IRRAS spectra are given for β-casein in the water band region. Upon compression of the surface the intensity of both the (negative-oriented) amide I and II bands and the (positive-oriented) water band at 3600 cm^{-1} increased.

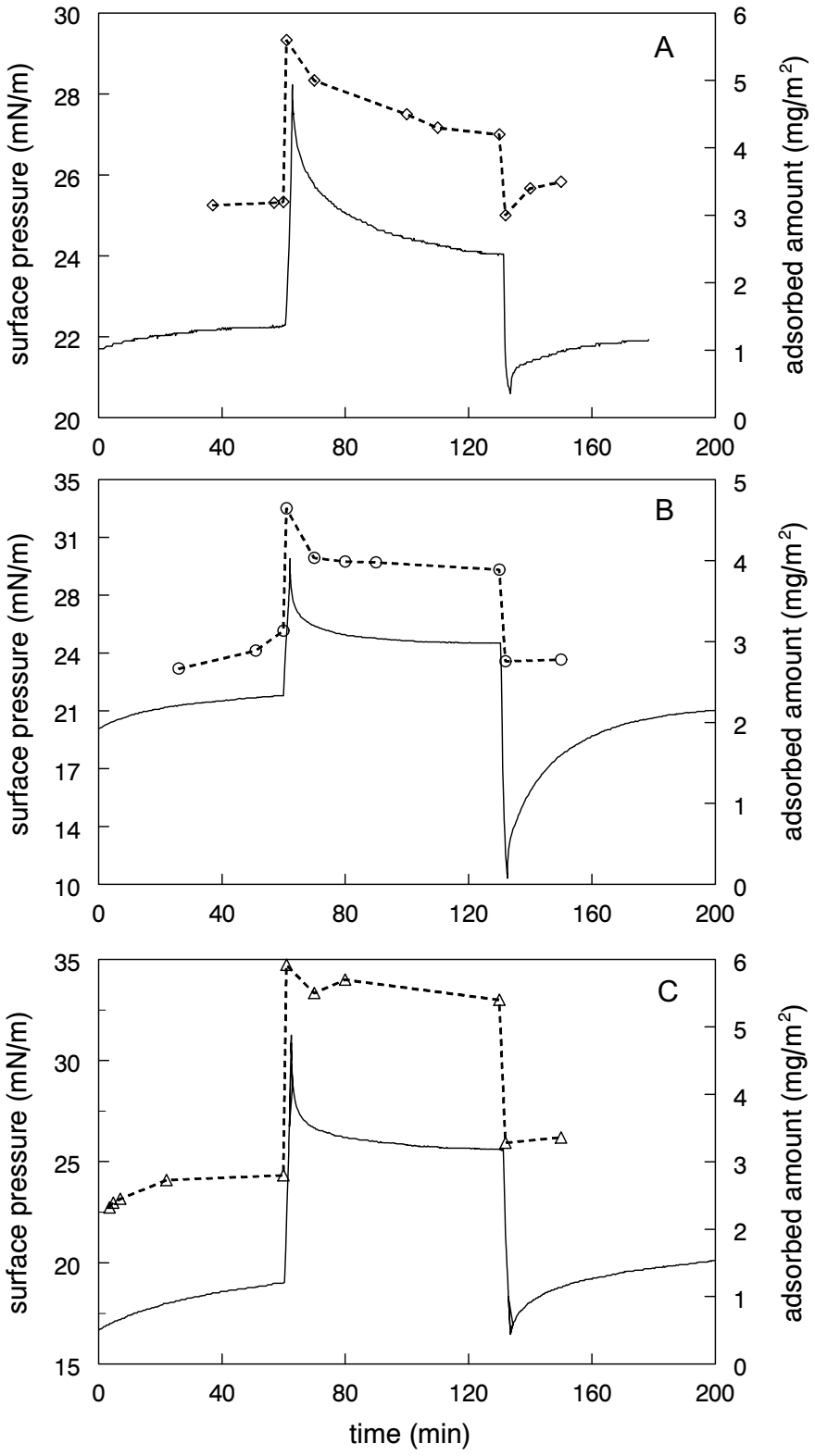

Figure 6.4 Relaxation of surface pressure (mN/m) (solid line) and adsorbed amount (mg/m^2) (dashed line) upon compression (at t=60 min) and expansion (at t=130 min) of the surface, measured simultaneously with IRRAS; (A) β-casein, (B) β-lactoglobulin and (C) glycinin (pH 3)

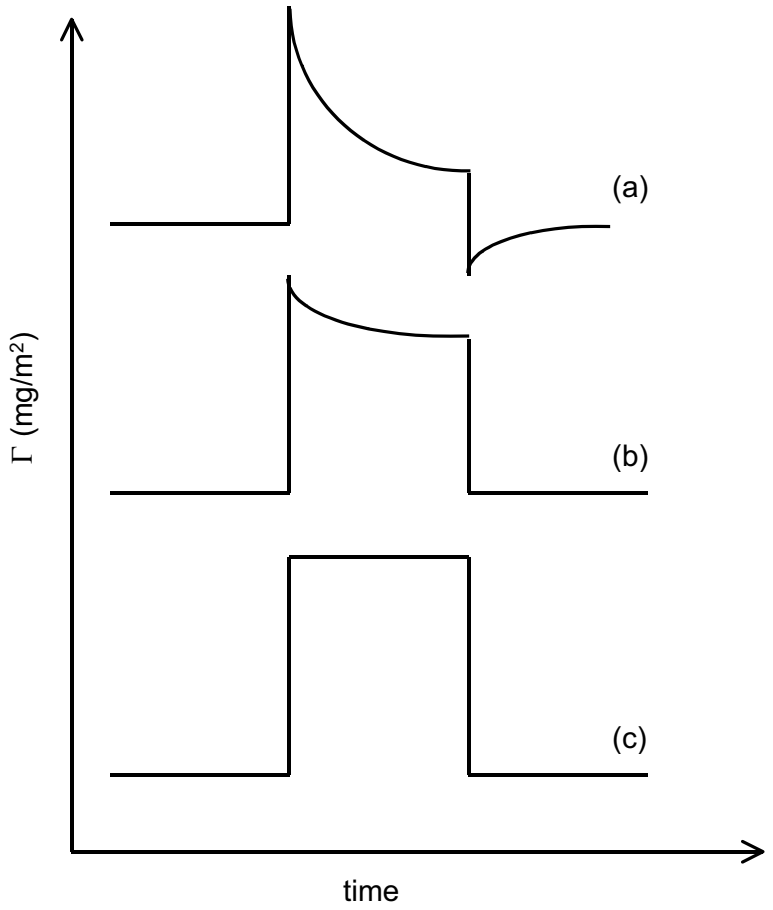

Figure 6.5 Three idealised relaxation profiles of Γ (mg/m^2) as a function of time upon compression and expansion of the surface (see also Figure 6.4); (a) predominantly viscous behaviour, (b) visco-elastic behaviour and (c) elastic behaviour

The increase in the amide I and II bands is due to an increase in protein concentration in the surface layer. Because the spectrum of the protein sample is measured relative to that of the protein free sample, an *increase* in intensity of the water band is related to a *decrease* of the volume fraction of water in the surface layer. It illustrates the depletion of water from the interface by the volume occupied by the protein. Hence, the amount of proteins per unit area increased upon compression, but also the water content of the layer decreased, which must imply the formation of a dryer and probably thicker protein film. During relaxation the intensity of the water band *decreases*; this is related to an *increase* in the volume fraction of water in the surface layer and therefore to a decrease in volume fraction of protein suggesting partial desorption of proteins. For glycinin (pH 3) (see Figure 6.6B) the intensity of the water band stayed constant during relaxation, indicating that no change in protein volume fraction took place, whereas β-lactoglobulin showed an

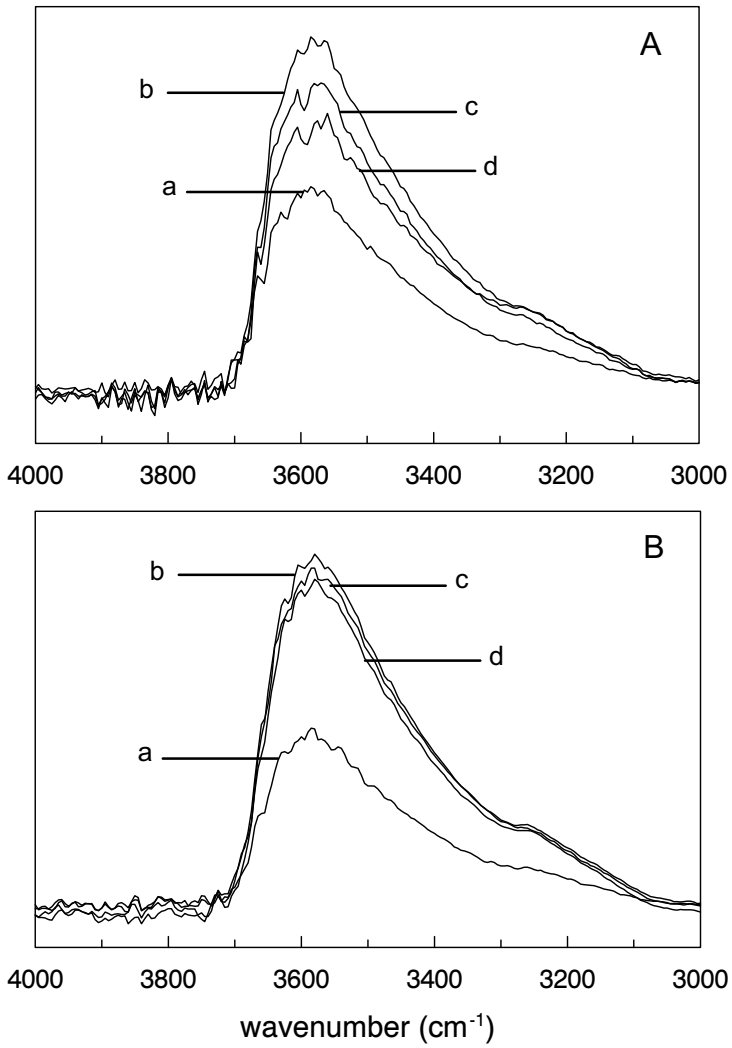

Figure 6.6 Experimental IRRAS spectra in the water band region of (A) β-casein (0.1 g/l) and (B) glycinin (pH 3) (0.1 g/l) adsorbed at the air/water interface; (a) area ~200 cm^2, (b) compression to area ~85 cm^2, (c) relaxation, t=10 min. after compression and (d) relaxation, t=30 min. after compression

initial decrease in intensity but after that, the protein volume fraction in the adsorbed layer remained constant too.

Also the packing density and the extent of elasticity of the protein film play a role in the way the protein layer responds to compression. Upon compression protein molecules are pushed together and a denser layer with a higher volume fraction of protein is formed (see Figure 6.6). β-Casein rearranges probably by forming a thicker layer with tails and loops; however, upon further compression protein molecules are pushed entirely out of the surface. This can be deduced from the decrease in Γ

during relaxation and from the decrease in intensity of the water band in the IRRAS spectra. Above a certain surface pressure the protein layer may collapse leading to a gradual displacement of the less hydrophobic segments of the protein molecule from the interface [27]. After expansion the interface is only partially occupied and will be refilled by adsorption from the solution, hence a small increase in Γ. For glycinin (pH 3), the layer behaves very elastically. Compression of the layer did not result in desorption of the protein from the surface. The compressed proteins merely go back to their original configuration upon expansion of the surface. After spontaneous adsorption the area per molecule available is initially large (see Table 6.2) but upon compression the proteins will do with less area. Glycinin molecules probably rearrange themselves in relation to each other during compression, thus decreasing the required area per molecule at the surface. Perhaps also buckling occurs, but not enough to induce a change in the layer thickness as measured by IRRAS (which is rather inaccurate). β-Lactoglobulin is an intermediate case: it is neither viscous like β-casein nor elastic like glycinin. During relaxation partial desorption plays a role, likely combined with buckling; the elastic part accounts for the facts that Γ reaches a steady state and that no re-adsorption takes place.

Table 6.2 Molecular properties of various proteins (pH 6.7); M = molecular weight; A_0 = area per molecule at Π~0; $d\Pi/d\Gamma$ (= maximum slope of Π-Γ curve); values for A_0 are derived from literature and own work: * = ref [28], # = ref [29], + = own work

	M (kDa)	A_0 (nm^2)	A_0 / M	$d\Pi/d\Gamma$ (mN·m/mg)
β-casein[*,#,+]	24	58	2.41	17
β-lactoglobulin[*,+]	18.3	28	1.53	30
glycinin (pH 3)[+]	44	62	1.41	38
ovalbumin[#]	45	75	1.67	32
lysozyme[#]	14.5	19	1.33	30
κ-casein[#]	19	37	1.94	14
bsa[*,#]	69	124	1.80	26

6.3.3 Molecular properties of proteins in relation to film properties

We will now attempt to correlate the behaviour of protein films in shear and dilation to the properties of a single protein molecule, namely its molecular dimensions and secondary structure.

Molecular dimensions

Upon adsorption proteins occupy a certain area at the interface and only above a certain coverage Π will start to increase. For each protein there exists a critical surface concentration (Γ_0) above which it can cause a measurable (and often steep) rise in Π. We define A_0 (= $1/\Gamma_0$) as the area (nm^2) occupied by a protein molecule at Π~0 mN/m just at the point where the protein film begins to sustain a pressure. A_0 can be determined from the intersection of the Π-Γ curve with the x-axis. Upon increasing Γ the surface pressure starts to rise and the maximum slope of this part of the curve is termed $d\Pi/d\Gamma$. In Table 6.2 A_0 and $d\Pi/d\Gamma$ are given for various proteins; the table includes values taken from literature. A_0 seems to be related to both the molecular weight M and molecular dimensions of the protein molecules: the larger M the larger A_0. Comparing the molecular dimensions of for example β-lactoglobulin, glycinin (pH 3) and β-casein we find that the size of a β-lactoglobulin molecule (~3 nm, globular) is smaller than that of glycinin (~5×7.5 nm [22]) or β-casein (1.5×15 nm, prolate ellipsoidal); per molecule β-lactoglobulin would therefore occupy less area. Razumovsky *et al.* [1] suggest that high values of A_0 correlate with strongly cohesive films. However, we could not confirm this correlation but by taking A_0/M and therefore ruling out the effect of the protein molecular weight, a correlation can be found between A_0/M and the mechanical properties of protein films. For each protein in Table 6.2 σ_{ss} was determined; values for σ_{ss} were taken either from Table 6.1 or deduced from literature [14,30]. Figure 6.7 shows that the lower A_0/M the stronger (in terms of mechanical properties) the protein film. The curve in Figure 6.7 can be described as $\sigma_{ss} \approx e^{-(A_0/M)}$ and because A_0/M (nm^2/mol) is related to $1/\Gamma_{\Pi\sim0}$ (m^2/mg), σ_{ss} coincides also with $1/\Gamma_{\Pi\sim0}$. Lower A_0/M values indicate molecules that spread less and remain more globular upon adsorption; it is therefore associated with molecules that have a low adaptability in changing their conformation e.g. upon surface area changes. Low A_0/M values seem to be a prerequisite for mechanically strong protein films but they do not account for intermolecular interactions (which may play an additional role in the build-up of a strong network) because A_0 is defined as the surface coverage above which surface pressure becomes detectable. In contrast to A_0/M, $d\Pi/d\Gamma$ is an indication for the compressibility of a protein film. High values of $d\Pi/d\Gamma$ correspond to a low compressibility of the protein film. The relation between $d\Pi/d\Gamma$ and the mechanical film properties, for example σ_{ss}, is similar to that between σ_{ss} and A_0/M because low values of A_0/M correspond to high values of $d\Pi/d\Gamma$. Conclusively, globular molecules may form stronger interfacial networks than flexible, random-like proteins.

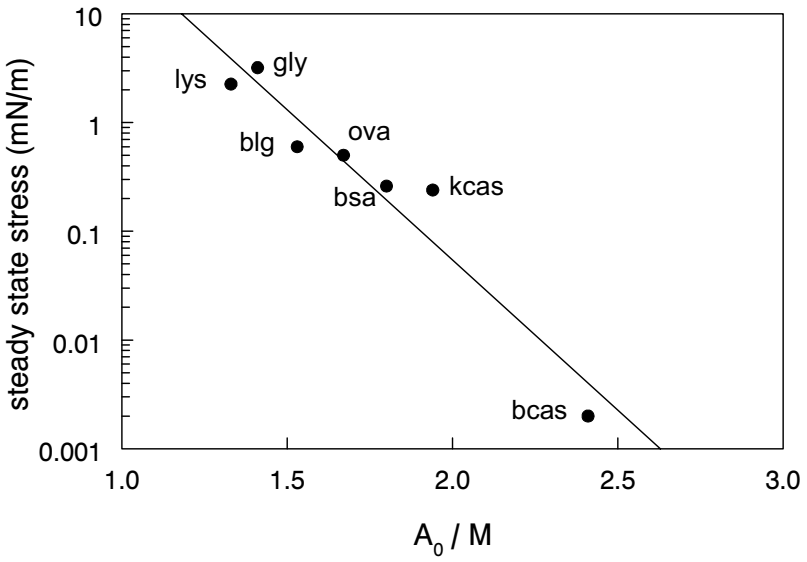

Figure 6.7 Correlation between A_0/M and σ_{ss} (mN/m) derived from values for various proteins; A_0/M values were all taken from table 6.2; σ_{ss} values from table 6.1, except for κ-casein and lysozyme [30] and BSA [14]

An adsorbed protein layer with visco-elastic properties can be seen as a 3-dimensional gel in which the dimension perpendicular to the interface is very small (< 0.01 μm) [17]. Therefore, the transition between an interfacial gel and a bulk gel is gradual from a single molecular layer via a multilayer to a system of which the smallest dimension is ≥ 1 mm. As mentioned above the packing density of proteins at the interface plays a role in the way protein layers respond to deformation in dilation and shear. The packing density or volume fraction occupied by the protein at the interface may change upon ageing or area changes. By calculating the volume fraction of proteins at the interface in an adsorbed protein layer, 'interfacial' gels can be compared with bulk gels. Moreover, a relation can be found between the volume fraction and the mechanical properties of interfacial protein layers. In Table 6.3 saturation values are given for Γ (mg/m^2) and the layer thickness d (nm), termed Γ_∞ and d_∞, respectively. Values for Γ_∞ and d_∞ are retrieved from ellipsometry and IRRAS measurements [13]. From Γ_∞ and d_∞ the density of proteins can be calculated; the volume fraction ϕ (m^3/m^3) is then calculated as follows:

$$\varphi = \frac{\rho}{M} \cdot N_{AV} \cdot \frac{4\pi \cdot R_g^{\,3}}{3} \qquad (6.3)$$

where R_g is the radius of gyration of a protein molecule; values for R_g were taken from literature [29,31,32]. Although values for ϕ are generally quite reasonable, β-lactoglobulin gives a somewhat high value of ϕ~0.74. Also β-casein exhibits a high

ϕ but because β-casein is a predominantly random coil structured protein (and not globular like β-lactoglobulin) it has a more open structure allowing interpenetration of chains. Discrepancies in the values of ϕ can be caused by an unclear definition of the layer thickness. The layer thickness as measured with ellipsometry and IRRAS is determined from a stratified layer model. The protein volume fraction is higher very near to the interface but as a function of distance perpendicular to the interface it decreases rapidly to a layer with a lower volume fraction [33,34]. The protein volume fraction in the layer will therefore depend on the definition of the layer thickness being the thickness of the layer with high ϕ only or taking into account the sub-layer as well. In addition, the layer thickness determined by IRRAS was generally found to be higher than with ellipsometry but the same trend in difference between proteins was found. Higher values of layer thickness will lead to lower protein volume fraction in the adsorbed layer.

Table 6.3 Protein volume fraction ϕ (m^3/m^3) in the adsorbed interfacial layer determined from the adsorbed amount Γ (mg/m^2) and layer thickness d (nm)

	Γ_∞ (mg/m^2)	d_∞ (nm)	ρ (10^3 kg/m^3)	ϕ (m^3/m^3)
β-casein	4 / 3.5	~5	0.75	0.99
β-lactoglobulin	2.7	~4	0.67	0.74
glycinin (pH 3)	2.8 / 3	~8	0.36	0.40
ovalbumin	1.9	~10	0.19	0.29
glycinin (pH 6.7)	2.9	~12	0.24	0.22

In literature we only find few reports in which the properties of interfacial and bulk gels have been compared. For glycinin a correlation was found between the gel formation behaviour in bulk and at interfaces [17]. Interfacial and bulk gels formed at low pH have a higher modulus, fracture at lower strain, while the fracture stress is higher than at basic pH. For bulk gels, these differences are caused by a difference in gel structure [35]: at low pH all protein is involved in the gel network and the structure itself is less coarse than at high pH where a considerable amount of protein does not take part in the gel network. For interfacial glycinin gels the differences found in gel structure are similar to those found in bulk gels (see Table 6.1 and 6.3). The volume fraction of protein in the 'gelled' interfacial layer is higher at low pH than at high pH. The differences in strength of an interfacial glycinin layer can therefore be explained by differences in the structure of the protein layer. For ovalbumin and β-lactoglobulin similarities are also found between interfacial and bulk gels. At

interfaces ovalbumin can be deformed much further before fracture occurs than β-lactoglobulin implying that it has a more yielding behaviour. This corresponds to similar differences in fracture strains in bulk and in interfacial rheology: for bulk gels fracture strains were reported of 0.27 and 0.47 for β-lactoglobulin and ovalbumin, respectively, at similar pH [36,37].

The differences in mechanical properties between β-casein, ovalbumin, glycinin (pH 6.7), β-lactoglobulin and glycinin (pH 3) indicate a transition from a more yielding (viscous) behaviour to a more fracturing (elastic) behaviour. This transition is also observed in gradual changes in ϕ, γ_f and A_0/M. Combining Tables 6.1, 6.2 and 6.3 it appears that in general protein layers with low ϕ and high A_0/M have a high γ_f and behave more viscous whereas solid-like behaviour is characterised by high ϕ, low A_0/M and low γ_f. The behaviour of ovalbumin and glycinin (pH 6.7) layers is more yielding whereas β-lactoglobulin and glycinin (pH 3) exhibit solid-like behaviour.

Conclusively, the strength of an interfacial protein network (or bulk gel) depends on (1) the volume fraction ϕ, (2) the interactions between proteins and (3) the deformability of the single proteins involved in the protein network. To form a strong gel at low ϕ the interactions between proteins are of major importance whereas at high ϕ also the deformability plays a role.

Table 6.4 Secondary structures of various proteins (pH 6.7) in solution

	α-helix	β-sheet
β-casein	10%	13%
β-lactoglobulin	15%	55%
glycinin (pH 3)	41%	-
ovalbumin	35%	47%
glycinin (pH 6.7)	67%	-
lysozyme	42%	-
κ–casein	14%	31%
BSA	55%	16%

Secondary structure

Upon adsorption at the air/water interface proteins may change conformation in order to form a protein network with specific mechanical properties. From previous experiments [11,13] it is known that only minor changes in secondary structure occur. At a protein concentration of 0.1 g/l no changes were found for β-casein whereas for

β-lactoglobulin and ovalbumin a conformational change from 10% β-sheet to random coil took place. For glycinin (pH 3) anti-parallel β-sheets were formed which are correlated to intermolecular aggregation of the protein at the interface. This aggregation phenomenon correlates directly with the strong mechanical properties of glycinin (pH 3). For glycinin at pH 6.7 however, no such aggregation phenomenon was found. No conformational changes occurred after 7 minutes but the interfacial protein layers continued to grow in strength. For glycinin at pH 6.7 the increase in strength was much larger than for glycinin at pH 3; at t=8 hours the same fracture stress was found for both pH values. The role of conformational changes in network formation by proteins is therefore not unequivocal.

According to literature the secondary structure of the protein is correlated with A_0 and $d\Pi/d\Gamma$ [1,38]. It is suggested that the α-helix structure plays a more dominant role in the magnitude of $d\Pi/d\Gamma$ than β-sheets and unordered structures, respectively [1]. Moreover, for sequential iso-peptides, which attained either an α-helix or β-sheet structure upon adsorption at the interface, A_0 was found to be significantly larger for the peptides rich in α-helices [38]. However, we did not observe such a relationship between the amount of α-helix (see Table 6.4) and A_0 (see Table 6.2). Several authors have studied the influence of the secondary structure on the compressibility of peptide layers [38-40]. They observed that peptide layers consisting of α-helical structures are more compressible than those containing predominantly β-sheets. Again, we could not clearly confirm this relation. We are aware that the behaviour of proteins containing several types of secondary structures, of which one is dominant, may differ from peptides containing only one type of secondary structure and that this probably causes the discrepancy between literature and our results.

Whether the differences observed in the compression experiments (see also section 6.3.2) between β-casein, β-lactoglobulin and glycinin (pH 3) can be directly related to differences in secondary structures is dubious. Upon compression of the interface ϕ will probably increase until a certain value, above which collapse of the layer will occur leading to buckling of the layer into the solution or even desorption. Both buckling and desorption may occur depending on the compressibility of the protein layer; whether desorption occurs may also depend on the internal coherence of an adsorbed protein layer. For β-casein, β-lactoglobulin and glycinin (pH 3) different behaviour was observed varying from desorption, partial desorption to probably (only) buckling, respectively. Adsorbed glycinin (pH 3) layers with ϕ~0.4 can still be compressed to higher ϕ. According to Figures 6.4 and 6.6 Γ stays more or less the same during relaxation, but the extent to which ϕ changes is unknown because we did not observe any significant changes in the layer thickness as measured by IRRAS. For β-casein and β-lactoglobulin (both very high ϕ) the

possibility for a further increase in ϕ is much lower than for glycinin (pH 3). Whether the volume fraction of a glycinin layer or the high content of α-helix is more characteristic for the solid-like behaviour of glycinin upon compression, is difficult to conclude. Extended research is needed to obtain systematic information on this. Moreover, upon compression organisational changes in secondary structure may occur. For example for glycinin (pH 3) and ovalbumin anti-parallel β-sheets were formed at the expense of random coil structures upon compression of the interface [13,41].

6.4 Conclusions

Differences observed in mechanical properties and relaxation behaviour indicate that the behaviour of a protein film may vary widely from predominantly viscous (yielding) to more elastic (fracture). This behaviour can in general be correlated with the molecular properties of single proteins in terms of molecular dimensions. When the molecular area occupied by a protein at Π~0 mN/m is corrected for the protein molecular weight (= A_0/M), it is strongly correlated to the mechanical properties of a protein film. Low values of A_0/M imply compact proteins and they seem to be a prerequisite for strong protein films in terms of the steady state stress. The role of intermolecular interactions in network formation is not related to A_0/M values, nor can information on this property be directly deduced from the slope of Π-Γ curves (=dΠ/dΓ).

Adsorbed protein layers can be defined as 3-dimensional 'interfacial' gels and in terms of volume fraction, fractures stress and fracture strain, they behave quite similarly to bulk gels, despite that these gels are usually heat-induced. Both ovalbumin and glycinin (pH 6.7) show more yielding behaviour both at interfaces and bulk whereas glycinin (pH 3) and β-lactoglobulin behave more solid-like and fracture more brittle upon large deformation.

Acknowledgements

The authors would like to thank Harmen de Jongh (WCFS) for critically reading the manuscript; Marcel Meinders (WCFS) is kindly acknowledged for helpful discussions.

References

1. Razumovsky, L.; Damodaran, S. *Langmuir* **1999**, *15*, 1392-1399.
2. Martin, A.H.; Grolle, K.; Bos, M.A.; Cohen Stuart, M.A.; van Vliet, T. *J. Coll. Interface Sci.* **2002**, *254*, 175-183.
3. Damodaran, S.; Song, K.B. *Biochim. Biophys. Acta* **1988**, *954*, 253.

4. Dickinson, E.; Murray, B.S.; Stainsby, G.; Dickinson, E.e. In: *Adv. Food Emulsions and Foams*; Ed. E. Dickinson and G. Stainsby, Elsevier; 1988, 123-162.
5. Graham, D.E.; Phillips, M.C. *J. Coll. Interface Sci.* **1979**, *70*, 403-414.
6. MacRitchie, F. In: *Proteins at Liquid Interfaces*; Ed. D. Möbius and R. Miller, Elsevier; 1998, 149-177.
7. Pezennec, S.; Gauthier, F.; Alonso, C.; Graner, F.; Croguennec, T.; Brulé, G.; Renault, A. *Food Hydrocoll.* **2000**, *14*, 463-472.
8. Graham, D.E.; Phillips, M.C. *J. Coll. Interface Sci.* **1979**, *70*, 427-439.
9. Lu, J.R.; Su, T.J.; Thomas, R.K.; Penfold, J.; Webster, J. *J. Chem.Soc.Far.Trans.* **1998**, *94*, 3279-3287.
10. Clark, D.C.; Smith, L.J.; Wilson, D.R. *J. Coll. Interface Sci.* **1988**, *121*, 136-147.
11. Meinders, M.B.J.; de Jongh, H.H.J. *Biospectroscopy* **2002**, *67*, 319-322.
12. Renault, A.; Pezennec, S.; Gauthier, F.; Vié, V.; Desbat, B. *Langmuir* **2002**, *18*, 6887-6895.
13. Martin, A.H.; Meinders, M.B.J.; Bos, M.A.; Cohen Stuart, M.A.; van Vliet, T. *Langmuir* **2003**, accepted for publ.
14. Graham, D.E.; Phillips, M.C. *J. Coll. Interface Sci.* **1980**, *76*, 240-250.
15. Graham, D.E.; Phillips, M.C. *J. Coll. Interface Sci.* **1980**, *76*, 227-239.
16. Bos, M.A.; van Vliet, T. *Adv. Coll. Interface Sci.* **2001**, *91*, 437-471.
17. van Vliet, T.; Martin, A.; Renkema, M.; Bos, M. In: *Plant Biopolymer Science, Food and Non Food Applications*; Ed. D. Renard, G. Della Valle and Y. Popineau, Royal Society of Chemistry; 2002, 241-252.
18. Jones, D.B.; Middelberg, P.J. *Langmuir* **2002**, *18*, 5585-5591.
19. de Jongh, H.H.J.; Gröneveld, T.; de Groot, J. *J. Dairy Sci.* **2001**, *84*, 562-571.
20. Swaisgood, H.E. In: *Developments in Dairy Chemistry-1*; Ed. P.F. Fox, Applied Science Publ.; 1982, 1-57.
21. Tanh, V.H.; Shibasaki, K. *J. Agric.Food Chem.* **1976**, *24*, 1117-1121.
22. Martin, A.H.; Bos, M.A.; van Vliet, T. *Food Hydrocoll.* **2002**, *16*, 63-71.
23. Martin, A.H.; Bos, M.A.; Cohen Stuart, M.A.; van Vliet, T. *Langmuir* **2002**, *18*, 1238-1243.
24. Whorlow, R.W. Rheological Techniques; Ellis Horwood Limited; New York; 1992.
25. Meinders, M.B.J.; van den Bosch, G.G.M.; de Jongh, H.H.J. *Eur. Bioph. J.* **2000**, *30*, 256-267.
26. Bertie, J.E.; Ahmed, M.K.; Eysel, H.H. *J. Phys. Chem.* **1989**, *93*, 2210-2218.
27. Mackie, A.R.; Gunning, A.P.; Wilde, P.J.; Morris, V.J. *J. Coll. Interface Sci.* **1999**, *210*, 157-166.
28. Meinders, M.B.J.; van Aken, G.A.; Martin, A.H. **2003**, in preparation.
29. Benjamins, J. **2000** PhD-thesis, Wageningen University, the Netherlands.
30. Murray, B.S. **1987** PhD-thesis, University of Leeds, United Kingdom.
31. Barteri, M.; Gaudiano, M.C.; Rotella, S.; Benagiano, G.; Pala, A. *Biochim. Biophys. Acta* **2000**, *1479*, 255-264.
32. Badley, R.A.; Atkinson, D.; Hauser, H.; Oldani, D.; Green, J.P.; Stubbs, J.M. *Biochim. Biophys. Acta* **1975**, *412*, 214-228.

33. Atkinson, P.J.; Dickinson, E.; Horne, D.S.; Richardson, R.M. *J. Chem.Soc.Far.Trans.* **1995**, *91*, 2847-2854.
34. Dickinson, E.; Horne, D.S.; Phipps, J.S.; Richardson, R.M. *Langmuir* **1993**, *9*, 242-248.
35. Lakemond, C.M.M.; de Jongh, H.H.J.; Paques, M.; van Vliet, T.; Gruppen, H.; Voragen, A.G.J. *Food Hydrocoll.* **2002**, accepted for publ.
36. Stading, M.; Hermansson, A.-M. *Food Hydrocoll.* **1991**, *5*, 339-352.
37. van Kleef, F.S.M. *Biopolymers* **1986**, *25*, 31-59.
38. Maget-Dana, R.; Lelièvre, D.; Brack, A. *Biopolymers* **1999**, *49*, 415-423.
39. Taylor, J.W. *Biochemistry* **1990**, *29*, 5364-5375.
40. De Grado, W.F.; Lear, J.D. *J.Am.Chem.Soc.* **1985**, *107*, 7684-7689.
41. Kudryashova, E.V.; Meinders, M.B.J.; Visser, A.J.W.G.; van Hoek, A.; de Jongh, H.H.J. *submitted.*

7 Practical Relevance

Background

The research described in this thesis was performed as part of a larger project named ‘Stability of Emulsions and Foams’. This project aimed at unravelling mechanisms responsible for the physical (in)stability of emulsions and foams at a molecular and mesoscopic level. Different sub-projects were defined each linked to a certain physical (in)stability mechanism, except for the sub-project described in this thesis. This sub-project was a more fundamental study on proteins at the air/water interface in general, which should provide knowledge on the properties of interfacial protein layers under conditions relevant for the other sub-projects within ‘Stability of Emulsions and Foams’.

In this thesis a schematic distinction was made between several molecular processes that occur at the interface, namely: (i) protein adsorption, (ii) conformational changes that occur upon adsorption, and (iii) the formation of a visco-elastic layer with specific mechanical properties. Each of these molecular processes supplied information for the other sub-projects within the project of ’Stability of Emulsions and Foams’ and for applications in industrial processes.

(i) Protein adsorption/anchoring at the interface

Foam formation and emulsification is strongly correlated to the rate at which the surface tension can be lowered; hence, knowledge is required about the adsorption rate of proteins to the interface, especially under dynamic circumstances (e.g. mixing, pumping). In *Chapter 5* the foamability of various proteins was studied and the results were compared to the adsorption rate of the corresponding proteins. It appeared that at a given concentration no foam could be formed with glycinin (pH 6.7) and ovalbumin because of the low adsorption rate. By changing the pH from 6.7 to 3 glycinin has a different quaternary structure (and a lower M) and behaves as a good foaming agent due to much faster adsorption (see *Chapter 2*). Another way to alter the foaming properties of a protein is by chemical modification. Upon lipophilisation of ovalbumin, the protein adsorbs faster due to the increased hydrophobicity; hence, the foaming properties of ovalbumin are greatly enhanced [1].

The knowledge obtained on the interfacial behaviour of various proteins may serve as a basis for modifying proteins in order to obtain desired functionality. The interfacial properties of soy glycinin, for example, had only occasionally been studied. Our work has shown that this protein, especially in the monomer form at pH 3, is a good substitute for proteins of animal origin for use in foams and emulsions. However, the monomer form is available only in a limited pH range. Glycinin should be modified in such a way that the monomeric form would also become available at other pH values; this could lead to a broader range of applications, both for food and non-food products.

(ii) Conformational changes

Conformational changes of proteins may occur upon adsorption. Such changes, either in secondary or in tertiary structure contribute to the lowering of the Gibbs energy for adsorption. Reports on in situ measurements of conformational changes of food proteins upon adsorption at the air/water interface (or oil/water interface) are very scarce in literature. The development of an infra-red reflection absorption spectroscopy (IRRAS) technique resulted in useful and unique experimental possibilities [2]. At first IRRAS spectra were recorded of adsorbed protein layers in equilibrium only. The IRRAS spectra needed to be interpreted and translated into parameters such as protein concentration and layer thickness, which could be done by simulation of the IRRAS spectra [2]. Understanding the IRRAS spectra allowed us to follow adsorption kinetics and the conformational changes that occur during the adsorption process [3]. Additional information could be retrieved by interpretation of simultaneously recorded values of surface pressure, adsorbed amount and conformational changes upon compression and expansion of the interface (see *Chapter 3*).

Only limited conformational changes (defined here in terms of secondary structure) were found upon adsorption of protein at the air/water interface. These relatively small changes in secondary structure may nevertheless suggest that the changes in tertiary structure are much larger. Unfortunately, lack of suitable techniques limits the possibilities to obtain information on tertiary structure changes. The importance of conformational changes for network formation and foam formation and stability is not really clear. Only for glycinin (pH 3) the conformational changes, in terms of intermolecular aggregation, correspond directly to the strong mechanical properties of the protein layer. It is suggested that protein unfolding is a prerequisite for the formation of intermolecular bonds leading to a protein network at the interface, but from the measurements presented in this thesis we can not draw a definite conclusion.

(iii) Mechanical properties

Various interfacial properties have been claimed to affect the stability of emulsions and foams in one way or another. It is thought that a rigid protein network around air or oil droplets retards destabilisation processes of foams and emulsions such as disproportionation, coalescence and drainage.

Regarding disproportionation we should point out that an interfacial protein gel layer with a thickness of molecular size can not stop the growth of large droplets, except for very mono-disperse systems. For hetero-disperse systems growth can only be stopped by an elastic network in the continuous phase or a ‘very’ thick interfacial gel network. Shrinkage of small droplets can in theory be stopped by an

ideally elastic interfacial layer around the droplet [4,5]. However, protein layers never behave purely elastically but always visco-elastically. Moreover, above a certain compression (or below a certain surface tension γ) collapse of the interfacial layer may occur, with the effect that further decrease of γ with ongoing shrinkage of the droplet will cease. The visco-elastic behaviour of adsorbed protein layers implies that the mechanical properties are time-dependent leading to stress relaxation over long time scales. Nevertheless, the presence of an interfacial protein layer may retard disproportionation of a foam as was shown in *Chapter 5*. Glycinin, which forms a mechanically strong layer, gave a foam with a lower coarsening rate than β-casein, which has weak network forming properties. Conclusively, surface elasticity slows down the disproportionation process but slow stress-relaxation in the adsorbed protein film allows disproportionation to proceed, albeit slowly. Strategies to obtain stabilisation of a protein stabilised foam against disproportionation are: (i) addition of components to the droplets that are insoluble in the continuous phase, (ii) presence of an elastic bulk of which the yield stress is above a critical value (e.g. inducing gel formation after foam formation) or (iii) stabilisation of small gas bubbles (< 0.5 μm) by very thick (> 0.1 μm) protein layers.

Mechanical properties of protein films may involve that the protein layer yields or fractures when it is exposed to large deformation. Fracture properties of interfacial layers have not extensively been dealt with in literature. Upon subjecting surfaces to large deformation (shear or dilation) cracks arise and eventually fracture occurs. Differences in the stress-strain characteristics were observed between various protein layers. Fracture mechanics was shown to play a role in the process of flow-induced coalescence [6] and also in entering and spreading phenomena of emulsion droplets at the air/water interface [7]. Both processes were themes of sub-projects within ‘Stability of Emulsions and Foams’.

Flow-induced coalescence plays a role during handling like stirring, pouring or eating of highly concentrated emulsions such as mayonnaise or cream. For flow-induced coalescence between two droplets to occur the following conditions must be fulfilled: (a) stresses exerted on the emulsion must result in local extension and compression of the interface, (b) stresses that are built up in the interfacial layer must become high enough to induce fracture of the interfacial protein layer and (c) the opposing bare interfaces formed due to fracture must stay bare long enough [8,9]. A correlation between the sensitivity to flow-induced coalescence and the fracture stress (as measured in shear (see *Chapter 4*) or dilation [10]) was not really observed. This apparent discrepancy can be explained by comparing flow-induced coalescence to macroscopic fracture of a solid foam with a polyhedral structure and by distinguishing fracture initiation and propagation [6,9]. Fracture is initiated if the local stress in the material exceeds the breaking stress of the bonds between the

structural elements (protein molecules) that give the solid-like properties to the material (adsorbed protein layers). In a polyhedral foam the stress is concentrated in the thin films between the droplets. After fracture of a single protein film the stress originally acting on this film will be divided over the adjacent films. These films become more heavily loaded than any other film in the (polyhedral) foam structure, which promotes their subsequent rupture. During crack growth extensive coalescence of the droplets at both sides of the crack formed will occur. If the cracks reach the edge of the highly concentrated emulsion, they may release part of their contents, which is visible macroscopically as the release of liquid oil. The role of the fracture stress of interfacial protein layers in flow-induced coalescence is probably only of importance for the fracture initiation process and not in the fracture propagation. It will therefore only play a minor role in determining the number of droplets that coalesce and the amount of oil separated from the emulsion. However, fracture of the interfacial protein layer is probably an essential first step for flow-induced coalescence to occur.

Entering and spreading of emulsion droplets at the air/water interface may occur during aeration of emulsions. Aeration involves the introduction of air bubbles into emulsions under a number of processing conditions including pouring, stirring, whipping and chewing. Whether intentional or not, aeration can have drastic effects on the physical properties and stability of the system. The result may be desirable, for example in systems such as whipped cream (where adsorbed fat globules act as a stabiliser of the interface) or undesirable such as with coalescence of emulsion droplets. During aeration, emulsion droplets encounter an expanding air/water interface and depending on the properties of that interface the emulsion droplets may enter and spread at the interface. By studying the entering and spreading of emulsion droplets in expanding spread films of β-casein, β-lactoglobulin and glycinin (pH 3) evidence was found that the mechanical properties of the interface influence entering and spreading events [7]. The differences in mechanical properties of β-casein, β-lactoglobulin and glycinin (pH 3) films (see *Chapter 4, 5 and 6*) vary from predominantly viscous (fluid-like) to more elastic, respectively. This is reflected in the entering and spreading behaviour as follows. In the case of β-casein the protein layer can flow to accommodate the spreading oil: upon expansion of the protein film the cloud of added emulsion droplets is enlarged beneath the protein film proportional to the expansion of the film itself. The insertion of emulsion droplets therefore happens at random over the enlarged cloud area. For β-lactoglobulin and glycinin (pH 3) the film is observed to fracture upon expansion and the emulsion quickly spreads to fill and expand the cracks [7]. The extent to which fracture occurs and propagates corresponds to the brittleness of protein films at the air/water interface increasing with β-casein < β-lactoglobulin < glycinin (pH 3) (see *Chapter 5*). Conclusively, film

elasticity and fracture mechanics play an important role in the entering and spreading behaviour of emulsion droplets at the air/water interface. The fracture behaviour is relevant when considering the stability of emulsions under aeration conditions where low or moderate expansion rates are applied (e.g. stirring, pouring, and chewing) [7].

With regard to sensory perception the three processes discussed above play a role in the mouth during eating. Upon consumption of an emulsion-type of product the emulsion droplets encounter the surface of the tongue, teeth and the palate. For flavour release and perception spreading of the emulsion droplets is useful but upon extensive coalescence of these emulsion droplets at tongue or palate surface a fatty layer may be formed (= fat surfacing) which is often not desired. Coalescence can be induced by flow, e.g. by chewing or by movement of the tongue. During consumption air can also be enclosed by the emulsion. Instead of spreading of emulsion droplets at the tongue or palate surface spreading can also occur at the surface of the introduced air bubbles. This allows a faster transfer of aroma components to the nasal cavity.

A final point is that in emulsions and foams the mechanical properties of the protein layers stabilising the interface have an influence on the appearance and fracture mechanics of the emulsion/foam itself. For example, proteins that form a very brittle film will give a different sensory perception to the foam than proteins that form viscous films. Foams made with glycinin were found be much dryer, more brittle and stiffer than β-casein foams at similar volume fractions of air (see *Chapter 5*).

References

1. Wierenga, P.; Meinders, M.B.J.; Egmond, M.; de Jongh, H.H.J. **2003**, submitted for publ.
2. Meinders, M.B.J.; van den Bosch, G.G.M.; de Jongh, H.H.J. *Eur. Bioph. J.* **2000**, *30*, 256-267.
3. Martin, A.H.; Meinders, M.B.J.; Bos, M.A.; Cohen Stuart, M.A.; van Vliet, T. In: *Food Colloids, Biopolymers & Materials*; Ed. E. Dickinson and T. van Vliet, Royal Society of Chemistry; 2003.
4. Kloek, W.; van Vliet, T.; Meinders, M.B.J. *J. Coll. Interface Sci.* **2001**, *237*, 158-166.
5. Meinders, M.B.J.; Kloek, W.; van Vliet, T. *Langmuir* **2001**,
6. van Aken, G.A. *Langmuir* **2002**, *18*, 2549-2556.
7. Hotrum, N.E.; Cohen Stuart, M.A.; Vliet van, T.; Aken, G.A., van **2003**, submitted for publ.
8. van Aken, G.A.; Zoet, F.D. *Langmuir* **2000**, *16*, 7131-7138.
9. van Vliet, T.; van Aken, G.A.; Bos, M.A.; Martin, A.H. In: *Food Colloids, Biopolymers & Materials*; Ed. E. Dickinson and T. van Vliet, Royal Society of Chemistry; 2003,
10. Bos, M.A.; Grolle, K.; Kloek, W.; van Vliet, T. **2002**, accepted for publ. in Langmuir.

Summary - Samenvatting

Summary

In food emulsions and foams proteins are often the main interfacial components stabilising air cells or oil droplets against destabilisation processes such as coalescence, drainage and disproportionation. Upon adsorption at interfaces proteins may form a visco-elastic network. To understand the role of these visco-elastic protein layers in the formation and stability of emulsions and foams a closer look was taken at the molecular processes occurring at the interface. In this thesis a rather simple distinction was made in these molecular processes: (i) protein adsorption, (ii) conformational changes that occur upon adsorption and (iii) the formation of a visco-elastic protein layer with specific mechanical properties. These three processes depend on the type of protein and on solution conditions like pH and ionic strength. The aim of this thesis was to obtain systematic information on the importance of mechanical and conformational aspects for the formation of a visco-elastic protein network. A series of proteins was therefore selected varying in structure from flexible to rigid/globular, namely (milk) β-casein, (milk) β-lactoglobulin, (egg) ovalbumin and (soy) glycinin.

In *Chapters 2 and 3* the conformational aspects of proteins upon adsorption at the air/water interface are discussed. In *Chapter 2* the quaternary structure of glycinin was studied as a function of pH. The association/dissociation behaviour as a result of the change in pH was related to differences in adsorption rate and interfacial rheological properties. At pH 3 glycinin is present in solution as a monomer, the so-called 3S form (M~44 kDa); at pH 6.7 it associates into a hexamer, the 11S form (M~350 kDa). The quaternary structure of glycinin therefore depends on the pH. Various interfacial rheological techniques show a difference in interfacial behaviour between the 3S form and the 11S form of glycinin. Due to the smaller molecular size and higher ability to unfold, the 3S form adsorbs faster, gives a higher adsorbed amount, a higher dilational modulus and a higher apparent surface shear viscosity after short ageing times. After longer ageing times however, the surface concentration and surface shear viscosity were more or less the same for pH 3 and pH 6.7. With regard to foaming properties, it was concluded that it was not possible to make foam with the 11S form at the given concentrations whereas the 3S form behaves as a good foaming agent.

Chapter 3 focused on changes in conformation in terms of secondary structure upon adsorption at the air/water interface of β-casein, β-lactoglobulin and glycinin. To study conformational changes a relatively new technique was used namely Infra-Red Reflection Absorption Spectroscopy (IRRAS). Spectral simulation of the absorption spectra obtained with IRRAS revealed information on conformational changes at a secondary folding level and the protein concentration at the surface. The adsorption behaviour of β-casein, β-lactoglobulin and glycinin was studied by following the

adsorbed amount (Γ) as a function of time. Obtained values for Γ were compared to ellipsometry data and agreed very well. Regarding conformational changes, only limited changes in secondary structure were found. For β-lactoglobulin loss of β-sheet structures was observed whereas the amount of unordered structure increased. For glycinin (pH 3) aggregation at the interface was observed by the appearance of an absorption band at 1630 cm^{-1}, which involves the formation of intermolecular anti-parallel β-sheet structures. This aggregation behaviour was not observed for glycinin at pH 6.7. For β-casein no conformational changes were observed at all. By comparison of adsorbed and spread protein layers it was found that spreading of a protein leads to a conformational state somewhat different from that when adsorbed from solution.

Chapters 4 and 5 deal with the mechanical aspects of the visco-elastic protein layer formed at the interface. Whereas *Chapter 4* only deals with the mechanical properties determined by deformation in shear, *Chapter 5* discusses both shear and dilation. In *Chapter 4* interfacial shear properties of adsorbed protein layers at the air/water interface were determined using a Couette-type surface shear rheometer. Such experiments have often been used to determine a steady state ratio between stress and rate of strain, which is then denoted as 'surface shear viscosity'. However, by measuring the stress on the protein layer as a function of time at a fixed shear rate, more information on the mechanical properties of the protein layers could be obtained. Initially the stress increased steadily with time, then it went through a maximum and next attained a steady-state value from which the surface shear viscosity is usually determined. Stress-strain curves could be calculated from the data obtained. Differences in the stress-strain curve were observed for the proteins studied (ovalbumin, β-lactoglobulin, glycinin). The maximum in the stress-strain curve can be regarded as a kind of fracture/yield stress. This implies that the strain at the maximum is a fracture strain and the decrease in stress reflects a kind of breakdown of the protein film structure.

In *Chapter 5* a series of proteins was studied with respect to their ability to form a network at the air/water interface and their suitability as foaming agents and foam stabilisers. Network forming properties were assessed in terms of surface dilational modulus (E), the critical falling film length (L_{still}) and flow rate (Q_{still}) below which a stagnant film exists (as measured with the overflowing cylinder technique) and the fracture stress and fracture strain measured in surface shear (see also *Chapter 4*). It was found that glycinin (pH 3) can form a strong interfacial gel in a very short time, whereas β-casein has very poor network forming properties. Hardly any foam could be produced at the chosen conditions with glycinin (pH 6.7) and with ovalbumin, whereas β-casein, β-lactoglobulin and glycinin (pH 3) were good foaming agents. It seems that adsorption and unfolding rate are most important for foam formation. Only

for stabilisation against disproportionation surface rheological properties were found to play a role. Due to a higher E, glycinin (pH 3) is more stable to coarsening than β-casein.

In *Chapter 6* the relation between mechanical film properties of various adsorbed protein layers at the air/water interface and molecular properties of the corresponding proteins is discussed. Mechanical film properties were determined by surface deformation in shear and dilation. In shear, the fracture stress σ_{ss} and strain γ_f were determined as well as the relaxation behaviour after macroscopic fracture. The dilational measurements were performed in a Langmuir-trough equipped with an IRRAS accessory. During compression and relaxation of the surface, the surface pressure Π and adsorbed amount Γ (determined from the IRRAS spectra) were determined simultaneously. In addition, IRRAS spectra revealed information on conformational changes in terms of secondary structure. We looked for correlations between macroscopic film properties and molecular properties of the proteins in terms of molecular dimensions and secondary structure. Molecular dimensions involve the area per protein molecule at Π~0 mN/m (A_0), A_0/M (M = molecular weight), the maximum slope of the Π-Γ curves ($d\Pi/d\Gamma$) and the volume fraction ϕ of the protein in the 'interfacial' gel. The differences observed in mechanical properties and relaxation behaviour indicate that the behaviour of a protein film may vary widely from predominantly viscous (yielding) to more elastic (fracture). The transition from viscous to elastic behaviour can be translated to the behaviour of protein layers: predominantly viscous behaviour involves low ϕ, higher A_0/M and a high γ_f, whereas more elastic protein films are characterised by high ϕ, low A_0/M and low γ_f.

In *Chapter 7* the practical relevance of the research described in this thesis is discussed. This thesis was part of a larger project named 'Stability of Emulsions and Foams' in which different sub-projects were defined each linked to a certain physical (in)stability mechanism. The fundamental study on the behaviour of proteins at the air/water interface in general should supply information for the other subprojects and for applications in industrial processes. In particular, the mechanical properties of protein layers appear to play a role in the destabilisation processes of foams and emulsions. Visco-elastic protein layers may slow down disproportionation but can not stop it altogether. The fracture behaviour of protein films was found to be important as a first step in flow-induced coalescence, but also in the entering and spreading of emulsions droplets at an expanding protein film adsorbed at the air/water interface.

Samenvatting

Eiwitten worden in de levensmiddelenindustrie vaak gebruikt als stabilisator van emulsies en schuimen. De functie van eiwitten is om de luchtbellen of olie-druppels te beschermen tegen destabilisatie-processen als coalescentie, drainage and disproportionering. Als gevolg van eiwitadsorptie aan grensvlakken, kunnen visco-elastische netwerken gevormd worden. Mogelijkerwijs spelen deze visco-elastische netwerken een rol in de vorming en stabiliteit van emulsies en schuimen. Om deze rol te begrijpen, zullen we de moleculaire processen die zich afspelen aan het grensvlak moeten bestuderen. In dit proefschrift worden de te bestuderen moleculaire processen op een vereenvoudigde wijze als volgt opgedeeld: (i) adsorptie van eiwit aan het grensvlak, (ii) conformatie-veranderingen die plaatsvinden als gevolg van en tijdens adsorptie en (iii) het ontstaan van een visco-elastische eiwitlaag met specifieke mechanische eigenschappen. Deze drie processen zijn afhankelijk van het type eiwit en van eigenschappen van de oplossing, zoals pH en ionsterkte. Het doel van dit proefschrift was om op een systematische manier informatie te krijgen over de belangrijkheid van mechanische eigenschappen en aspecten betreffende eiwit-conformatie voor het ontstaan van een visco-elastisch netwerk. Hiertoe is een aantal eiwitten geselecteerd die in structuur verschillen van flexibel naar star/globulair. Deze eiwitten zijn: β-caseïne (een melk-eiwit), β-lactoglobuline (een melk-eiwit), ovalbumine (een ei-eiwit) en glycinine (een soja-eiwit).

De onderverdeling die hierboven is gemaakt in moleculaire processen kan als leidraad in het proefschrift worden gebruikt. In *hoofstuk 2 en 3* wordt gekeken naar de conformatie van het eiwit en veranderingen hierin ten gevolge van adsorptie aan een lucht/water grensvlak. *Hoofdstuk 4 en 5* behandelen de mechanische eigenschappen van het eiwitnetwerk dat onstaat na adsorptie en in *hoofstuk 6* wordt, ter overkoepeling van het geheel, geprobeerd het mechanische gedrag van eiwitlagen te koppelen aan de moleculaire eigenschappen van de individuele eiwitmoleculen.

In *Hoofdstuk 2* wordt de conformatie van glycinine bestudeerd als functie van de pH. Door van pH 3 naar pH 6.7 te gaan verandert de quaternaire structuur van glycinine (in oplossing) van monomeer (M~44 Da) naar hexameer (M~350 kDa). Deze structuren worden respectievelijk ook wel 3S en 11S genoemd. Met behulp van verschillende technieken werd het adsorptiegedrag van glycinine bepaald, als mede de oppervlakte-reologische eigenschappen van de geadsorbeerde laag. Deze metingen leidden tot dezelfde, eenduidige conclusie: de 3S vorm adsorbeert sneller dan de 11S vorm en vormt op korte tijdschaal een laag met een hogere geadsorbeerde hoeveelheid eiwit, een hogere dilatatie modulus en een hogere schijnbare viscositeit. Op langere tijdschaal daarentegen werd er geen verschil meer

gevonden in de schijnbare viscositeit en geadsorbeerde hoeveelheid tussen de 3S en de 11S vorm. Wat schuimvorming betreft, was het niet mogelijk om met de 11S vorm schuim te maken onder de gekozen omstandigheden; met de 3S vorm daarentegen kon een goed schuim gemaakt worden.

Hoofdstuk 3 behandelt de veranderingen in conformatie ten gevolge van adsorptie van het eiwit aan een lucht/water grensvlak. Hierbij wordt voornamelijk gedoeld op veranderingen in secundaire structuur. Om conformatie veranderingen te bestuderen werd gebruik gemaakt van een vrij nieuwe techniek, namelijk Infra-Rood Reflectie Absorptie Spectroscopie (IRRAS). Door simulatie van de verkregen IRRAS spectra, kon informatie verkregen worden over de conformatie van het eiwit en de geadsorbeerde hoeveelheid eiwit aan het lucht/water grensvlak. Het adsorptie gedrag van β-caseïne, β-lactoglobuline en glycinine werd bestudeerd en de waarden voor de geadsorbeerde hoeveelheid kwamen overeen met eerder uitgevoerde metingen met ellipsometrie. De gevonden veranderingen in conformatie bleken slechts gering te zijn wat betreft secundaire structuur. De secundaire structuur van β-lactoglobuline veranderde 10%, waarbij een afname in β-sheets gepaard ging met een toename in random coil structuren. Voor glycinine (pH 3) kon uit de IRRAS spectra afgeleid worden dat aggregatie plaats had gevonden aan het lucht/water grensvlak. Het ontstaan van een absorptieband bij 1630 cm^{-1} duidde op de vorming van anti-parallelle β-sheets, die verschillende eiwitmoleculen met elkaar vormen. Deze vorm van aggregatie werd niet gevonden voor glycinine bij pH 6.7. Voor β-caseïne werden helemaal geen conformatie-veranderingen waargenomen. De verandering in conformatie is dus afhankelijk van het type eiwit, maar ook van de manier waarop de laag gevormd wordt. De resultaten hierboven betreffen allemaal geadsorbeerde eiwitlagen; uit metingen met gespreide lagen bleek dat de conformatie van de eiwitten ietwat anders was dan in geadsorbeerde lagen.

In *hoofdstuk 4* worden de mechanische eigenschappen van eiwitlagen besproken als bepaald door afschuiving (shear). De metingen met een Couette-type shear rheometer worden normaal gebruikt om de stationaire toestand te bepalen tussen de spanning (stress) en relatieve vervorming (strain); dit wordt dan schijnbare viscositeit genoemd. In dit proefschrift werden de metingen op een andere manier geïnterpreteerd. Het meten van de spanning als functie van de tijd bij constante afschuifsnelheid leverde meer informatie op over de mechanische eigenschappen van de eiwitlaag. Het verloop van de spanning-tijd curves kan als volgt worden beschreven: de spanning neemt ongeveer lineair toe met de tijd totdat een maximum wordt bereikt, waarna de spanning naar een evenwichtswaarde gaat. Deze evenwichtswaarde komt overeen met de schijnbare viscositeit. Spanning-tijd curves kunnen omgerekend worden naar spanning-relatieve vervorming curves en deze curves blijken verschillend, dus karakteristiek, te zijn voor elk eiwit. Op het maximum

in deze curves treedt breuk op in de eiwitlaag. Dit betekent dat de relatieve vervorming waarbij dit gebeurt iets zegt over de mate waartot een eiwitlaag vervormd kan worden eer breuk optreedt. De daling in spanning na het maximum lijkt op een afbraak van de eiwitlaagstructuur.

Naast shear metingen, worden in *hoofdstuk 5* ook metingen in dilatatie beschreven, welke informatie verschaffen over de aanleg van eiwitten om een netwerk te vormen aan een lucht/water grensvlak. In *hoofdstuk 5* wordt getracht de invloed van deze netwerkvorming aan schuimvorming –en stabiliteit te relateren. Parameters die iets zeggen over de netwerkvorming zijn: de oppervlaktedilatatie modulus (E), de kritieke valhoogte (L_{still}) and debiet (Q_{still}) (zoals bepaald met de overlopende cylinder) en de spanning en relatieve vervorming bij breuk (afgeleid uit de metingen gedaan in afschuiving). Uit de resultaten bleek dat glycinine (pH 3) een zeer sterk netwerk kan vormen op korte tijdschaal, maar dat β-caseïne deze eigenschap niet bezit. Van ovalbumine en glycinine (pH 6.7) kon geen schuim gevormd worden, terwijl met β-caseïne, β-lactoglobuline en glycinine (pH 3) dit wel mogelijk was. Hieruit volgt dat voornamelijk adsorptie –en ontvouwingssnelheid belangrijke aspecten zijn in het maken van schuim. De relatie tussen mechanische eigenschappen en schuimstabiliteit komt alleen naar voren in de stabiliteit tegen disproportionering. Doordat glycinine een hogere E heeft, blijkt het stabieler te zijn tegen vergroven dan β-caseïne.

Ter overkoepeling van het geheel, wordt in *hoofdstuk 6* getracht de relatie tussen de mechanische eigenschappen en de moleculaire eigenschappen van individuele eiwitten, in kaart te brengen. Mechanische eigenschappen werden bepaald in afschuiving en in dilatatie. In afschuiving werden de spanning en relatieve vervorming bij breuk bepaald en ook het relaxatiegedrag van de eiwitlaag nadat macroscopische breuk had plaatsgevonden. De dilatatie metingen werden uitgevoerd in een Langmuir-trog voorzien van een IRRAS-meetopstelling. Tijdens compressie en relaxatie van het grensvlak konden op deze manier de oppervlaktespanning en de geadsorbeerde hoeveelheid (bepaald uit de IRRAS spectra) tegelijkertijd worden bepaald. Bovendien bevatten de IRRAS spectra informatie over eventuele veranderingen in conformatie. Er is gezocht naar een relatie tussen de macroscopische eigenschappen van geadsorbeerde eiwitfilms en de moleculaire eigenschappen, welke opgedeeld werden in moleculaire dimensies en secundaire structuur. Met moleculaire dimensies wordt bijvoorbeeld het oppervlak (A_0) dat een eiwit inneemt bij een oppervlaktedruk van 0 mN/m bedoeld, als ook A_0/M (M=molgewicht), de maximale helling van een Π/Γ-curve ($d\Pi/d\Gamma$) en de volumefractie eiwit in de eiwitlaag. De verschillen die we gevonden hebben in mechanische eigenschappen leiden tot de conclusie dat het gedrag van een eiwitlaag enorm kan verschillen tussen visceus (zwicht) tot elastisch (breuk). De overgang tussen

overwegend visceus en elastisch wordt teruggevonden in de moleculaire eigenschappen: visceuse eiwitlagen hebben een lage volumefractie eiwit, een hoge A_0/M en zwichten bij grote relatieve vervorming terwijl elastische eiwitfilms gekarakteriseerd worden door een hoge volumefractie, lage A_0/M en breken bij kleine relatieve vervorming.

In *hoofdstuk 7* wordt de praktische relevantie van het in dit proefschrift beschreven onderzoek verhaald. Dit onderzoek maakte deel uit van een groter project, te weten 'Stabiliteit van Schuim en Emulsies'. In dit project zijn verschillende sub-projecten gedefinieerd, die elk aan een ander instabiliteitsmechanisme zijn gekoppeld. Het meer fundamentele onderdeel naar het gedrag van eiwitten aan lucht/water grensvlakken zoals beschreven in dit proefschrift, moest informatie genereren voor de andere sub-projecten, maar ook voor toepassingen in industriële processen. De mechanische eigenschappen blijken met name een rol te spelen in destabilisatie processen van schuim en emulsies. De aanwezigheid van een visco-elastisch eiwitnetwerk vertraagt disproportionering, maar kan het proces niet stoppen. Het breukfenomeen van eiwitlagen dat waargenomen wordt bij grote vervorming, speelt o.a. een rol in de eerste stap van coalescentie geïnduceerd door afschuiving, maar ook bij het inserteren en spreiden van emulsiedruppels aan expanderende eiwitfilms.

List of publications

Bos, M.; Martin, A.; Bikker, J.; van Vliet, T. **2001** Surface rheological properties of soy glycinin; gel layer formation and conformational aspects. In E. Dickinson and R. Miller, *Food Colloids, Fundamentals of Formulation* (223-232). Cambridge Royal Society of Chemistry.

Martin, A.H.; Bos, M.A.; van Vliet, T. **2002** Interfacial rheological properties and conformational aspects of soy glycinin at the air/water interface. *Food Hydrocoll.,* 16, 63-71.

Martin, A.H.; Bos, M.A.; Cohen Stuart, M.A.; van Vliet, T. **2002** Stress-strain curves of adsorbed protein layers at the air/water interface measured with surface shear rheology. *Langmuir,* 18, 1238-1243.

van Vliet, T.; Martin, A.; Renkema, M.; Bos, M. **2002** Gel formation by soy glycinin in bulk and at interfaces. In D. Renard, G. Della Valle and Y. Popineau, *Plant Biopolymer Science, Food and Non Food Applications* (241-252). Cambridge Royal Society of Chemistry.

Martin, A.H.; Grolle, K.; Bos, M.A.; Cohen Stuart, M.A.; van Vliet, T. **2002** Network forming properties of various proteins adsorbed at the air/water interface in relation to foam stability. *J. Coll. Interface Sci.,* 254, 175-183.

van Vliet, T.; Martin, A.H.; Bos, M.A. **2002** Gelation and interfacial behaviour of vegetable proteins. *Curr. Op. Coll.Interface Sci.,* 7, 462-468.

Martin, A.H.; Meinders, M.B.J.; Bos, M.A.; Cohen Stuart, M.A.; van Vliet, T. **2003** Adsorption properties and conformational aspects of proteins at the air/water interface measured by IRRAS. In E. Dickinson and T. van Vliet, *Food Colloids, Biopolymers & Materials* Cambridge Royal Society of Chemistry.

van Vliet, T.; van Aken, G.A.; Bos, M.A.; Martin, A.H. **2003** Failure behaviour of adsorbed protein layers, consequences for emulsion and foam stability. In E. Dickinson and T. van Vliet, *Food Colloids, Biopolymers & Materials* Cambridge Royal Society of Chemistry.

Martin, A.H.; Meinders, M.B.J.; Bos, M.A.; Cohen Stuart, M.A.; van Vliet, T. **2003** Conformational aspects of proteins at the air/water interface studied by IRRAS. *Langmuir,* accepted for publ.

Martin, A.H.; Cohen Stuart, M.A.; Bos, M.A.; van Vliet, T. **2003** Mechanical behaviour of protein films at the air/water interface in relation to the protein molecular properties, to be submitted.

Levensloop

Anneke Martin werd op 26 juni 1975 geboren in Hamont, België. Na het behalen van het VWO-diploma in 1993 aan het Lorentz Lyceum in Eindhoven begon zij in datzelfde jaar met de studie Levensmiddelentechnologie aan de Landbouwuniversiteit Wageningen (LUW). Tijdens haar studie deed zij afstudeervakken bij de toenmalige sectie Zuivel en Levensmiddelennatuurkunde (LUW), het NIZO (in Ede) en de Landbouwuniversiteit van Zweden in Uppsala (SLU). In september 1998 sloot zij haar studie af met als specialisatie zuivelkunde. Van februari 1999 t/m februari 2003 was zij in dienst bij het Wageningen Centre for Food Sciences (WCFS) als Assistent in Opleiding, gedetacheerd bij Wageningen Universiteit. Gedurende deze 4 jaar verrichtte zij het in dit boekje beschreven onderzoek bij de Laboratoria van Fysische Chemie & Kolloïdkunde en Levensmiddelenfysica.

Dankwoord

Eindelijk is het tijd om al diegenen te bedanken die mij op wat voor manier dan ook hebben bijgestaan de afgelopen vier jaar. Collega's, vrienden en familie hebben elk op hun eigen manier ervoor gezorgd dat ik op een zeer prettige manier aan dit proefschrift heb kunnen werken. Enkele mensen wil ik met name noemen.

Allereerst mijn begeleiders Martien, Ton en Martin, promotor and co-promotoren. Hoewel de namen (inclusief de mijne) enige gelijkenis vertonen, mocht ik profiteren van een divers gezelschap. Martien, jij benaderde eiwitten en grensvlakken telkens weer op een voor mij verfrissende manier; bovendien hebben je correcties veel bijgedragen aan de leesbaarheid en helderheid van mijn artikelen. Ton, je hield het overzicht over mijn werk maar vooral stimuleerde je me om eens wat langer na te denken over mijn resultaten, hetgeen in het begin tot enige onrust van mijn kant leidde; er gebeurde immers 'niks. Gelukkig ging ik dit anders inzien. Martin, jouw interesse in mij en mijn onderzoek en jouw immer aanwezige enthousiasme werkten aanstekelijk en zorgden dat ik zeer gemotiveerd en gestructureerd heb kunnen werken.

Mijn onderzoek werd geïnitieerd door het WCFS en hier ben ik hen dan ook zeer erkentelijk voor. Bij deze wil ik dan ook al mijn collega's van *programma 2* bedanken. Marcel, je hebt me wegwijs gemaakt in de wereld van IRRAS en spectroscopie, maar ook aan jouw logische manier van redeneren en je tientallen waarom-vragen heb ik veel gehad. Bovendien was het altijd erg gezellig om 'boven' langs te komen. Dat laatste geldt ook voor Harmen; voor specifieke vragen over eiwitten en om mijn chemische kennis weer wat op te vijzelen voorzag jij me op je eigen manier van wat ik wilde weten. Jolan wil ik bedanken voor het zuiveren van de eiwitten en praktische tips daaromtrent. Peter, alias Mister IRRAS, ik vond het erg leuk om samen met jou aan de IRRAS te werken en om onze frustraties en resultaten te delen. Ik ben benieuwd naar de uitkomst van al je plannen.

In de *SEF*-groep heb ik me altijd erg thuis gevoeld en de sfeer tijdens meetings en uitstapjes was altijd erg fijn. George, bedankt voor je suggesties en ideëen. Katja, Franklin en Wim voorzagen de vele experimenten die ik heb uitgevoerd in het lab ter plekke van 'kritiek'; bij hun kon ik terecht voor praktische tips (en ander ongevraagd advies), meestal voorzien van kilo's (!) drop. Katja, jouw schuimwerk en andere metingen hebben mij een stuk verder geholpen in mijn onderzoek. Franklin, de smilestone heb ik niet meer nodig. Mijn mede-AIO's in het project, Natalie en Theo, waren tevens mijn kamergenoten. Ik heb met jullie ontzettend veel plezier beleefd de afgelopen 4 jaar. Door het delen van onze resultaten, twijfels en frustraties (ook die van het dagelijkse leven) werd onze kamer soms een kippenhok, maar zonder had ik

niet gekund. Het laatste jaar zorgden Catriona en Jeannet voor een toename in gezelligheid en verse thee op de kamer. Bedankt hiervoor.

In het kader van hun studie hebben Joanke en Elsbeth gewerkt aan soja –en tarwe-eiwitten ten gunste van mijn project; door hun waardevolle resultaten heb ik een vliegende start kunnen maken. Dennis, je was mijn enige student en ondanks dat jouw resultaten niet terug te vinden zijn in dit boekje, vond ik het fijn om met je samen te werken.

Al de niet-genoemde collega's van pdq, fysica en fysko hebben natuurlijk ook bijgedragen aan de prettige werksfeer; door alle labuitjes, borrels, hét AIO-reisje en de dagelijkse kletspauzes is mijn promotietijd ook een aangename tijd geweest.

Naast het werk was er gelukkig genoeg afleiding, zowel doordeweeks als in het weekend. Muziekvrienden dank ik voor de vrolijke noot; IAAS-oldies en andere lui, voor de steun en gezelligheid tijdens weekendjes, kroegavonden en 'brood en spelen'.

Pap, mam, Gert, jullie zijn altijd een zeer grote steun en stimulans geweest en gaven mij alle ruimte om mijn eigen weg te kiezen. Dank voor de onvoorwaardelijke steun en nuchtere kijk op het leven. Lieve Bart, veel dank voor het aanhoren, meedenken en vooral relativeren.

Anneke

The research described in this thesis was carried out at Wageningen University (the Netherlands) and was part of the research carried out in the scientific programme ‘Structure and Functionality’ of the Wageningen Centre for Food Sciences. Furthermore, the research was part of the Graduate School VLAG (Food Technology, Agrobiotechnology, Nutrition & Health Sciences).

Printing Ponsen & Looijen BV, Wageningen

Cover Protein layers (blue lines) on air bubbles